

200-1-1



FACILITY FORM 602

N71 - 36809
(ACCESSION NUMBER)

141
(PAGES)

CR-122949
(NASA CR OR TMX OR AD NUMBER)

1.7
(THRU)

63
(CODE)

15
(CATEGORY)



Reproduced by
NATIONAL TECHNICAL
INFORMATION SERVICE
Springfield, Va 22151



NORTHWESTERN UNIVERSITY

THE TECHNOLOGICAL INSTITUTE

EVANSTON, ILLINOIS

NORTHWESTERN UNIVERSITY

DYNAMIC RESPONSE AND STABILITY OF A
GAS-LUBRICATED RAYLEIGH-STEP PAD

by

CHI CHENG

and

H. S. CHENG

Prepared under Grant No. NGR 14-007-093

by Department of Mechanical Engineering

and Astronautical Sciences

Northwestern University

Evanston, Illinois 60201

for Lewis Research Center

NASA, Cleveland, Ohio

July 1971

ABSTRACT

The quasi-static, pressure characteristics of a gas-lubricated thrust bearing with shrouded, Rayleigh-step pads are determined for a time-varying film thickness. The axial response of the thrust bearing, to an axial forcing function or an axial rotor disturbance is investigated by treating the gas-film as a spring having nonlinear restoring and damping forces. These forces are related to the film thickness by a power relation. The nonlinear equation of motion in axial mode is solved by the Ritz-Galerkin method as well as the direct, numerical integration. Results of the nonlinear response by both methods are compared with the response based on the linearized equation.

Further, the gas-film instability of an infinitely-wide Rayleigh step thrust pad is determined by solving the transient Reynolds equation coupled with the equation of the motion of the pad. Results show that the Rayleigh step geometry is very stable for bearing number, Λ , up to 50. The stability threshold is shown to exist only for ultra high values of $\Lambda \geq 100$ where the stability can be achieved by making the mass heavier than the critical mass.

ACKNOWLEDGMENT

The authors are grateful for the financial support received under a research grant by the National Aeronautics and Space Administration, Lewis Research Center, Cleveland, Ohio

NOMENCLATURE

A	array of coefficients for pressure Eqs. (4.16) and (4.23).
A_o, A	amplitudes of zero and first order Fourier series representation of response.
$B = \frac{C_1}{m\delta(\omega^*)^2}$	nondimensional gas film force constant of stiffness.
B	array of constants for pressure Eqs. (4.16).
B	width of Rayleigh step pad.
B_1, B_2	width of Rayleigh step pad with gas film.
$C = \frac{C_2\omega}{m\omega^*}$	nondimensional constant of gas film damping coefficient.
C	array of coefficients for pressure Eq. (4.16).
D	array of constants for pressure Eq. (4.23).
D_1, D_2	conventional constants in relations (3.30) and (3.40).
$E_n = \epsilon n/\delta$	nondimensional amplitude of Fourier series expansion of disturbance.
F, G	algebraic equations of A and A_o .
$H = h/\delta$	nondimensional gas film thickness.
$\dot{H} = \frac{dH}{dT}$	nondimensional velocity of gas film thickness.
$H_{s,i} = (H_i + H_{i-1})^3$	array of coefficients in (4.10).
I_1, I_4, I_5	nonlinear integrals in (3.26)(3.27) and (3.28) respectively.
$I = \int_0^1 P_R dX$	in phase gas film reaction of complex pressure profile.
N	number of grids in Chapter II.

$P = P/P_a$	nondimensional pressure of gas film.
P_o, P_c	zero and first order of P in (4.12).
P_I, P_R	imaginary and real part of P_c .
$Q = PH$	pressure field parameter in (2.27).
$Q = q/m\delta\omega^2$	nondimensional force excitation.
R	universal gas constant.
$R = r/r_o$	nondimensional radius.
R	residue in (3.13).
$R = \int_0^1 P_I dX$	out of phase gas film reaction of complex pressure profile.
S_1, S_2	parameters in (3.29).
$T, \tau = \omega t$	nondimensional time.
T	torque in Section 2.3.
$U = \omega r$	velocity of the driving surface.
$W_o = \frac{C_1}{H_o^{2.5}}$	load acted on the ring to get equilibrium at $H = H_o$.
$X = H_o - H$	coordinate and response of gas film in (3.2).
$X = x/B$	coordinate for infinite-width pad.
$X = [P_R, P_I]$	vector of unknown $P_{R,i}$ and $P_{I,i}$ in (4.23).
$a_o, b_o, c_o, d_o, e_o, f_o$	arrays of coefficients in pressure Eqs. (4.17).
$a_s, b_s, c_s, a_n, b_n, c_n,$ d, e, f	arrays of coefficients in pressure Eqs. (4.15).
c_1, c_2	constants in gas film force approximation (2.16).
$\epsilon = H - H_o$	disturbance of gas film thickness in (4.11).
h	gas film thickness.
j	imaginary number in (4.21).

$$k = \frac{5}{2} \frac{c_1}{H_0^{3.5}}$$

stiffness of gas film force.

m

mass of the ring in (3.1); mass of the pad per unit length in (4.26).

m_c

critical mass for stability in (4.29).

$n = 2\pi\omega$

number of revolution of the motor per second.

n_1, n_2

powers of H for gas film force in (2.16).

p

pressure of gas film.

p_a

ambient pressure of gas film

q_i

mass flow rate.

q

magnitude of excitational force.

r

radius

t

time

x

coordinate in the length of infinitely wide step pad.

Dimensions

ρ

FT^2L^{-4}

density of gas film

μ

FTL^{-2}

coefficient of viscosity

δ

L

step deepth.

$$\Lambda = \frac{6\mu L/B}{P_a \delta^2}$$

0

bearing number

$$\Delta = H_{i,i}^+ - H_{i,j}^-$$

0

stepped discontinuity at (i,j) grid point.

θ

θ

angular position

θ_G

θ

angle of ground area of step pad.

θ_L

θ

angle of landing area of step pad.

ω	θT^{-1}	rotational velocity.
ω_f	θT^{-1}	frequency of excitational force.
$\omega^* = \sqrt{\frac{k}{m}}$	θT^{-1}	natural frequency based on the linearization of Eq. (3.1).
$\bar{\omega} = \frac{\omega_f}{\omega^*}$	0	Normalized facing frequency.
ϵ_n	L	magnitude n-th order excitation.
α		phase difference between the response and the excitation.
Δ	0	determinent defined in (3.35).
ν	θT^{-1}	threshold frequency.
$\sigma = \frac{12\nu B^2}{\delta^2 P_a}$	0	squeeze number in (4.9).

LIST OF TABLES

	Page
1. Gas Film Forces (lb_f)	48
2. Load (lb_f) Calculated And Error Occurred (%)	49
3. Dynamic Bearing Reaction For $B_1/B = 0.75$, $H_2 = 0.5$	50
4. Dynamic Bearing Reaction For $B_1/B = 0.75$, $H_2 = 0.75$	51
5. Dynamic Bearing Reaction For $B_1/B = 0.5$, $H_2 = 0.5$	52

LIST OF FIGURES

		Page
Figure 1	The Geometry Of A Shrouded, Rayleigh-Step Thrust Bearing.	53
Figure 2	Flow Balance Around A Typical Grid Point.	54
Figure 3	Pressure Distribution For $h = -1$. in/sec., $H_{\min} = 0.5$	55
Figure 4	Pressure Distribution For $h = 1$. in/sec., $H_{\min} = 0.5$	56
Figure 5	Pressure Distribution For $h = -1$. in/sec., $H_{\min} = 1$	57
Figure 6	Pressure Distribution For $h = 1$. in/sec., $H_{\min} = 1$	58
Figure 7	Contour Map For Pressure Distributions For $h = -1$ in/sec., $H_{\min} = 0.5$	59
Figure 8	Variation Of Static, Gas Film Force ($H = 0$) With The Normalized Film Thickness.	60
Figure 9	Variation of $\frac{\partial F}{\partial h}$ With The Normalized Film Thickness	61
Figure 10	Simplified Seal Ring-Rotor System	62
Figure 11	Nonlinear Response For $H_o = 0.5$, $m = 0.2$ Slug.	63
Figure 12	Nonlinear Response For $H_o = 0.5$, $m = 1$ Slug.	64
Figure 13	Nonlinear Response For $H_o = 0.75$, $m = 0.2$ Slug.	65
Figure 14	Nonlinear Response For $H_o = 0.75$, $m = 1$ Slug.	66
Figure 15	Nonlinear Response For $H_o = 0.5$, $m = 0.2$ Slug, $C = 1.52 \frac{\text{lb}_f}{\text{in/sec}}$	67
Figure 16	Nonlinear Response For $H_o = 0.5$, $m = 0.2$ Slug, $C = 0.38 \frac{\text{lb}_f}{\text{in/sec}}$	68
Figure 17	Comparison Of The Approximate And Exact Upward Amplitudes Of Response	69

Figure 18	Comparison Of The Approximate And Exact Downward Amplitudes Of Response	70
Figure 19	Phase Plot With Second Harmonics.	71
Figure 20	Phase Plot With Third Harmonics	72
Figure 21	Phase Plot With Fourth Harmonics.	73
Figure 22	Phase Plot With Second Order Subharmonics	74
Figure 23	Phase Plot With Limiting Cycle Of Large Amplitude	75
Figure 24	Phase Plot With Limiting Cycle Of Small Amplitude	76
Figure 25	Phase Plot At Natural Frequency	77
Figure 26	Flow Balance And Geometry Of A Infinitely Wide Rayleigh Step-Pad.	78
Figure 27	Pressure Profile For $B_1/B = 0.5$, $H_2 = 0.5$	79
Figure 28	Real Pressure Profile For $\Lambda = 42$, $H_2 = 0.5$, $B_1/B = 0.75$	80
Figure 29	Imaginary Pressure Profile For $\Lambda = 42$, $H_2 = 0.5$, $B_1/B = 0.75$	81
Figure 30	Real Pressure Profile For $\Lambda = 100$, $H_2 = 0.5$, $B_1/B = 0.75$	82
Figure 31	Imaginary Pressure Profile For $\Lambda = 100$, $H_2 = 0.5$, $B_1/B = 0.75$	83
Figure 32	Real Pressure Profile For $\Lambda = 8.4$, $H_2 = 0.5$, $B_1/B = 0.5$	84
Figure 33	Imaginary Pressure Profile For $\Lambda = 8.4$, $H_2 = 0.5$, $B_1/B = 0.5$	85
Figure 34	Real Pressure Profile For $\Lambda = 42$, $H_2 = 0.5$, $B_1/B = 0.5$	86
Figure 35	Imaginary Pressure Profile For $\Lambda = 42$, $H_2 = 0.5$, $B_1/B = 0.5$	87
Figure 36	Variation Of Dynamic Bearing Forces With The Excitation Frequency, σ , For $B_1/B = 0.75$, $\Lambda = 42$, $H_2 = 0.5$	88

TABLE OF CONTENTS

	Page
ABSTRACT.	i
ACKNOWLEDGMENTS	ii
NOMENCLATURE.	iii
LIST OF TABLES.	vii
LIST OF FIGURES	viii
CHAPTER I - INTRODUCTION	
1.1 Introduction.	1
1.2 Historical Survey	2
CHAPTER II - GAS FILM FORCES	
2.1 Statement Of The Problem.	5
2.2 Pressure Equation	6
2.3 Method Of Solution.	9
2.4 Approximation For Gas Film Forces	13
CHAPTER III - NONLINEAR AXIAL RESPONSE	
3.1 Mathematical Modeling	14
3.2 Equation Of Motion.	15
3.2.1 Force-Excited Motion	15
3.2.2 Displacement-Excited Motion.	16
3.3 Linearized Solution	17
3.4 Nonlinear Solution.	18
3.4.1 Method of Galerkin	18
3.4.2 Direct Integration	25
3.5 Results of Nonlinear Response	26
3.5.1 Results By Method of Galerkin.	26
3.5.2 Results By Direct Integration.	30

CHAPTER IV - STABILITY OF AN INFINITELY-WIDE RAYLEIGH-STEP PAD	
4.1 Statement Of The Problem.	31
4.2 Governing Equations	32
4.3 Method Of Solution.	32
4.4 Stability Criterion	40
4.5 Results	42
CHAPTER V - SUMMARY OF RESULTS.	44
REFERENCES.	46
TABLES.	48
FIGURES	53
APPENDIX A - PROGRAM RSEAL.	89
APPENDIX B - PROGRAM RSGALN	103
APPENDIX C - PROGRAM RSRKIT	113
APPENDIX D - PROGRAM RSTAB.	118
VITA.	131

I. INTRODUCTION

1.1 Introduction

Among many geometrical profiles which generate hydrodynamic pressure in fluid-film bearings, the step geometry is one of the most proficient methods to achieve this purpose. This discovery was first made by Lord Rayleigh in 1918 (Ref. 1), and subsequently there have been many contributions (Refs. 2 to 8) on the prediction of the performance of the Rayleigh-step thrust as well as journal bearings.

Recently, there has been another significant application of the Rayleigh-step bearing in the field of dynamic sealing in advanced air-breathing propulsion systems (Ref. 9). In this application, a series of Rayleigh-step pads is employed on the high-pressure side of a face seal in order to maintain a small steady gap (in the order of 0.001") between a one-tooth labyrinth and the high-speed rotor surface (Fig. 1). The flat step is shrouded in order to minimize the side leakage. These pads function strictly as hydrodynamic thrust bearings operate in the high-ambient pressure, and provide the necessary stiffness to maintain a steady gap. The satisfactory operation of this type of seals depends critically on the dynamic performance of these thrust pads in the presence of an oscillatory force or a disturbance due to rotor run-out or rotor unevenness.

So far, the investigations on shrouded, Rayleigh-step bearings have been restricted to the prediction of the static performance (Ref. 10) only. The dynamic characteristics of this type of thrust-pads have not been given much attention. It is the main objective of this report to study the influence of the nonlinear, gas-film, restoring and damping forces upon the response of the pad to a given forcing function or disturbance.

Specifically, the work reported herein fulfills the following objectives:

1. To develop a gas-film analysis of purely hydrodynamic, Rayleigh-Step pad to calculate the quasistatic stiffness and damping, which depend not only on the operating conditions but also on the vibration of the system.
2. To extend the analysis to the nonlinear axial response of the stationary ring due to any external force excitation or any disturbances induced by the rotor misalignment or surface waviness.
3. To develop a stability analysis of the infinitely wide, single-step pad to explore whether there exists any thresholds of stability for the system.

1.2 Historical Survey

In 1918, after Reynolds' theory of thick film lubrication became generally accepted, Lord Rayleigh (Ref. 1) first applied the theory and discovered that an optimum profile for the load capacity of a slider bearing is a flat step. The method of the calculus of variations was used to optimize the shape of slider bearing to an infinitely long, incompressible film. From then on, any hydrodynamic bearings composing of two sections of parallel surface film are called Rayleigh-step bearings.

The optimized geometry of a Rayleigh-step slider and its corresponding optimized, non-dimensional, load capacity for an incompressible film can be found in most textbooks on lubrication (Ref. 11). For compressible gas film, the optimized, one-dimensional, Rayleigh-step bearing was analyzed by Wylie and Maday in 1970 (Ref. 2). The load capacity of an optimized step

bearing was found to be slightly lower at low bearing number but much higher at higher bearing number than the load capacity of an incompressible, optimized, slider bearing.

The problem of a two-dimensional, Rayleigh-step, thrust bearing has not received much attention until 1954, C. F. Kettleborough (Ref. 3) solved the pressure profile and calculated the load capacity for the step thrust bearing by Relaxation methods. In 1955 (Ref. 17) he applied the analogy method contributed by A. Kingsbury (Ref. 12) to investigate the pressure profile for an oil-lubricated step bearing by an electrolytic tank.

In 1959, using air as the lubricant, K. C. Kochi (Ref. 6) showed the characteristics of an infinitely-wide, Rayleigh-step, thrust pad by the use of semi-graphical method. He demonstrated that an analytical solution to express the pressure profile explicitly is extremely difficult, because the Reynolds equation for a compressible film is nonlinear.

In 1961, J. S. Ausmann (Ref. 7) made certain approximations to linearize the Reynolds equation for a compressible film, and obtained a series solution of the pressure and load for a self-acting, stepped, sector, thrust bearing by the aid of Neumann polynomial. He obtained the numerical solutions for the optimized number of sectors and step depth for the maximum load carrying capacity.

Recently, Cheng, Chow and Wilcock (Ref. 8) presented some results for shrouded, Rayleigh-step pad used as a flexible face seal. The pressure generation and static stability of this type of surface profiles using as a flexible seal ring was discussed, and the effectiveness of hydrodynamic action was confined to the static stiffness characteristics of gas film. The influence of the nonlinear gas-film forces and the question of gas-film stability of the hydrodynamic, Rayleigh-step pad

has not been investigated. Therefore, to ensure a safe operation of Rayleigh-step, thrust pads, it is necessary to conduct a full-scale nonlinear study, which is the major objective of this work.

II. GAS FILM FORCES

2.1 Statement of the Problem

The major concern in this section is the determination of the time-dependent, pressure distribution within the gas film between two annular surfaces containing a series of Rayleigh-step pockets as shown in Fig. 1. This problem is formulated within the framework of the conventional theory of lubrication for a compressible lubricant.

The major assumptions commonly used for gas-lubrication theories are:

1. The pressure across the film is constant
2. The flow is laminar
3. Inertia forces are neglected
4. The film is isothermal
5. The flow is Newtonian.

Under these assumptions, the governing equation for a transient, continuous, pressure field becomes the well-known, transient, Reynolds equation for a compressible fluid. Various analytical and numerical methods for the solution to this equation have been outlined by Castelli and Peviric (Ref. 13). For the present problem, the abrupt geometry introduced by the Rayleigh pocket makes it rather difficult to solve the pressure equation by any analytical methods. For this reason, a numerical method is employed in solving the discretized pressure field based on the solution of a system, non-linear algebraic equations by the Newton-Raphson procedure. The numerical integration of the discretized pressure field gives rise to the time-dependent gas-film forces which are required for investigating the nonlinear response of this type gas-film to a prescribed forcing function or disturbance function.

2.2 Pressure Equation

The discretized pressure equation is derived by considering a flow balance within an element of the gas film as shown in Fig. 2. The mass flow rate into the left boundary, AD, and the bottom boundary, AB, are designated as q_1 and q_2 . The mass flow rates out of the boundaries, DC and BC are, likewise, designated as q_3 and q_4 . In addition, there are mass stored in the volume which is designated as q_5 .

Based on the assumption in 2.1, the velocity is parabolic across the film. Integrating the velocity across the film, one may express the mass flow rate in terms of the boundary velocities and the pressure gradients. These can be written as

$$q_1 = \left[\rho \frac{urh}{2} - \frac{\rho h^3}{12\mu r} \frac{\partial p}{\partial \theta} \right]_{j-\frac{1}{2}, i} \left(\frac{r_{i+1} - r_{i-1}}{2} \right) \quad (2.1)$$

$$q_2 = \left[\rho \frac{U_r h}{2} - \frac{\rho h^3}{12\mu} \frac{\partial p}{\partial r} \right]_{i-\frac{1}{2}, j} \left(\frac{\theta_{i+1} - \theta_{i-1}}{2} \right) r_{i-\frac{1}{2}} \quad (2.2)$$

$$q_3 = \left[\rho \frac{urh}{2} - \frac{\rho h^3}{12\mu r} \frac{\partial p}{\partial \theta} \right]_{j+\frac{1}{2}, i} \left(\frac{r_{i+1} - r_{i-1}}{2} \right) \quad (2.3)$$

$$q_4 = \left[\rho \frac{U_r h}{2} - \frac{\rho h^3}{12\mu} \frac{\partial p}{\partial r} \right]_{i+\frac{1}{2}, j} \left(\frac{\theta_{i+1} - \theta_{i-1}}{2} \right) r_{i+\frac{1}{2}} \quad (2.4)$$

$$q_5 = \frac{\partial(\rho h)}{\partial t} \left(\frac{r_{i+1} - r_{i-1}}{2} \right) r_i \left(\frac{\theta_{i+1} - \theta_{i-1}}{2} \right) \quad (2.5)$$

The flow balance requires

$$q_1 + q_2 = q_3 + q_4 + q_5 \quad (2.6)$$

Introducing the following nondimensional variables:

$$P = \frac{p}{p_a}, \quad H = \frac{h}{\delta}, \quad R = \frac{r}{r_o}, \quad \tau = \omega t, \quad Q = PH, \quad \text{and} \quad \Lambda = \frac{6\mu\omega r_o^2}{p_a \delta^2}$$

and using the equation of state $\rho = \frac{p}{RT}$, Equation (2.6) becomes

$$\begin{aligned} & \left[\left(\Lambda R H \frac{Q}{\sqrt{Q}} - \frac{H^3}{2R} \frac{\partial Q}{\partial \theta} \right)_{i,j-\frac{1}{2}} - \left(\Lambda R H \frac{Q}{\sqrt{Q}} - \frac{H^3}{2R} \frac{\partial Q}{\partial \theta} \right)_{i,j+\frac{1}{2}} \right] \left(\frac{R_{i+1} - R_{i-1}}{2} \right) \\ & + \left[\left(-\frac{H^3}{2} \frac{\partial Q}{\partial R} \right)_{i-\frac{1}{2},j} R_{i-\frac{1}{2}} + \left(\frac{H^3}{2} \frac{\partial Q}{\partial R} \right)_{i+\frac{1}{2},j} R_{i+\frac{1}{2}} \right] \left(\frac{\theta_{j+1} - \theta_{j-1}}{2} \right) \\ & = \left[2\Lambda \left(\frac{\partial PH}{\partial \tau} \right)_{i,j} \left(\frac{R_{i+1} - R_{i-1}}{2} \right) R_i \left(\frac{\theta_{j+1} - \theta_{j-1}}{2} \right) \right] \end{aligned}$$

Further simplification leads to,

$$\begin{aligned} & \frac{1}{(\theta_{j+1} - \theta_{j-1})} \left[\left(\Lambda R H \frac{Q}{\sqrt{Q}} - \frac{H^3}{2R} \frac{\partial Q}{\partial \theta} \right)_{i,j-\frac{1}{2}} - \left(\Lambda R H \frac{Q}{\sqrt{Q}} - \frac{H^3}{2R} \frac{\partial Q}{\partial \theta} \right)_{i,j+\frac{1}{2}} \right] \\ & + \frac{1}{(R_{i+1} - R_{i-1})} \left[\left(-\frac{H^3}{2} \frac{\partial Q}{\partial R} \right)_{i-\frac{1}{2},j} R_{i-\frac{1}{2}} + \left(\frac{H^3}{2} \frac{\partial Q}{\partial R} \right)_{i+\frac{1}{2},j} R_{i+\frac{1}{2}} \right] \\ & = 2\Lambda \left(\frac{\partial PH}{\partial \tau} \right)_{i,j} R_i \end{aligned} \tag{2.7}$$

Introducing the following finite difference approximations:

$$\begin{aligned} \left(\frac{\partial Q}{\partial \theta} \right)_{i,j-\frac{1}{2}} &= (Q_j - Q_{j-1})_i / (\theta_j - \theta_{j-1})_i \\ \left(\frac{\partial Q}{\partial R} \right)_{i-\frac{1}{2},j} &= (Q_i - Q_{i-1})_j / (R_i - R_{i-1})_j \\ Q_{i,j-\frac{1}{2}} &= \frac{Q_{i,j} + Q_{i,j-1}}{2} \end{aligned} \tag{2.8}$$

one obtains a system of first order differential equations in time for the discretized pressures.

To obtain the exact, time-dependent, gas-film forces, it is necessary to solve this equation simultaneously with the equations of motion of the supported mass by an explicit or implicit, numerical procedure for the initial-valued problems. This procedure necessitates the calculation of the pressure field at each time interval during the transient, and it is extremely uneconomical and cumbersome.

In the case of a high, ambient pressure, the effect produced by the term containing $\frac{\partial P}{\partial \tau}$ becomes insignificant comparing to that by $\frac{\partial H}{\partial \tau}$, one may neglect the $\frac{\partial P}{\partial \tau}$ effect, and thus decoupled the gas-film force calculation from the dynamics of the supporting mass. Ignoring the contribution by $\frac{\partial P}{\partial \tau}$, the pressure distribution can be solved independently as a function of H and $\frac{\partial H}{\partial \tau}$ or \dot{H} . The assumption of a negligible $\frac{\partial P}{\partial \tau}$ effect is made in the subsequent analysis. Expanding the terms in Equation (2.7) by using relations (2.8) one obtains

$$\begin{aligned} a_3 Q_{i,j-1} + a_1 \sqrt{Q_{i,j-1}} + a_5 Q_{i-1,j} - (a_3 + a_4 + a_5 + a_6) Q_{i,j} + a_6 Q_{i+1,j} \\ + \left[\frac{a_1}{H_{i,j-1}} \Delta - a_6 \right] \sqrt{Q_{i,j}} + a_4 Q_{i,j+1} - a_2 \sqrt{Q_{i,j+1}} = 0 \end{aligned} \quad (2.9)$$

where $\Delta = H_{i,j}^+ - H_{i,j}^- = \begin{cases} 1 & \text{at the end of the pocket} \\ 0 & \text{otherwise} \end{cases}$

and

$$\begin{aligned}
 (a_1)_{i,j} &= \frac{\Lambda R_i}{2(\theta_{j+1} - \theta_{j-1})} (H^1)_{i,j-1} \\
 (a_2)_{i,j} &= \frac{\Lambda R_i}{2(\theta_{j+1} - \theta_{j-1})} (H^1)_{i,j+1} \\
 (a_3)_{i,j} &= \frac{1}{2R_i(\theta_{j+1} - \theta_{j-1})(\theta_j - \theta_{j-1})} (H^3)_{i,j-\frac{1}{2}} \\
 (a_4)_{i,j} &= \frac{1}{2R_i(\theta_{j+1} - \theta_{j-1})(\theta_{j+1} - \theta_j)} (H^3)_{i,j+\frac{1}{2}} \\
 (a_5)_{i,j} &= \frac{(R_i + R_{i-1})}{4(R_{i+1} - R_{i-1})(R_i - R_{i-1})} (H^3)_{i-\frac{1}{2},j} \\
 (a_6)_{i,j} &= \frac{(R_{i+1} + R_i)}{4(R_{i+1} - R_{i-1})(R_{i+1} - R_i)} (H^3)_{i+\frac{1}{2},j} \\
 (a_8)_{i,j} &= \Lambda R_i \dot{H}_i = \Lambda R_i \frac{\partial H}{\partial \tau}
 \end{aligned} \tag{2.10}$$

2.3 Method of Solution

The set of nonlinear, algebraic equations to be solved for the pressure field, $Q_{i,j}$, is

$$\begin{aligned}
 \bar{\Phi}_{i,j} &= a_3 Q_{i,j-1} + a_1 \sqrt{Q_{i,j-1}} + \\
 &+ a_5 Q_{i-1,j} - (a_3 + a_4 + a_5 + a_6) Q_{i,j} + \left[\frac{a_1}{H_{i,j-1}} \Delta - a_8 \right] \sqrt{Q_{i,j}} + \\
 &+ a_6 Q_{i+1,j} + a_4 Q_{i,j+1} - a_2 \sqrt{Q_{i,j+1}} = 0
 \end{aligned} \tag{2.9}$$

where $\bar{\Phi}_{i,j}$ is the implicit function for the node point (i,j) . Newton-Raphson method has been employed here to solve these equations.

Based on this method, $Q_{i,j}^n$ can be improved by calculating the difference $\Delta Q_{i,j}^n$ which is found from first order approximation of Taylor's expansion for $\Phi_{i,j}$. Using Taylor's expansion, eq. (2.9) becomes

$$\begin{aligned} \Phi_{i,j}^{n+1} = \Phi_{i,j}^n &+ \left(\frac{\partial \Phi_{i,j}}{\partial Q_{i,j-1}} \right) \Delta Q_{i,j-1}^n + \frac{\partial \Phi_{i,j}}{\partial Q_{i,j}} \Delta Q_{i,j}^n + \frac{\partial \Phi_{i,j}}{\partial Q_{i,j+1}} \Delta Q_{i,j+1}^n \\ &+ \left(\frac{\partial \Phi_{i,j}}{\partial Q_{i-1,j}} \right) \Delta Q_{i-1,j}^n + \left(\frac{\partial \Phi_{i,j}}{\partial Q_{i+1,j}} \right) \Delta Q_{i+1,j}^n + O(\epsilon^2) = 0 \quad \dots (2.11) \end{aligned}$$

From Equations (2.9) and (2.11), one obtains

$$\begin{aligned} -\Phi_{i,j}^n &= \left(a_3 + \frac{a_1}{\sqrt{Q_{i,j-1}^n}} \right) \Delta Q_{i,j-1}^n + a_5 \Delta Q_{i-1,j}^n \\ &+ \left\{ -(a_3 + a_4 + a_5 + a_6) + \left[\frac{a_1}{H_{i,j-1}} \Delta - a_8 \right] \frac{1}{\sqrt{Q_{i,j}^n}} \right\} \Delta Q_{i,j}^n \\ &+ a_6 \Delta Q_{i+1,j}^n + \left(a_4 - \frac{a_2}{2\sqrt{Q_{i,j+1}^n}} \right) \Delta Q_{i,j+1}^n \end{aligned} \quad (2.12)$$

Since $Q_{i,j}^n$ are known from the previous iteration, the set of linear simultaneous equations (2.12) are solved for the difference $\Delta Q_{i,j}$, by Gaussian Elimination Method.

The new iterated Q becomes,

$$Q_{i,j}^{n+1} = Q_{i,j}^n + \Delta Q_{i,j}$$

and the procedure is repeated until all $\Delta Q_{i,j}$ becomes less than a prescribed convergence error.

A computer-program RSS-FILM has been written to calculate $Q_{i,j}$, for a given nondimensional, gas-film thickness H and a nondimensional, velocity \dot{H} . The nondimensional, pressure distribution can be obtained by dividing Q by the nondimensional gas film thickness H . The horsepower required to overcome the friction resistance is calculated as

$$T = \int r \tau_s dA = \frac{\mu \omega r_o^3}{h} \int_{R_1}^{R_2} R^3 dR \int_0^{\theta_G + \theta_L} \frac{1}{H} d\theta \quad (2.13)$$

and

$$HP = \frac{n \times T \times N \times 60}{63000} \quad (2.14)$$

Also, the load perpad is obtained by the following integration

$$\begin{aligned} W &= p_a \int_A (P - 1) r d\theta dr \\ &= p_a r_o^2 \int_{R_i}^{R_o} R dR \int_0^{\theta_G + \theta_L} (P - 1) d\theta \end{aligned} \quad (2.15)$$

Figures 3, to 7 show the effects of change in H and \dot{H} on the pressure distributions in a shrouded, Rayleigh-step gas pad.

2.4 Approximation for Gas-Film Forces

The gas-film forces are shown to be dependent upon H , $\frac{\partial H}{\partial T}$, and the following operating and geometrical parameters

$$\Lambda = \frac{6\mu_{ax} \omega_o^2}{p_a \delta^2} = \text{Bearing Parameter}$$

$$\frac{\theta_L}{\theta_G + \theta_L} = \text{Step Length Parameter}$$

$$\frac{2B}{R_o - R_i} = \text{Shroud Width Parameter}$$

$$\frac{2\pi R_o}{N(R_o - R_i)} = \text{Length to Width Ratio}$$

Table 1 lists the gas-film forces for an annular bearing surface containing 20 Shrouded-Rayleigh-Step pads, with geometrical dimensions shown in Fig. 1. By plotting data on a log-log scale in Fig.8 & Fig.9 it is found that they can be fitted with the following function for a wide range of dimensionless thickness, H .

$$F = \frac{C_1}{H^{n_1}} - \frac{C_2}{H^{n_2}} \delta \omega \frac{dH}{dT} \quad (2.16)$$

Tables 2 list the approximate, gas-film force based on Eq. (2.16) and the actual values interpolated from Table 1. The errors introduced by using the fitted Equation (2.16) are also listed in these tables.

The values for C_1 , C_2 , n_1 , and n_2 for the gas-film forces listed in

Table 1 are found to be

$$C_1 = 2.32 \quad \text{lb}$$

$$C_2 = 0.76 \quad \text{lb}/(\text{in}/\text{sec})$$

$$n_1 = 2.5$$

$$n_2 = 2.5$$

The above constants, of course, only apply to the operating and geometrical parameters shown in Fig.1 . For other parameters, a different set of C_1 , C_2 , n_1 and n_2 will be required to approximate the gas-film forces.

Letting H_o be the equilibrium nondimensional gas film thickness, and defining x as the nondimensionalized displacement from H_o , positive for a decreasing of H , the gas film force can be alternatively expressed as,

$$F = \frac{C_1}{(H_o - X)^{n_1}} + \frac{C_2}{(H_o - X)^{n_2}} \omega \delta \frac{dX}{dT} \quad (2.17)$$

where $H = H_o - X$

and $\frac{dH}{dT} = - \frac{dX}{dT}$

III. NONLINEAR AXIAL RESPONSE

3.1 Mathematical Modeling

The main problem in this chapter is to determine the dynamic response of the stationary ring to any external force excitation or to any disturbances produced by the rotor misalignment and by the rotor surface waviness. Knowing the detailed motion of the stationary ring with respect to the rotor motion, one may calculate time-dependent gap distribution between the surfaces. In general, the dynamic response of the stationary ring is measured by the axial translation and by the rotations about two mutually perpendicular diameters of the ring. However, for a stationary ring with a narrow width and a large diameter, the response in the axial mode is very weakly coupled with the oscillation in the angular mode. Furthermore, the equation governing the angular oscillation is very nearly the same as that governing the axial motion. Thus, it is only necessary to concentrate the analysis on the non-linear characteristics of the motion in the axial mode. This reduces the problem from a complicated, three-degrees-of-freedom dynamical system to a single-degree-of-freedom problem for which a more thorough analysis can be afforded. The weak coupling between the axial and angular oscillation is demonstrated analytically in Reference 14.

Figure 10 shows the mathematical modelling of the non-linear vibration of the stationary ring in the axial direction. It consists of a stationary ring of mass m subjected to a steady load W_0 . The back face of the ring is flexibly mounted to the frame through a soft spring of stiffness K_s and the front face is supported on a very stiff, non-linear gas-film whose restoring force is represented by the power relations

formulated in Chapter 2, Eq. (2.17). The major problem here is to investigate the motion of the stationary ring for one of the two following conditions:

- a, a force excitation, $q \cos \omega_f t$, acting on the stationary ring.
- b, a prescribed rotor disturbance characterized by a Fourier series

$$\sum_{n=1}^N e_n \cos n\omega_f t .$$

3.2 Equation of Motion

3.2.1 Force-Excited Motion

The equation of motion due to a force excitation $q \cos \omega t$ is considered first. Recalling from Eq. (2.16), the force balance on the stationary ring gives the following equation,

$$m \frac{d^2 x}{dt^2} + \frac{C_1}{H^{2.5}} - \frac{C_2}{H^{2.5}} \frac{dh}{dt} - W_0 + k_s x = q \cos \omega_f t \quad (3.1)$$

where $k_s x$ is small comparing with W_0 and other terms.

Introducing the following nondimensional variables

$$X = x/\delta$$

$$T = \omega_f t$$

$$\omega = \frac{\omega_f}{\omega^*}$$

$$B = \frac{C_1}{m\delta(\omega^*)^2}$$

$$C = \frac{C_2 \bar{\omega}}{m \omega^*}$$

$$Q = \frac{q}{m \delta (\omega^*)^2}$$

where ω^* is the natural frequency of the system based on the linearized equation of Eq. (3.1). Equation (3.1) becomes

$$\begin{aligned} \bar{\omega}^2 \ddot{X} + C \dot{X} \frac{1}{(H_o - X)^{2.5}} + B \left[\frac{1}{(H_o - X)^{2.5}} - \frac{1}{H_o^{2.5}} \right] \\ = Q \cos T \end{aligned} \quad (3.2)$$

where

$$H = H_o - X$$

$$\omega_o = \frac{C_1}{H_o^{2.5}}$$

$$\cdot = \frac{d}{dT}$$

3.2.2 Displacement-Excited Motion

Consider now the disturbance function $\sum_{n=1}^N e_n \cos n \omega_f t$ resulted from the rotor misalignment, commonly known as the run out, and the non-flatness of the rotor-surface. The film thickness H will be perturbed by this disturbance, and becomes

$$H = H_o - X + \sum_{n=1}^N E_n \cos n T \quad (3.3)$$

where $E_n = e_n / \delta$.

The equation of motion in the absence of the excitation $q \cos \omega_f t$ becomes

$$m \frac{dx^2}{dt^2} + \frac{C_1}{H^{2.5}} - \frac{C_1}{H_0^{2.5}} - \frac{C_2}{H^{2.5}} \frac{dh}{dt} = 0 \quad (3.4)$$

Substituting Eq. (3.3) into (3.4) and letting $X' = X - \sum_{n=1}^N E_n \cos n T$, one obtains

$$\begin{aligned} & \omega^2 \ddot{X}' + C \dot{X}' \frac{1}{(H_0 - X')^{2.5}} + B \left[\frac{1}{(H_0 - X')^{2.5}} - \frac{1}{H_0^{2.5}} \right] \\ & = \sum_{n=1}^N Q'_n \cos n T \end{aligned} \quad (3.5)$$

where

$$Q'_n = n^2 \omega^2 E_n \quad (3.6)$$

Equation (3.5) is identical to (3.2) with the exception that X , and $Q \cos \omega t$ are replaced by X' and $\sum_{n=1}^N Q'_n \cos nT$ respectively. Thus, the solution for the force-excited oscillations is also applicable to the displacement-excited motion provided the proper substitutions are made for X' and Q'_n .

3.3 Linearized Solution

If the motion of the stationary ring is such that the resulting gap variation, $H - H_0$, is only a small fraction of the equilibrium film thickness H_0 , the response can be estimated from the solution of the linearized equation about the equilibrium film thickness H_0 . Linearizing Eq. (3.2) for the force-excited motion, one obtains

$$\frac{-2}{\omega} \ddot{X} + \frac{C}{H_o^{2.5}} \dot{X} + X = Q \cos T \quad (3.7)$$

Similarly, linearization of Eq. (3.4) for the displacement-induced motion leads to

$$\frac{-2}{\omega} \ddot{X} + \frac{C}{H_o^{2.5}} \dot{X} + X = \epsilon \cos T \quad (3.8)$$

Eqs. (3.7) and (3.8) are clearly the standard, damped vibration equation for a single mass, and its solution can be readily written as

$$A = \frac{Q}{\left[(1 - \frac{-2}{\omega})^2 + \frac{C^2}{H_o^5} \right]^{1/2}} \quad (3.9)$$

$$\alpha = \tan^{-1} \frac{(1 - \frac{-2}{\omega}) H_o^{2.5}}{C} \quad (3.10)$$

where $X = A \cos (T - \alpha)$

3.4 Non-Linear Solution

Two methods have been employed to obtain the non-linear response characterized by the solution to Eqs. (3.2). The first is the method of Galerkin. (Ref.18) which gives an approximate solution to the nonlinear equation. The degree of approximation is governed by the number of terms considered in the assumed function in the Galerkin procedure. The second method is the direct, step by step, numerical integration using a Runge-Kutta procedure. Details of these two methods are given next.

3.4.1 Method of Galerkin

The non-linear equation in question, Eq. (3.2), can be represented, implicitly as

$$f(\ddot{X}, \dot{X}, X, T) = 0$$

where

$$f = \ddot{X} + \frac{C\dot{X} + B}{(H_0 - X)^{2.5}} - \frac{B}{H_0^{2.5}} - Q \cos T = 0 \quad (3.11)$$

According to the method of Galerkin, one may assume that the unknown response $X(T)$ can be represented approximately by a truncated Fourier series,

$$X = \sum_{n=0}^N a_n \cos nT + b_n \sin nT \quad (3.12)$$

The substitution of (3.12) into the differential equation gives arise to the residue function,

$$R(T) = f(\ddot{X}, \dot{X}, X, T) \quad (3.13)$$

The $R(T)$ will not vanish unless $X(T)$ exactly satisfy the differential equation. The Galerkin method provides a set of equations by which one can solve for the constants a_n and b_n for which the residue function will be made extremely small. These conditions are obtained by requiring that the integration of the residue function as weighted by each individual Fourier component ($\cos nT$ or $\sin nT$) be made equal to zero. Stating mathematically, one obtains,

$$\int_0^{2\pi} R(T) \cos nT \, dT = 0 \quad (3.14)$$

$$\int_0^{2\pi} R(T) \sin nT \, dT = 0$$

for $n = 0, 1, 2, \dots, N$

where

$$\begin{aligned}
 R(T) = & \sum_{n=0}^N -\omega^2 n^2 (a_n \cos nT + b_n \sin nT) \\
 & + \frac{B + C \sum_{n=0}^N n(-a_n \sin nT + b_n \cos nT)}{\left[H_0 - \sum_{n=0}^N (a_n \cos nT + b_n \sin nT) \right]^{5/2}} - \frac{B}{H_0^{5/2}}
 \end{aligned} \tag{3.15}$$

$$- Q \cos T$$

For $N > 1$, integration of Equation (3.14) involves definite integrals of $-\frac{5}{2}$ th power of the Fourier series. A gallant attempt was made in reducing these integrals in some manageable form, but was unsuccessful. Thus, the inclusion of any terms beyond $N = 1$ was not made.

For $N = 1$,

$$X = a_0 + a_1 \cos T + b_1 \sin T \tag{3.16}$$

Further simplification is made by representing X with

$$X = A \cos (T - \alpha) - A_0 \tag{3.17}$$

where

$$A_0 = -a_0$$

$$A = (a_1^2 + b_1^2)^{1/2}$$

$$\alpha = \tan^{-1} \frac{b_1}{a_1}$$

Substituting (3.17) into (3.14), one obtains

$$\int_0^{2\pi} \left[-\omega^2 A \cos T + \frac{B - CA \sin T}{\left[H_0 + A_0 \right]^{2.5} \left[1 - \frac{A}{H_0 + A_0} \cos T \right]^{2.5}} \right. \\ \left. - Q(\cos \alpha \cos T - \sin \alpha \sin T) \right] \begin{Bmatrix} 1 \\ \sin T \\ \cos T \end{Bmatrix} dT = 0 \quad (3.18)$$

Integrating Eqs. (3.18) and noting the following relations:

$$\int_0^{2\pi} \begin{Bmatrix} \cos T \\ \sin T \\ \sin T \cos T \end{Bmatrix} dT = 0 \quad (3.19)$$

$$\int_0^{2\pi} \begin{Bmatrix} \cos^2 T \\ \sin^2 T \end{Bmatrix} dT = \pi \quad (3.20)$$

$$\int_0^{2\pi} \frac{\sin T \cos T}{\left(1 - \frac{A}{H_0 + A_0} \cos T \right)^{5/2}} dT = 0 \quad (3.21)$$

$$\int_0^{2\pi} \frac{\sin T}{\left(1 - \frac{A}{H_0 + A_0} \cos T \right)^{5/2}} dT = 0 \quad (3.22)$$

Equation (3.18) reduces to the following algebraic equations

$$- A \omega^2 + \frac{B}{\pi} I_1 - Q \cos \alpha = 0 \quad (3.23)$$

$$- \frac{CA}{\pi} I_4 + Q \sin \alpha = 0 \quad (3.24)$$

$$I_5 - 2\pi = 0 \quad (3.25)$$

where

$$I_1 = \frac{2}{D_1} \int_0^{\frac{\pi}{2}} S_1 \cos T \, dT \quad (3.26)$$

$$I_4 = \frac{2}{D_1} \int_0^{\frac{\pi}{2}} S_2 \sin^2 T \, dT \quad (3.27)$$

$$I_5 = \frac{2H_o^{2.5}}{D_1} \int_0^{\frac{\pi}{2}} S_2 dT \quad (3.28)$$

$$\begin{Bmatrix} S_1 \\ S_2 \end{Bmatrix} = \frac{1}{\left(1 - \frac{A}{H_o + A_o} \cos T\right)^{2.5}} \begin{Bmatrix} - \\ + \end{Bmatrix} \frac{1}{\left(1 + \frac{A}{H_o + A_o} \cos T\right)^{2.5}} \quad (3.29)$$

$$D_1 = (H_o + A_o)^{5/2} \quad (3.30)$$

Eliminating α from (3.23) and (3.24), one obtains a system of two non-linear equations to be solved for A and A_o . These two equations are

$$F(A, A_o) = \left(\frac{BI_1}{\pi} - A \omega^2\right)^2 + \left(\frac{CAI_4}{\pi}\right)^2 - Q^2 = 0 \quad (3.31)$$

$$G(A, A_o) = I_5 - 2\pi = 0 \quad (3.32)$$

Using Newton-Raphson procedure, the successive corrections ΔA , ΔA_o can be expressed in terms of F , G , $\frac{\partial F}{\partial A}$, $\frac{\partial F}{\partial A_o}$, $\frac{\partial G}{\partial A}$, and $\frac{\partial G}{\partial A_o}$, evaluated at the last iterates of A and A_o .

$$\Delta A = \frac{1}{\Delta} \begin{vmatrix} -F & \frac{\partial F}{\partial A_o} \\ -G & \frac{\partial G}{\partial A_o} \end{vmatrix} \quad (3.33)$$

$$\Delta A_o = \frac{1}{\Delta} \begin{vmatrix} \frac{\partial F}{\partial A} & -F \\ \frac{\partial G}{\partial A} & -G \end{vmatrix} \quad (3.34)$$

$$\text{where } \Delta = \begin{vmatrix} \frac{\partial F}{\partial A} & \frac{\partial F}{\partial A_o} \\ \frac{\partial G}{\partial A} & \frac{\partial G}{\partial A_o} \end{vmatrix} \quad (3.35)$$

$$\frac{\partial F}{\partial A} = 2 \left(\frac{BI_1}{\pi} - A \bar{\omega}^2 \right) \left(\frac{B}{\pi} \frac{\partial I_1}{\partial A} - \bar{\omega}^2 \right) + 2 \frac{C^2 AI_4}{\pi^2} \left(I_4 + A \frac{\partial I_4}{\partial A} \right) \quad (3.36)$$

$$\frac{\partial F}{\partial A_o} = 2 \left(\frac{BI_1}{\pi} - A \bar{\omega}^2 \right) \frac{B}{\pi} \frac{\partial I_1}{\partial A_o} + 2 \frac{C^2 A^2}{\pi^2} I_4 \frac{\partial I_4}{\partial A_o} \quad (3.37)$$

$$\frac{\partial G}{\partial A} = \frac{\partial I_5}{\partial A} \quad (3.38)$$

$$\frac{\partial G}{\partial A_o} = \frac{\partial I_5}{\partial A_o} \quad (3.39)$$

The differentials of nonlinear integrals can be derived from equations (3.36) - (3.28). They are

$$\frac{\partial I_1}{\partial A} = \frac{1}{D_2} \left\{ 5 \int_0^{\frac{\pi}{2}} \cos^2 T S_3 dT \right\} \quad (3.40)$$

$$\frac{\partial I_1}{\partial A_o} = \frac{-1}{D_2} \left\{ 5 \int_0^{\frac{\pi}{2}} \cos T S_4 dT \right\}$$

Equation (3.40) cont'd.

$$\frac{\partial I_4}{\partial A} = \frac{1}{D_2} \left\{ 5 \int_0^{\frac{\pi}{2}} \sin^2 T \cos T S_4 dT \right\}$$

$$\frac{\partial I_4}{\partial A_0} = \frac{-1}{D_2} \left\{ 5 \int_0^{\frac{\pi}{2}} \sin^2 T S_3 dT \right\}$$

$$\frac{\partial I_5}{\partial A} = \frac{H_0^{2.5}}{D_2} \left\{ 5 \int_0^{\frac{\pi}{2}} \cos T S_3 dT \right\}$$

$$\frac{\partial I_5}{\partial A_0} = - \frac{H_0^{2.5}}{D_2} \left\{ 5 \int_0^{\frac{\pi}{2}} S_4 dT \right\}$$

where $D_2 = (H_0 + A_0)^{3.5}$

and

$$\begin{Bmatrix} S_3 \\ S_4 \end{Bmatrix} = \frac{1}{\left(1 - \frac{A}{H_0 + A_0} \cos T\right)^{3.5}} \begin{Bmatrix} - \\ + \end{Bmatrix} \frac{1}{\left(1 + \frac{A}{H_0 + A_0} \cos T\right)^{3.5}}$$

Being provided with values of A, and A_0 , α can be solved from Equations

(3.23) and (3.24) as

$$\alpha = \tan^{-1} \frac{CAI_4}{BI_1 - \pi A \omega^2} \quad (3.41)$$

A computer program has been written to solve for A , A_0 and α , from which, X_{\max} and X_{\min} can be determined by

$$\begin{aligned} X_{\max} &= A - A_0 \\ X_{\min} &= -A - A_0 \end{aligned} \quad (3.42)$$

The integrals I_1 , I_4 , I_5 and their derivatives with respect to A and A_0 are evaluated numerically. Tables have been prepared for various values of $A/(H_0 + A_0)$ varying in the range, $[0,1]$ at intervals of 0.01.

3.4.2 Direct Integration

The step-by-step numerical integration of Eq. (3.2) is achieved by splitting it into two first order equations:

$$\dot{X} = Y$$

$$\dot{Y} = \frac{1}{\omega} \left[\frac{B}{H_0^{2.5}} - \frac{B + CY}{(H_0 - X)^{2.5}} + Q \cos T \right]$$

(Ref. 16)

The popular Runge-Kutta method _A has been employed in obtaining the solution for X and Y with a given set of initial conditions X_0 , Y_0 . The response is represented by the trajectories in the phase space plot (X,Y) . The response is considered to have reached a steady state if the trajectory approaches a limit cycle, which could be a single or multiple-looped cycle. A library subroutine at the Vogelback computer center has been used for this numerical integration. Fortran listings for the Computer program, RSGALN, which calculates A , A_0 , and α by the Galerkin method, and the computer program, RSRKIT, which calculates the trajectories in the phase space, are included in the Appendices and

3.5 Results of Non-Linear Response

The results of the nonlinear response are presented in two parts. The first part is obtained from the method of Galerkin one-term approximation, and the second part from the Runge-Kutta direct integration. Since the gas-film is an unsymmetrical spring, i.e., the relation between the displacement and restoring force is not symmetric with respect to the equilibrium position, the amplitude of response during an upstroke is different from that during a downstroke. During an upstroke, the gas film stiffness is softer, and the amplitude is greater than that during a downstroke when the gas-film is considerably stiffer. For this reason, the response in the upstroke and downstroke are plotted separately against the non-dimensional excitation frequency in Figs. 11 to 19 .

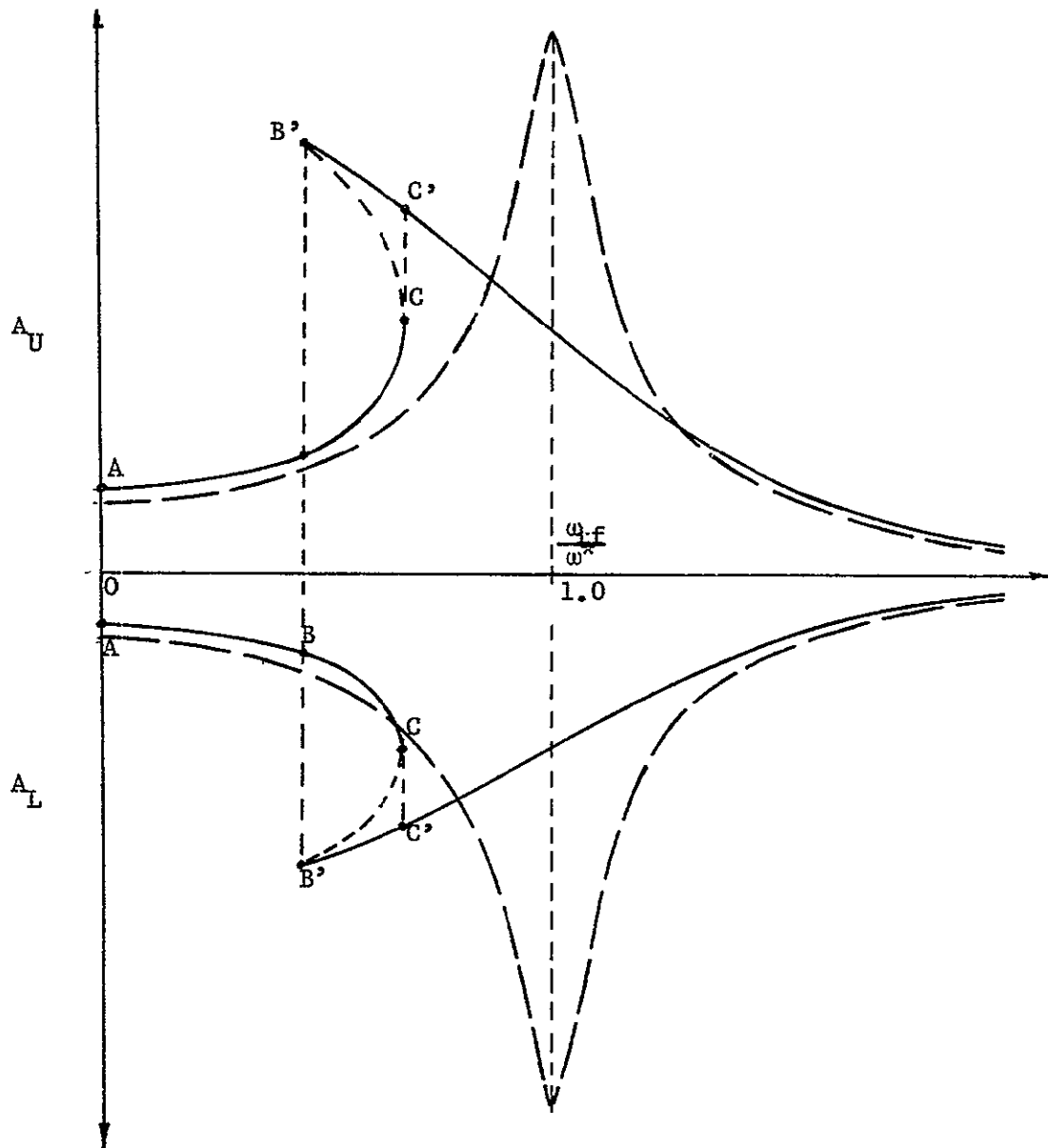
3.5.1 Results by Method of Galerkin

Referring to the equation of motion, Eq.(3.2', it is seen that the parameters affecting the dynamic response are:

$$\begin{aligned}
 B &= \text{stiffness parameter} &= \frac{C_1}{m\delta(\omega^*)^2} \\
 C &= \text{damping parameter} &= \frac{C_2\omega_f}{m\omega^*} \\
 H_o &= \text{static-film parameters} &= h_o/\delta \\
 Q &= \text{forcing intensity parameter} &= \frac{q}{m\delta(\omega^*)^2} \\
 \bar{\omega} &= \text{frequency parameter} &= \omega_f/\omega^*
 \end{aligned}$$

The general characteristics of the upper and lower amplitudes as

a function of excitation frequency are illustrated in the sketch below.



The nonlinear response based on one-term Galerkin method is shown as solid lines except with a small portion of the unstable oscillations, which are shown as dotted lines. The dashed lines show the response predicted from the linearized solution. In the region AB, the excitation frequency

is smaller than the natural frequency, ω^* , based on the linear theory, and the non-linear solution predicts a smaller lower amplitude but a greater upper amplitude comparing to the linear response. As ω_f increases to the region BC, the non-linear theory yields three possible solutions, one along the path BC, one along the path B'C, and another one along the path B'C'. The solution along BC is in-phase with the forcing function and is the most stable mode of response; the solution along B'C is unstable and only exists mathematically; and the solution along B'C' is out-of-phase with the excitation and is less stable than the solution along BC. For excitation frequency beyond the region BC, the characteristics of the non-linear response are similar to that of the linear response in the region where $\omega_f > \omega^*$. In this region, the pad is insensitive to the excitation and would not track any disturbance introduced by rotor runout or waviness.

The non-symmetrical nonlinear gas-film produces a response characteristics which resemble more to the response due to a symmetrical, soft, nonlinear spring, for which the resonance occurs at a frequency considerably lower than the natural frequency based on the linear theory. This correlation is really not surprising, since the mean position of the oscillation shifts to the region of softer stiffness, and the nonlinear oscillations are dominated by the softer part of the gas-film stiffness.

Fig. 11 shows typical response curves for the following dimensional parameters:

$$h_o = 0.0005 \quad \text{inches}$$

$$\delta = 0.001 \quad \text{inches}$$

$$m = 0.2 \quad \text{slug or } 6.44 \text{ lbm}$$

$$C_1 = 2.32 \quad \text{lb}$$

$$C_2 = 0.76 \quad \text{lb/(in/sec)}$$

$$q = 1, 2, \text{ and } 5 \text{ lb}$$

The corresponding non-dimensional parameters are listed in Fig. 11 . The inward bending of the resonant peak in the region $\bar{\omega} < 1$ is clearly visible in all three cases. Fig. 12 shows the effect of increasing the mass of the pad from 0.2 slug to 1.0 slug. The increase in mass does not alter the parameters, B , H_0 , and Q , since $(\omega^*)^2$ is inversely proportional to m . The only parameter affected by changing of m is the non-dimensional damping parameter. A five fold increase in mass is equivalent to a $\sqrt{5}$ times reduction in the effective damping factor C_2 . The more peaky response near the resonance is clearly visible in Fig. 12 when the mass is increased by five fold.

Figs. 13 and 14 shows the effect of increasing the equilibrium film thickness from 0.5 to 0.75. The natural frequency is reduced sharply by the increase in the film thickness, and the level of response is also much greater with a thick film than with a thin film for the same forcing function.

To investigate the effect of damping the value of C_2 has been doubled and halved from the case shown in Fig. 11 . The curves in Fig. 15 show that when the damping is doubled, the response near the resonance is considerably suppressed. The opposite effect is introduced if the damping is halved as shown in Fig. 16 .

3.5.2 Results by Direct Integration

Both the upper and lower amplitudes obtained by using the step-by-step, Runge-Kutta, direct integration are plotted against the excitation frequencies in Figs. 17 and 18 . A case of heavy mass, small equilibrium film thickness, and large excitation force has been selected to illustrate the nonlinear effects. The linear response curve and the approximate nonlinear response by Galerkin method are also plotted as dashed and dotted lines for comparison. It is seen that the agreement between the Runge-Kutta results and the Galerkin results is good near $\bar{\omega} = 1$. This clearly shows that even with one term approximation the Galerkin method yields a reasonably accurate prediction for the synchronous response. For $\bar{\omega} < 1$, the Runge-Kutta results show a series of superharmonic resonances at $\bar{\omega}$ approximately equal to 1/2, 1/3, 1/4, etc. The magnitude of these superharmonic amplitudes is, of course, governed by the damping factor.

Fig. 19 shows the trajectory in the phase-space plot for condition near the second superharmonic resonance. The final limit cycle forms a two-loop orbit showing typical characteristics of a superharmonic response. Other trajectories at the third and fourth superharmonic resonances are also shown in Figs. 20 to 22 . A subharmonic resonance is also found for $\bar{\omega} \sim 2.0$, but the amplitude is small and harmless. The Characteristics of the phase space trajectories near $\bar{\omega} = 1$ are plotted in Figs. 23 to 25.

IV. STABILITY OF AN INFINITELY-WIDE RAYLEIGH-STEP PAD

4.1 Statement of the Problem

It is well known in hydrodynamic lubrication that a dynamic system involving any fluid-film supports may, under certain conditions, encounter detrimental self-excited oscillations commonly known as dynamical instability of fluid-film bearings. The gas-film bearings are particularly susceptible to this type of instability. The fractional frequency whirl of a shaft supported on gas-bearings and the pneumatic hammer in externally pressurized gas-bearings are two of the prominent examples of the fluid-film instability. For journal bearings, the gas-film instability usually occurs if either the rotating frequency or the supported mass becomes large. There have been considerable data available to predict the threshold speed or critical mass of the journal bearing. However, for gas-lubricated thrust pads, the problem of instability is relatively unexplored. Since present trends in gas-bearing are always toward higher and higher speeds, it is important to determine whether there exists any stability threshold associated with a gas-lubricated thrust pad.

This chapter is devoted to the stability analysis of a thrust pad with a Rayleigh-step. The geometry of such a thrust pad is shown in Fig.26 . In order not to impose excessive burdens on the analysis, the assumption of an infinitely wide pad has been made. Moreover, the motion of the pad is assumed to be restricted in the transverse direction only. With these two assumptions, the problem is reduced to the stability of a single-degree-of-freedom dynamical system with restoring pressures governed by a partial differential equation in space and time.

4.2 Governing Equations

The one-dimensional, time-dependent pressure distribution is governed by the Reynolds equation,

$$\frac{\partial}{\partial x} \left(ph^3 \frac{\partial p}{\partial x} \right) = 6\mu u \frac{\partial(ph)}{\partial x} + 12\mu \frac{\partial(ph)}{\partial t} \quad (4.1)$$

where $h = \delta + h_o + e(t)$ for $0 < x < B_1$

$h = h_o + e(t)$ for $B_1 < x < B$

$e(t)$ is the upward motion of the pad.

The boundary conditions for Eq. (4.1) are

$$p = p_a \text{ at } x = 0 \text{ and } x = B \quad (4.2)$$

The equation governing the pad motion is,

$$m \frac{d^2 e}{dt^2} = \int_0^B (p - p_a) dx - W_o \quad (4.3)$$

where m is the mass per unit length of the pad, B the length of the pad, and W_o the static load imposed on the pad. The dynamic system represented by the coupled equations, (4.1) and (4.3) are to be investigated for the stability for an equilibrium position.

4.3 Method of Solution

The time-dependent, nonlinear, pressure equation, Eq. (4.1), is difficult to solve analytically. A numerical approach has been used here in solving a set of discretized, time-dependent, pressures along the coordinate X .

The discretization of pressure is achieved by considering the flow

balance in an elemental volume within the gas film as shown in Fig. 26 for the i -th element. The flow rates in and out the element are respectively q_1 and q_2 , and

$$\begin{aligned} q_1 &= \left(-\frac{\rho h^3}{12\mu} \frac{\partial p}{\partial x} + \frac{u_1 + u_2}{2} \rho h \right)_{i-\frac{1}{2}} \\ q_2 &= \left(-\frac{\rho h^3}{12\mu} \frac{\partial p}{\partial x} + \frac{u_1 + u_2}{2} \rho h \right)_{i+\frac{1}{2}} \end{aligned} \quad (4.4)$$

where $u_1 = u$ and $u_2 = 0$

Considering the flow balance,

$$q_1 - q_2 = \text{rate of mass stored within the elemental volume}$$

It follows,

$$\begin{aligned} & - \left(\frac{\rho h^3}{12\mu} \frac{\partial p}{\partial x} \right)_{i-\frac{1}{2}} + \left(\frac{\rho h^3}{12\mu} \frac{\partial p}{\partial x} \right)_{i+\frac{1}{2}} \\ & + \frac{u}{2} \left[(\rho h)_{i-\frac{1}{2}} - (\rho h)_{i+\frac{1}{2}} \right] \\ & = \frac{\partial}{\partial t} \left[\rho_i \left(h_{i-\frac{1}{2}} \frac{\Delta x_{i-1}}{2} + h_{i+\frac{1}{2}} \frac{\Delta x_i}{2} \right) \right] \end{aligned} \quad (4.5)$$

Using the isothermal relation,

$$\frac{p}{\rho} = R T_e = \text{constant} \quad (4.6)$$

Introducing the non-dimensional parameters,

$$\begin{aligned} P &= p/p_a \\ X &= x/B \end{aligned} \quad (4.7)$$

Equation (4.7) cont'd

$$H = \frac{h}{\delta} = \frac{h}{h_2 - h_1}$$

$$\Lambda = \frac{6\mu BU}{p_a \delta^2}$$

$$\sigma = \frac{12\mu \nu B^2}{p_a \delta^2}$$

$$T = \nu t$$

$$\nu = \text{excitation frequency}$$

and using the following finite approximations for $\left(\frac{\partial P}{\partial X}\right)_{i-\frac{1}{2}}$, $P_{i-\frac{1}{2}}$, $H_{i-\frac{1}{2}}$

$$\left(\frac{\partial P}{\partial X}\right)_{i-\frac{1}{2}} = \frac{P_i - P_{i-1}}{X_i - X_{i-1}} = \frac{P_i - P_{i-1}}{\Delta X_{i-1}}$$

$$P_{i-\frac{1}{2}} = \frac{1}{2} (P_i + P_{i-1}) \quad (4.8)$$

$$H_{i-\frac{1}{2}} = \frac{1}{2} (H_i + H_{i-1})$$

the discretized pressure equation becomes

$$\begin{aligned} & \frac{1}{4\Delta X_i} (P_{i+1}^2 - P_i^2) H_{s,i} - \frac{1}{4\Delta X_{i-1}} (P_i^2 - P_{i-1}^2) H_{s,i-1} \\ & - \Lambda (P_{i+1} + P_i)(H_{i+1} + H_i) + \Lambda (P_i + P_{i-1})(H_i + H_{i-1}) \\ & = \sigma \left\{ \frac{\partial}{\partial T} [P_i (H_i + H_{i-1})] \Delta X_{i-1} + \frac{\partial}{\partial T} [P_i (H_{i+1} + H_i)] \Delta X_i \right\} \end{aligned} \quad (4.9)$$

where

$$H_{s,i} = (H_{i+1} + H_i)^3 \quad (4.10)$$

where $A_i = a_{o,i} P_{i+1,o} + d_{o,i}$

$$B_i = b_{o,i} P_{i,o} + e_{o,i}$$

$$C_i = c_{o,i} P_{i-1,o} + f_{o,i}$$

$$a_{o,i} = \frac{H_{s,i}}{4\Delta X_i}, \quad d_{o,i} = -\Lambda(H_{i+1,o} + H_{i,o})$$

$$c_{o,i} = \frac{H_{s,i-1}}{4\Delta X_{i-1}}, \quad f_{o,i} = \Lambda(H_{i,o} + H_{i-1,o})$$

$$b_{o,i} = -a_{o,i} - c_{o,i}, \quad e_{o,i} = d_{o,i} + f_{o,i} \quad (4.17)$$

and

$$P_{1,o} = P_{n,o} = 1 \quad (4.18)$$

Since the algebraic equations (4.16) are nonlinear, Taylor's expansion is used to reach the following simultaneous equations for $\Delta P_{i,o}$,

$$\Delta \bar{\Phi}_i = -\bar{\Phi}_i(P_{i,o}) \quad (4.19)$$

where
$$\begin{aligned} \Delta \bar{\Phi}_i &= (A_i + a_{o,i} P_{i+1,o}) \Delta P_{i+1,o} \\ &+ (B_i + b_{o,i} P_{i,o}) \Delta P_{i,o} \\ &+ (C_i + c_{o,i} P_{i,o}) \Delta P_{i-1,o} \end{aligned}$$

Equations(4.19) are inverted directly for successive $\Delta P_{i,o}$ until the convergence is reached.

In equation (4.9), both the discretized pressure P_i and H_i are dependent on time. For transient studies, they have to be solved simultaneously with the dynamic equation of motion, Eq. (4.3). However, for small oscillations and stability analysis, the variation of H and P with time can be considered as small perturbations about the equilibrium solution, H_0 and P_0 . These small perturbed quantities can be expressed as

$$H_i(T, X) = H_{i,0}(X) + \epsilon(T) \quad (4.11)$$

$$P_i(T, X) = P_{i,0}(X) - \epsilon(T) P_{i,c}(X) \quad (4.12)$$

where $\epsilon = e/\delta$

$$\left| \frac{\epsilon}{H_i} \right| \ll 1$$

The minus sign in (4.12) is due to the fact that an increase in thickness leads to a decrease of pressure of the gas film. Substituting (4.11) and (4.12) into Equation (4.9), the equilibrium equation and the first order, perturbed equations can be obtained. They are

$$\begin{aligned} & \frac{1}{4\Delta X_i} (P_{i+1,0}^2 - P_{i,0}^2) H_{s,i} - \frac{1}{4\Delta X_{i-1}} (P_{i,0}^2 - P_{i-1,0}^2) H_{s,i-1} \\ & - \Lambda (P_{i+1,0} + P_{i,0}) (H_{i+1,0} + H_{i,0}) + \Lambda (P_{i,0} + P_{i-1,0}) (H_{i,0} + H_{i-1,0}) \\ & = 0 \end{aligned} \quad (4.13)$$

and

$$\begin{aligned} & (P_{i+1,0} a_{s,i} + a_{n,i}) P_{i+1,c} + (P_{i,0} b_{s,i} + b_{n,i}) P_{i,c} \\ & + (P_{i-1,0} c_{s,i} + c_{n,i}) - d_i \\ & = \frac{1}{\epsilon} \frac{\partial \epsilon}{\partial T} [P_{i,0} f_i + e_i P_{i,c}] \end{aligned} \quad (4.14)$$

where

$$\begin{aligned}
 a_{s,i} &= \frac{H_{s,i}}{8\Delta X_i} \quad , \quad a_{n,i} = -\frac{\Lambda}{4} (H_{i+1,o} + H_{i,o}) \\
 c_{s,i} &= -\frac{H_{s,i-1}}{8\Delta X_{i-1}} \quad , \quad c_{n,i} = \frac{\Lambda}{4} (H_{i,o} + H_{i-1,o}) \\
 b_{s,i} &= -a_{s,i} - c_{s,i} \quad , \quad b_{n,i} = a_{n,i} + c_{n,i} \\
 d_i &= \frac{1}{4\Delta X_i} (P_{i+1,o}^2 - P_{i,o}^2) (H_{i+1,o}^2 + H_{i+1,o}H_{i,o} + H_{i,o}^2) \\
 &\quad - \frac{1}{4\Delta X_{i-1}} (P_{i,o}^2 - P_{i-1,o}^2) (H_{i,o}^2 + H_{i,o}H_{i-1,o} + H_{i-1,o}^2) \\
 &\quad - \frac{\Lambda}{2} (P_{i+1,o} - P_{i,o}) \\
 e_i &= \frac{\sigma}{4} [(H_{i+1,o} + H_{i,o})\Delta X_i + (H_{i,o} + H_{i-1,o})\Delta X_{i-1}] \\
 f_i &= -\frac{\sigma}{2} (\Delta X_{i-1} + \Delta X_i)
 \end{aligned} \tag{4.15}$$

Equations (4.13) are nonlinear simultaneous algebraic equations for the pressure distribution $P_{i,o}$. They are solved numerically by Newton-Raphson method. The boundary conditions are $P_o(1,n) = 1$.

Rewrite equation (4.13) as

$$\Phi_i(P_{i,o}) = A_i P_{i+1,o} + B_i P_{i,o} + C_i P_{i-1,o} = 0 \tag{4.16}$$

for $i = 2, \dots, n-1$.

After the equilibrium pressure distribution is found, Equations (4.14) are solved for the first order pressure distribution, $P_{i,c}$. In Equations (4.14), both $P_{i,c}$ and $\epsilon(T)$ are complex quantities, and they are assumed to be

$$P_{i,c} = P_{i,R} + jP_{i,I} \quad (4.20)$$

and

$$\epsilon = \epsilon_o e^{jT} \quad (4.21)$$

The boundary conditions are $P_{i,c} = 0$ at entrance and exit, which gives

$$P_{1,R} = P_{n,R} = P_{1,I} = P_{n,I} = 0 \quad (4.22)$$

Substituting Eqs. (4.20) and (4.21) into Eq. (4.14), one obtains a system of $2n - 4$ simultaneous, linear equations,

$$A_{i+1,i} X_{i+1} + A_{i,i} X_i + A_{i-1,i} X_{i-1} + A_{i+n-2,i} X_{i+n-2} = D_i \quad (4.23)$$

for $i = 1, \dots, n-2$

$$A_{i-n+2,i} X_{i-n+2} + A_{i+1,i} X_{i+1} + A_{i,i} X_i + A_{i-1,i} X_{i-1} = D_i$$

for $i = n-1, \dots, 2n-4$

In the above, A and X for $i = 1, \dots, n-2$ are defined by,

$j = i+1$

$$\begin{aligned} A_{i+1,i} &= P_{j+1,o} a_{s,j} + a_{n,j} & , & & X_{i+1} &= P_{i+2,R} \\ A_{i,i} &= P_{j,o} b_{s,j} + b_{n,j} & , & & X_i &= P_{i+1,R} \\ A_{i-1,i} &= P_{j-1,o} c_{s,j} + c_{n,j} & , & & X_{i-1} &= P_{i,R} \\ A_{i+n-2,i} &= e_j & , & & X_{i+n-2} &= P_{i+1,I} \\ D_i &= d_j \end{aligned} \quad (4.24)$$

and for $i = n - 1, \dots, 2n - 4$, they are defined by,

$$j = i - n + 3$$

$$\begin{aligned} A_{i+1,i} &= P_{j+1,o} a_{s,j} + a_{n,j} & , & & X_{i+1} &= P_{i-n+4,I} \\ A_{i,i} &= P_{j,o} b_{s,j} + b_{n,j} & , & & X_i &= P_{i-n+3,I} \\ A_{i-1,i} &= P_{j-1,o} c_{s,j} + c_{n,j} & , & & X_{i-1} &= P_{i-n+2,I} \\ A_{i-n+2,i} &= -e_j & , & & X_{i-n+2} &= P_{i-n+3,R} \\ D_i &= f_j P_{j,o} \end{aligned} \quad (4.25)$$

The boundary conditions become

$$\begin{aligned} X_o &= P_{1,R} = 0 & \text{for equations with } i = 1, \\ & & n - 2, \text{ respectively} \\ X_{n-1} &= P_{n,R} = 0 \end{aligned} \quad (4.26)$$

and

$$\begin{aligned} X_{n-2} &= P_{1,I} = 0 & \text{for equations with } i = n - 1, \\ & & 2n - 4 \text{ respectively} \\ X_{2n-3} &= P_{n,I} = 0 \end{aligned} \quad (4.27)$$

These simultaneous equations (4.23) can now be solved for $[X]$ vector by direct matrix inversion. A computer program has been written to solve for $P_{i,o}$ and $P_{i,c}$ for different real values of ν , and the Fortran listing of this program is included in Appendix D.

Once the real and imaginary part of the gas film pressure are determined, the integration of $P_{i,R}$ and $P_{i,I}$ gives respectively the in-phase and

out-of-phase bearing forces. The in-phase force $\int_0^1 P_R dX$, can be interpreted as the stiffness of the film, whereas the out-of-phase, $\int_0^1 P_I dX$, represents the damping factor of the film. It should be emphasized that both the in-phase and out-of-phase perturbed pressure are dependent upon σ , or the excitation frequency ν of the mass. The frequency-dependent characteristics of the gas-film reactions is a direct consequence of the inclusion of the term $\frac{\partial P}{\partial T}$. The use of these frequency-dependent bearing forces in determining the dynamic stability of the gas-film and pad system is described in the next section.

4.4 Stability Criterion

The stability of the gas-film and pad is governed by the equation of motion, Eq. (4.3), which, in its non-dimensional form, appears as

$$\frac{d^2 \epsilon}{dT^2} = \frac{p_a^B}{m\delta\nu^2} \int_0^1 (P - 1) dX - \frac{W_o}{m\delta\nu^2} \quad (4.28)$$

Recalling the pressure is the summation of the equilibrium pressure, P_o , and the dynamic pressure, $- \epsilon P_c$, one obtains

$$\frac{p_a^B}{m\delta\nu^2} \int_0^1 (P - 1) dX - \frac{W_o}{m\delta\nu^2} = - \frac{p_a^B}{m\delta\nu^2} \epsilon \int_0^1 P_c dX \quad (4.29)$$

It follows that

$$\left(\frac{m\delta\nu^2}{p_a^B} \right) \frac{d^2 \epsilon}{dT^2} + \epsilon \int_0^1 P_c dX = 0 \quad (4.30)$$

Mathematically, Eq. (4.30) represents a free oscillation problem which contains stiffness and damping factors depending upon the frequency of the oscillations. A direct approach in determining of the stability of this

single-degree of freedom problem is to look for the eigenvalue of this system. If the real part of the eigenvalue is negative, the system is stable; otherwise it is unstable. If the eigenvalue is purely imaginary, then the system is at its threshold of instability.

Alternatively, one can also determine the stability thresholds by assuming that the eigenvalue is a purely imaginary number and inquire what would be the mass parameter, $\frac{m\delta v^2}{p_a^B}$, for a purely imaginary eigenvalue.

Let the eigenvalue be represented by $\lambda + jv$, and for a pure imaginary eigenvalue, $\lambda = 0$. It follows that

$$\epsilon = \epsilon_o e^{jvt} = \epsilon_o e^{jT} \quad (4.31)$$

Substituting Eq. (4.27) into Eq. (4.26), and separating the real from the imaginary part, one obtains

$$\int_0^1 P_I(v) dX = 0 \quad (4.32)$$

$$\int_0^1 P_R(v) dX - \frac{m\delta v^2}{p_a^B} = 0 \quad (4.33)$$

where $P_I(v)$ and $P_R(v)$ are solutions of Equations (4.23) for a given value of v . The pure imaginary eigenvalue v may be determined by evaluating the integral, $\int_0^1 P_I(v) dX$, for various values of v until the integral changes its sign. The exact eigen frequency v may be calculated by a linear interpolation. Once the eigen frequency is found, the critical mass at the threshold of instability can be determined by Eq. (4.28), and

$$m_{cr} = \frac{p_a^B}{\delta v^2} \int_0^1 P_R(v) dX \quad (4.34)$$

Equation (4.29) predicts a quantitative value of the critical mass, but does not furnish any information on which side the stable region lies. To determine the region of stability, one may use the criterion developed by Malanowski and Pan (ref. 17). Their criterion can be stated in the following manner.

Stability Criterion - The system consisting of a thrust bearing of mass, m , with Rayleigh Shrouded-Step Seal is in a state of self-sustained oscillation at frequency ω_0 when and only when the out-of-phase component of the bearing reaction, $\int_0^1 P_I(\omega) dX$, vanishes, and when the mass, m_0 has the critical magnitude to be in resonance with the in-phase bearing reaction, Equation (4.28). The system will become unstable if the mass exceeds the critical value provided the out-of-phase bearing reaction increases with the frequency in the algebraic sense in the neighborhood of the critical frequency ω_0 , and conversely.

4.5 Results

The steady state pressure distribution, P_0 , has been calculated numerically for the following parameters:

$$B_{1/B} = 0.5, \text{ and } 0.75$$

$$H = \frac{h}{\delta} = 0.5 \text{ and } 0.75$$

$$\Lambda = \frac{6\mu b U}{P_a \delta^2} = 8.4, 42, \text{ and } 100$$

The resulting pressure curves are plotted in Fig. 27, and they are in excellent agreement with the analytical solution provided by Kochi (Ref. 6). This comparison confirms the accuracy of the present numerical solution of the steady state pressure distribution, P_0 .

For each steady-state pressure distribution, the dynamic pressure distributions, P_R and P_I are calculated for a series value of σ . Figs. 28 to 35 show a typical series of the dynamic pressure profiles for $B_1/B = 0.5$ and 0.75 , $H = 0.5$, and $\Lambda = 42$. For small excitation frequencies, the real part of the dynamic pressure is dominated by the bearing parameter Λ , and the profile is similar to the static pressure distribution, and is relatively independent of σ . As σ increases, the pressure distribution, P_R , becomes slightly wavy at both edges. The waviness penetrates deeper as σ further increases. As σ approaches infinity, the effect of Λ disappears, and P_R approaches the asymptotic solution,

$$(P_R)_{\sigma \rightarrow \infty} = \frac{P_o}{H_o} \quad (4.35)$$

The imaginary part of the dynamic pressure takes a wavy pattern even for small values of σ . For σ approaches infinity, the values for P_I vanishes throughout the entire region.

The in-phase and out-of-phase forces are plotted as a function of σ in Fig. 36, and also listed in Tables 3 to 5. It is seen that for small or moderate values of Λ , the out-of-phase force never becomes negative. This indicates that for nearly incompressible cases, there exists no stability threshold, and all equilibrium solutions are stable. As Λ becomes extremely large, the out-of-phase force does become negative at a fairly high value of σ . This crossing-over of zero line indicates that for a highly compressible film, there does exist a stability threshold, and the gas film will exhibit a self-excited oscillation at a fairly high frequency. Moreover, the criterion in Reference 16 suggests that the stable region lies in the area where the mass of the pad is greater than the critical mass calculated according to Eq. (4.34).

V. SUMMARY OF RESULTS

1. The gas-film restoring forces in a Rayleigh-Shrouded-Step thrust pad can be determined numerically by solving the discretized time-dependent Reynolds equation with irregular grid-spacings to account for any abrupt changes of pressure at the step and at the exit edge.

2. For conditions of high ambient pressure, for which the term of $h \frac{\partial p}{\partial t}$ can be neglected in comparison with other terms at the right side of the Reynolds equation, the gas-film force is found to be approximately inversely proportional to n th power of the film thickness and directly proportional to the squeeze-film velocity. The exact value of n is a function of the step geometry. In general, n lie between 2 and 3.

3. The axial, non-linear response of the Rayleigh-Shrouded-Step pad to a sinusoidal, axial forcing function or a sinusoidal disturbance due to the rotor misalignment or surface waviness can be determined by one of the following two methods:

a, By assuming the response to be a truncated Fourier series in multiples of the excitation frequency, the Ritz-Galerkin procedure can be employed to predict the non-linear behavior of the pad motion.

b, By integrating directly the equation of motion of the thrust pad using a step-by-step, numerical routine, the Runge-Kutta procedure.

4. Results obtained by using the Ritz-Galerkin method with the first harmonic terms show considerably departures from the linear response curve as the frequency approaches the resonance based on the linear theory. The asymmetric spring characteristics of the gas film result into a non-linear response similar to that caused by a symmetric, soft, non-linear

spring. The resonating peak bends inward and occurs at a frequency less than the resonating frequency based on the linear theory. The peak can be suppressed by decreasing the mass, increasing the damping, and increase the stiffness.

5. Results obtained by the step-by-step direct integration confirms the approximate solution in the vicinity of the resonance. The direct integration also predicts a number of additional peaks at frequencies less than the resonating frequency known as the superharmonic resonance.

6. The gas-film instability of an infinitely-wide Rayleigh step thrust pad can be determined by solving the complete, time dependent, Reynolds equation coupled with the equation of the motion of the pad. Results show that for bearing numbers, Λ , up to 50, the Rayleigh step geometry is very stable, and no stability threshold has been discovered. For ultra high values of $\Lambda \geq 100$, a stability threshold is shown to exist, and the stability can be achieved by making the mass heavier than the critical mass.

REFERENCES

1. Rayleigh, Lord, "Notes on Theory of Lubrication," Phil. Mag., 35, 1912, p.1-12.
2. Wylie, G. M. and Maday, C. J., "The Optimum One-Dimensional Hydrodynamic Gas Rayleigh Step Bearing," J. Lub. Tech., Trans., ASME, V.93, No.3, July 1970, p.504-508.
3. Kettleborough, C. F., "Stepped Thrust Bearing-Solution by Relaxation Methods," J. Appl. Mechanics, Trans., ASME, 76, 1954, p.19-24.
4. Archibald, F. R., and Hamrock, B. J., "The Rayleigh Step Bearing Applied to a Gas-Lubricated Journal of Finite Length," J. Lub. Tech., Trans. ASME, Series F, V.90, No.1, Jan. 1967, p.38-47.
5. Hamrock, B. J., "Rayleigh-Step Journal Bearing, Part 1- Compressible Fluid," J. Lub. Tech., Trans. ASME, Series F, V.90, No.1, Jan. 1968, p.271-280.
6. Kochi, K. C., "Characteristics of Self-Lubricated Stepped Thrust Pad of Infinite Width with Compressible Lubricant," J. Basic Engineering, Trans. ASME, June 1959, p.135-146.
7. Ausman, J. S., "An Approximation Analytical Solution for Self-Acting Gas Lubrication of Stepped Sector Thrust Bearing," ASLE Trans., 4, 1961, p.304-314.
8. Cheng, H. S., Chow, C. Y., and Wilcock, D. F., "Behavior of Hydrostatic and Hydrodynamic Noncontacting Face Seal," J. Lub. Tech., Trans. ASME, V.90, No.2, April 1968, p.510-519.
9. Pratt & Whitney Aircraft Co. and Mechanical Technology Inc., "Self Annual Report No.1 & No.2, Development of Compressor End Seals, Stator Interstage Seals, and Stator Pivot Seals in Advanced Air Breathing Propulsion Systems," PW&A 2752 & 2875 Contract NAS3-7605.
10. Chow, C. Y., Cheng H. S., and Wilcock, D. F., "Optimum Surface Profile for the Enclosed Pocket Hydrodynamic Gas Thrust Bearing," J. Lub. Tech., Trans. ASME, V.92, No.2, April 1970, p.318-324.
11. Pinkus, O. and Sternlicht, B., "Theory of Hydrodynamic Lubrication," Mc-Graw-Hill, N. Y., 1961.
12. Kingsbury, A., "On Problems in the Theory of Fluid-Film Lubrication with an Experimental Method of Solution," Trans. ASME, 53, 1931, p.59-75.

13. Castelli, V., and Pirvics, J., "Review of Numerical Methods in Gas Bearing Film Analysis," J. Lub. Tech., Trans. ASME, V.90, No.4, Oct. 1968, p.777-792.
14. Chiang, T., and Cheng, H. S., "An Analysis of Flexible Seal Ring," ASLE Trans., V.LL, No.3, July 1968, p.204-215.
15. Mc-Lachlan, N. W., "Ordinary Nonlinear Differential Equations," Oxford University Press, Amen House, London E. C. 4, 1950.
16. Malanoski, S. B., and Pan, C. H. T., "The Static and Dynamic Characteristic of the Spiral-Grooved Thrust Bearing," MTI-64TR11.
17. Kettleborough, C. F., "An Electrolytic Tank Investigation into Stepped Thrust Bearings," Proc. Inst. Mech. Engrs., 169, 1955, p.679-688.
18. Cunningham, W. J., "Nonlinear Analysis," Mc-Graw-Hill, N. Y., 1958.

TABLE 1

GAS FILM FORCES (lb_f)

$$d_o = 6.46 \text{ ins} \quad d_i = 5.96 \text{ ins}$$

$$\delta = 0.001 \text{ in (step)}$$

$$\omega = 277 \text{ rev./sec.}$$

$$P_a = P_o = 315 \text{ psia.: Ambient Pressure}$$

$\frac{H_{\min}}{dh/dt}$	2.0	1.5	1.0	0.75	0.50	0.30	0.20
-1 in/sec.	0.50635	1.10134	3.2606	6.9965	19.949	65.138	139.729
-0.5	0.45104	0.97913	2.8878	6.1765	17.499	56.041	115.531
-0.25	0.42338	0.91801	2.7015	5.7667	16.275	51.529	103.734
+0.25	0.36806	0.79580	2.3290	4.9477	13.833	42.576	80.750
+0.5	0.34040	0.73470	2.1428	4.5384	12.615	38.135	69.559
+1	0.28509	0.61250	1.7704	3.7204	10.182	29.325	47.778
0	0.3957	0.8569	2.515	5.357	15.06	47.124	92.8
$\frac{F_{g1} - F_{g2}}{h_2 - h_1}$	0.1106	0.2444	0.7450	1.6380	4.8836	17.907	45.975

$$\mu = 6 \times 10^{-9} \frac{\text{lb}_f \cdot \text{sec}}{\text{in}^2}$$

$$\Lambda = 8.30076$$

TABLE 2

LOAD ($1b_f$) CALCULATED AND ERROR OCCURRED (%)

$\frac{H_{min}}{h}$ in/sec.	2.0	1.5	1.0	0.75	.50	.30	0.20
-1	0.544	1.116	3.08	6.33	17.403	62.7	171.2
	+ 1.5%	+ 1.45%	- 5.53%	- 9.5%	- 12.5%	- 3.7%	+ 22.5%
-0.5	0.477	0.978	2.70	5.55	15.28	54.95	150.1
	+ 5.78%	- 0.1%	- 6.5%	- 10.1%	- 6.29%	+ 6.65%	+ 30%
-0.25	0.4435	0.909	2.51	5.16	14.205	51.075	139.05
	+ 4.78%	- 0.98%	- 7.07%	- 10.5%	- 12.3%	- 0.89%	+ 33%
+0.25	0.3765	0.771	2.13	4.38	12.055	43.325	118.95
	+ 2.34%	- 3.01%	- 8.2%	- 11.5%	- 12.9%	+ 1.76%	47.4%
0.5	0.344	0.703	1.94	3.99	10.98	39.45	107.9
	+ 1.18%	- 4.22%	- 9.35%	- 11.8%	- 12.9%	+ 3.46%	55.2%
1	0.276	0.564	1.56	3.21	8.83	31.7	86.8
	- 3.15%	- 7.85%	- 11.85%	- 13.7%	- 15%	+ 8.2%	+ 82%

TABLE 3
DYNAMIC BEARING REACTION FOR

$$B_1/B = .75 \quad H_2 = 0.5$$

$$\Lambda = 8.4$$

σ	$\int_0^1 P_I dX$	$\int_0^1 P_R dX$
20	.13373	1.1836
50	.21003	1.2694
100	.27600	1.4097
200	.24248	1.5930
300	.18121	1.6590
450	.12761	1.6887

$$\Lambda = 42$$

1	.005975	1.5018
10	.057536	1.5144
50	.11984	1.6844
100	.020667	1.7192
200	.031105	1.5013
300	.26865	1.5269
500	.37916	1.8392
2×10^3	.079279	2.0095
10^4	.045201	2.0296

$$\Lambda = 100$$

10	.05897	1.0295
50	.28043	1.1019
100	.47831	1.3014
200	.47977	1.7884
300	.13904	1.9829
500	-.12737	1.5789

TABLE 4
DYNAMIC BEARING REACTION FOR
 $B_1/B = .75 \quad H_2 = 0.75$

$\Lambda = 8.4$

σ	$\int_0^1 P_I dX$	$\int_0^1 P_R dX$
10	.15200	.55179
50	.16382	.78737
100	.15032	.84853
200	.14273	.92439
300	.12283	.96835
500	.08910	1.0045

$\Lambda = 42$

1	.009264	.61777
10	.090506	.63251
50	.27479	.86727
100	.17722	1.0606
200	.052296	1.0238
300	.10195	.99666
500	.15700	1.0797

$\Lambda = 100$

1	.004522	.46999
10	.045139	.47216
50	.21611	.52320
100	.37708	.66548
200	.42895	1.0325
300	.22267	1.2315
500	-.036699	1.0725

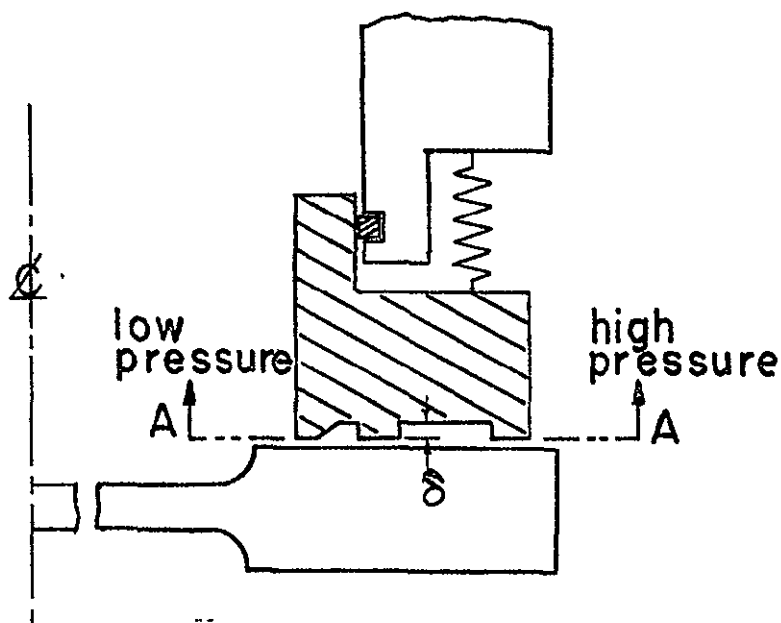
TABLE 5
DYNAMIC BEARING REACTION FOR

$$B_1/B = 0.5 \quad H_2 = 0.5$$

σ	$\Lambda = 8.4$	
	$\int_0^1 P_I dX$	$\int_0^1 P_R dX$
1	.04398	.9242
10	.40067	1.0473
50	.65404	1.9523
100	.34743	2.2234
200	.17872	2.2381
300	.14173	2.2543
500	.10469	2.2785
800	.07845	2.2960

$\Lambda = 42$		
1	.00519	2.3313
10	.05146	2.3349
50	.22100	2.3947
100	.38003	2.4791
200	.66419	2.7731
300	.65252	3.1907
500	.22427	3.3674

$\Lambda = 100$		
1	.00727	1.9138
10	.07261	1.9170
50	.34848	1.9943
100	.61342	2.2089
200	.73899	2.7584
300	.49508	3.0561
500	.29231	2.8927



$$r_o = 3.23 \text{ in}$$

$$r_i = 2.98 \text{ in}$$

$$\delta = 0.001 \text{ in (step)}$$

$$\omega = 1740 \text{ rad/sec}$$

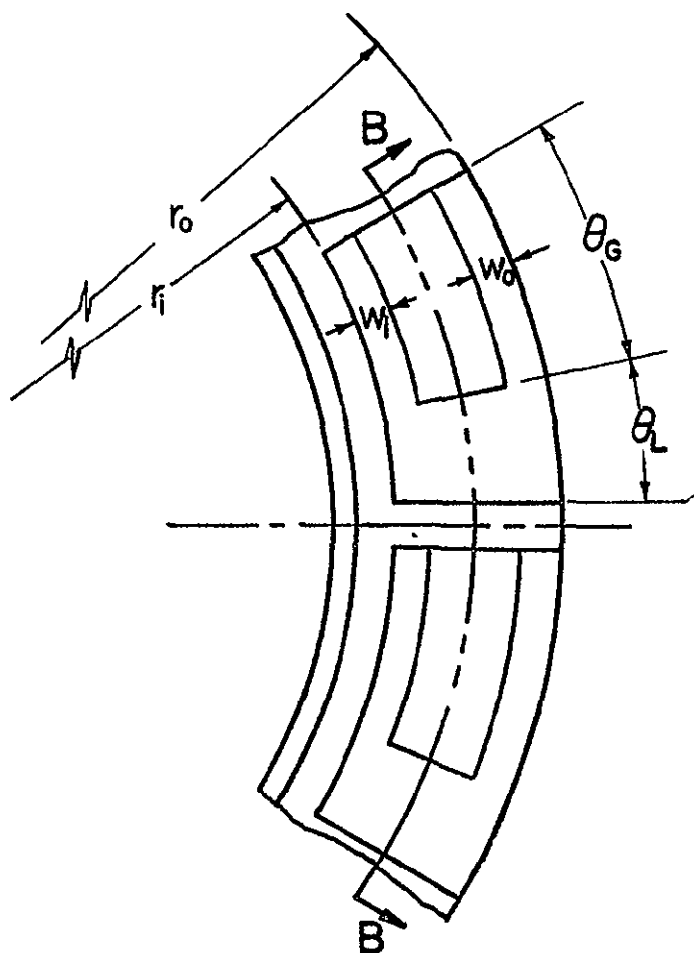
$$\frac{w_o}{r_o - r_i} = \frac{w_i}{r_o - r_i} = 0.08$$

$$p_o = p_i = 315 \text{ psia}$$

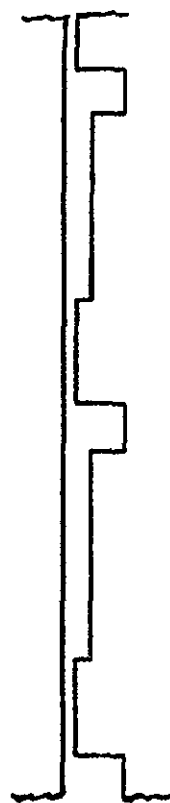
$$\Lambda = 8.30076$$

$$\theta_G = 10.9^\circ$$

$$\theta_L = 5.32^\circ$$



View A-A



View B-B

Fig.1 The geometry of a shrouded, Rayleigh-step thrust bearing

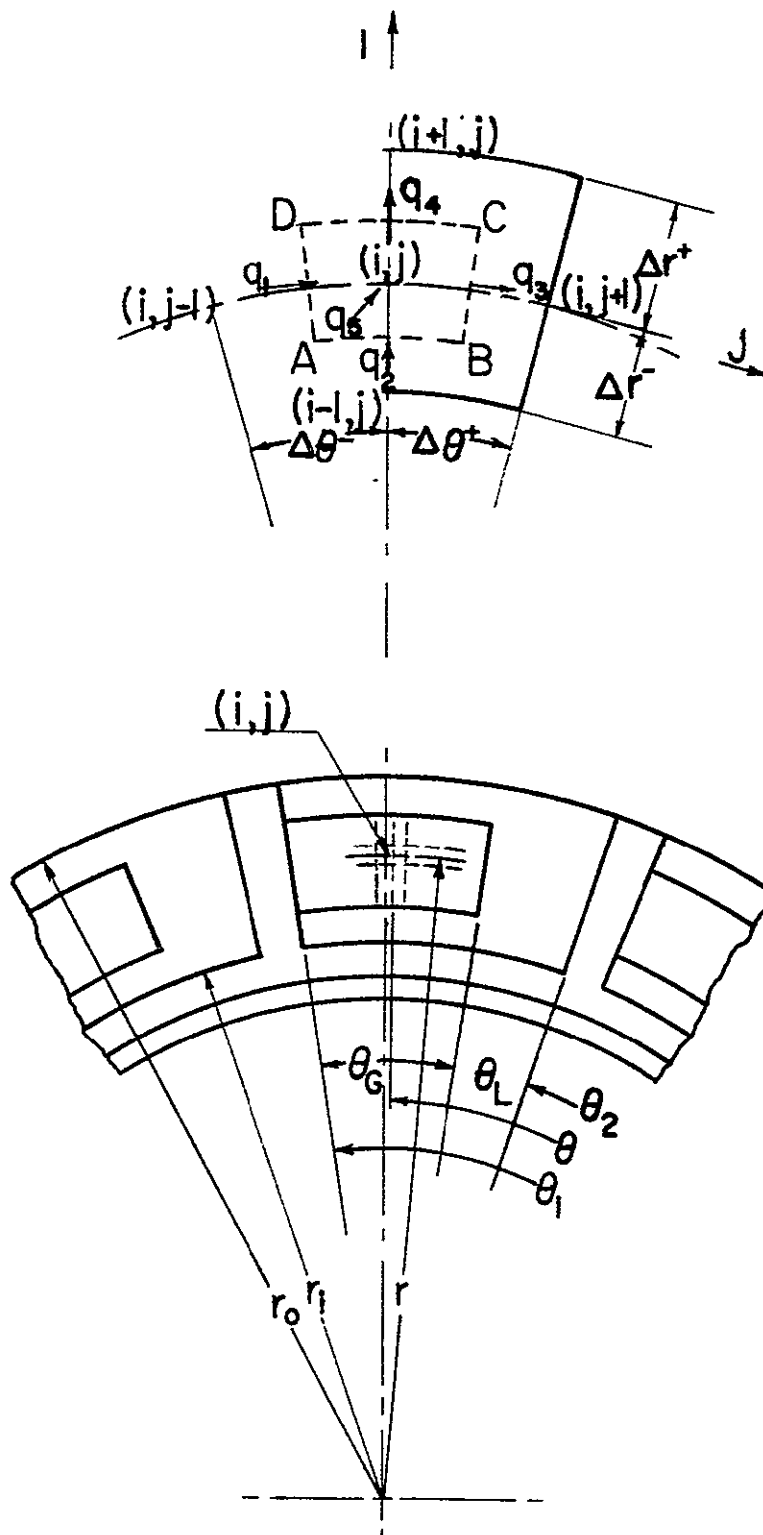


Fig.2 Flow balance around a typical grid point

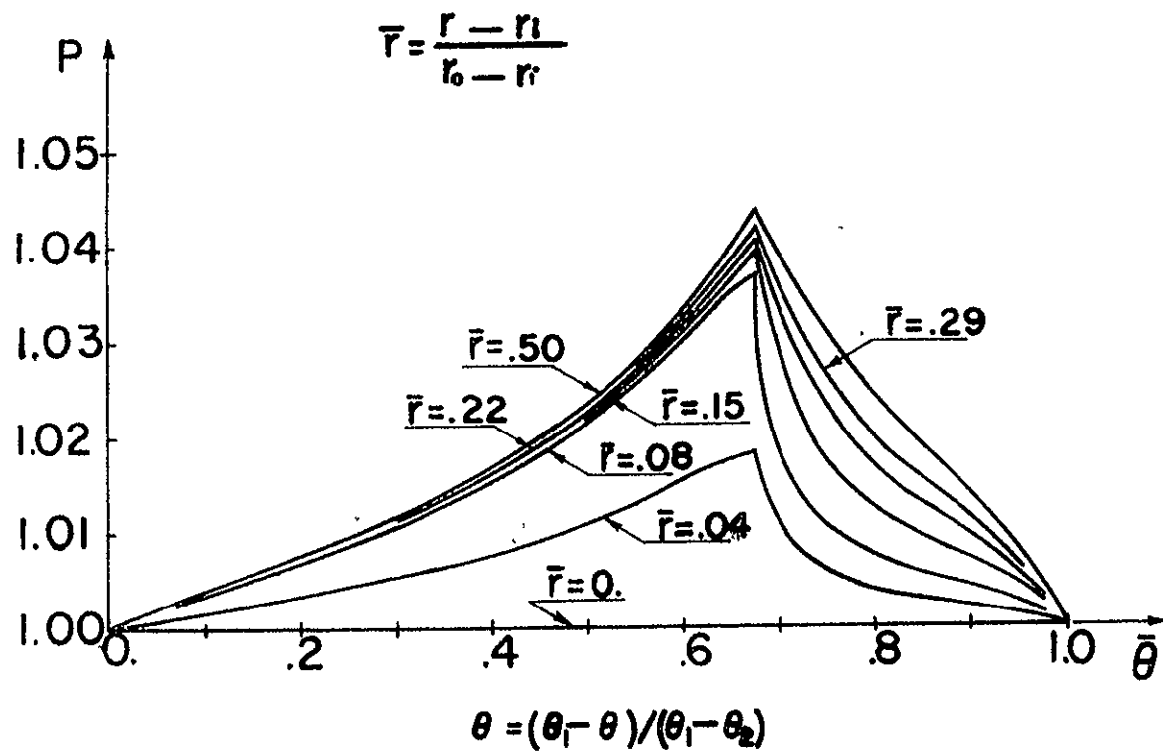


Fig.3 Pressure distribution for $h = -1.1ps$, $H_{min} = 0.5$

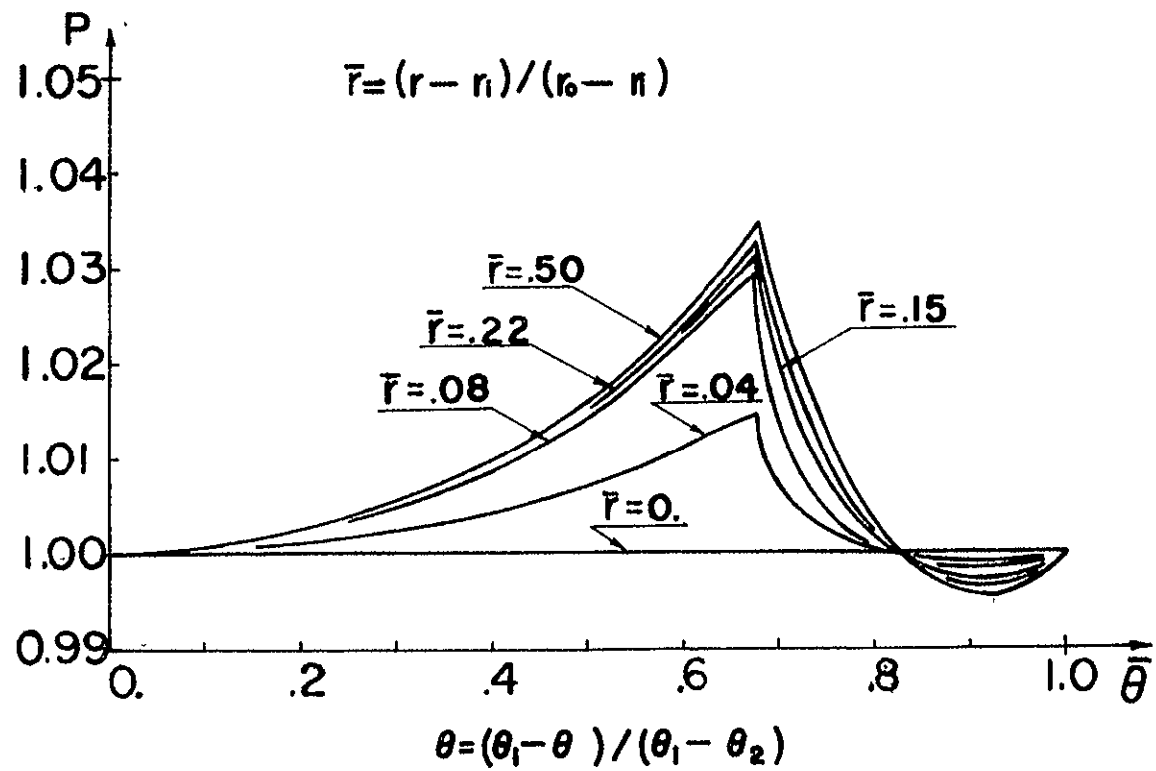


Fig.4 Pressure distribution for $h = 1 \text{ ips. } H_{\min} = 0.5$

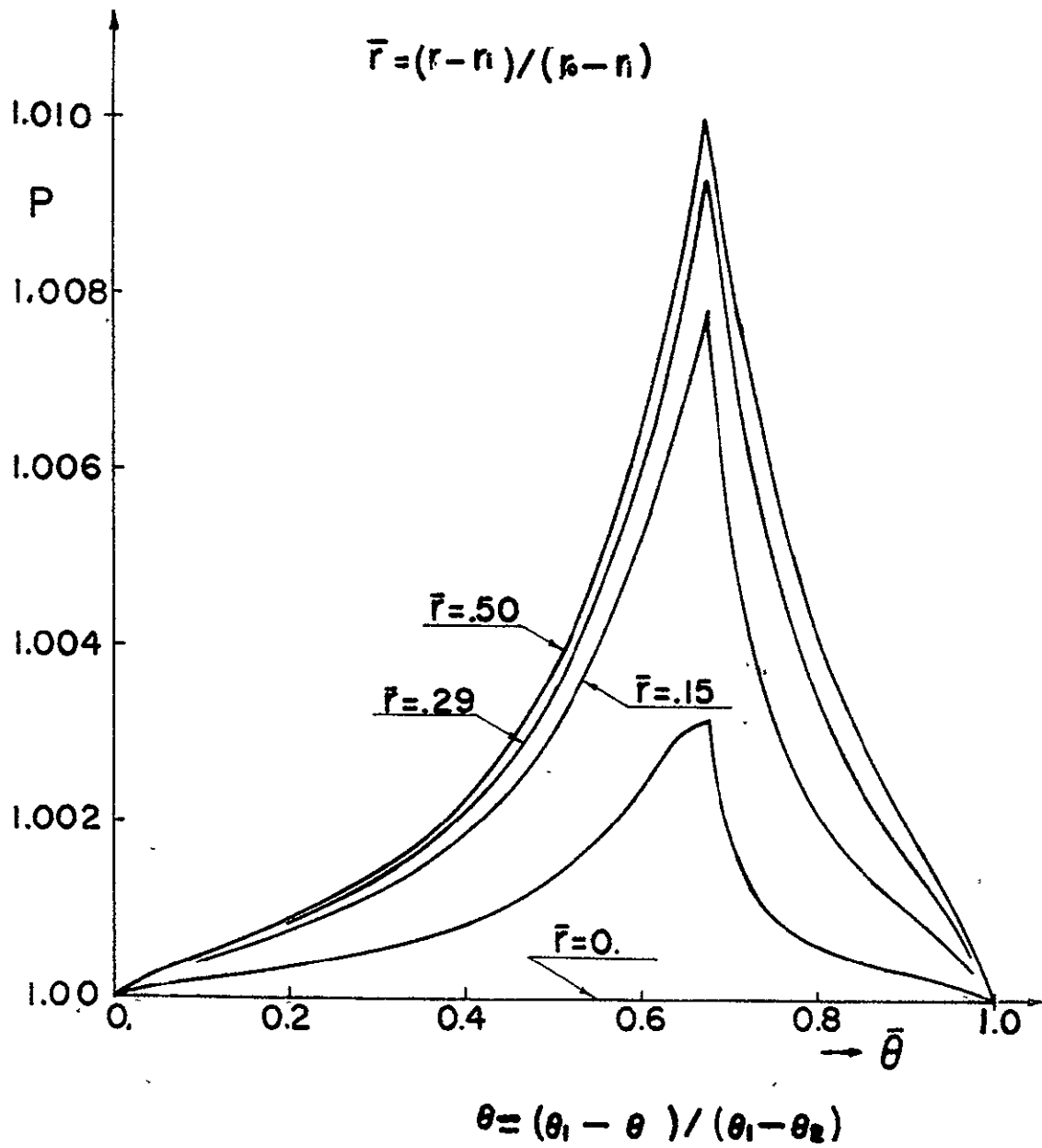
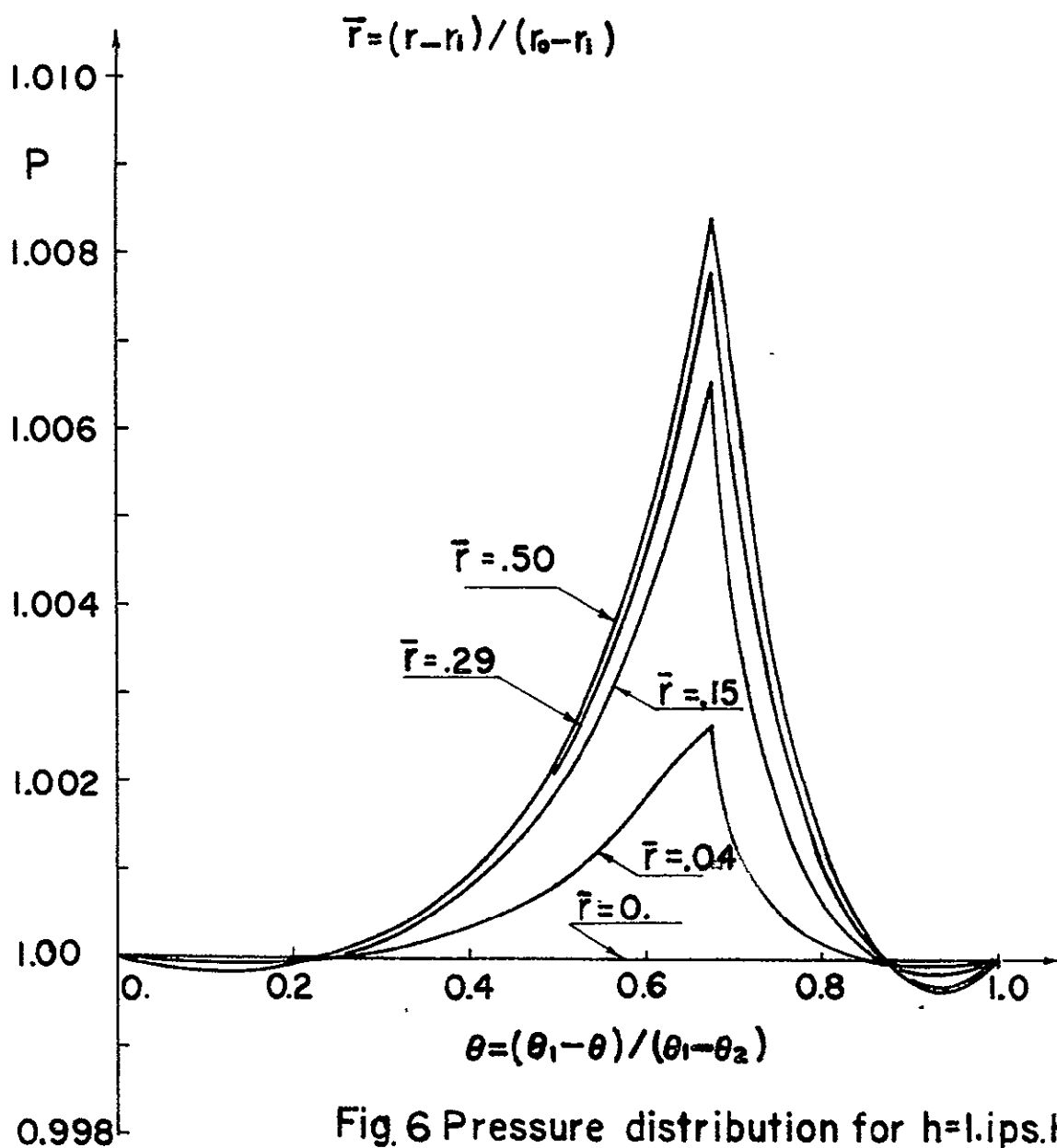


Fig. 5 Pressure distribution for $h = -1$ ips. $H_{\min} = 1$.



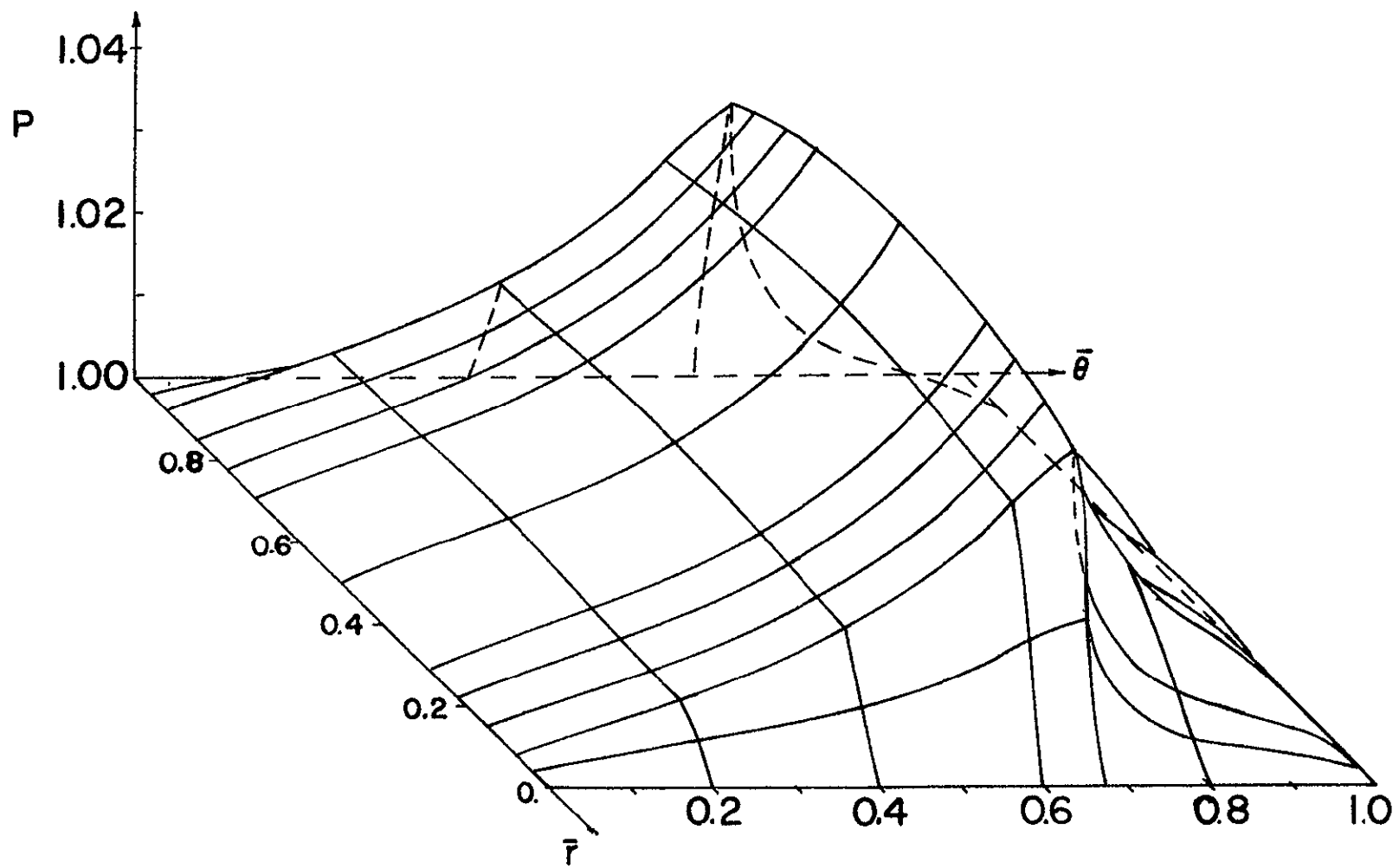


Fig.7 CONTOUR MAP FOR PRESSURE DISTRIBUTIONS
for $\dot{h} = -1$ in/sec, $H_{min} = 0.5$

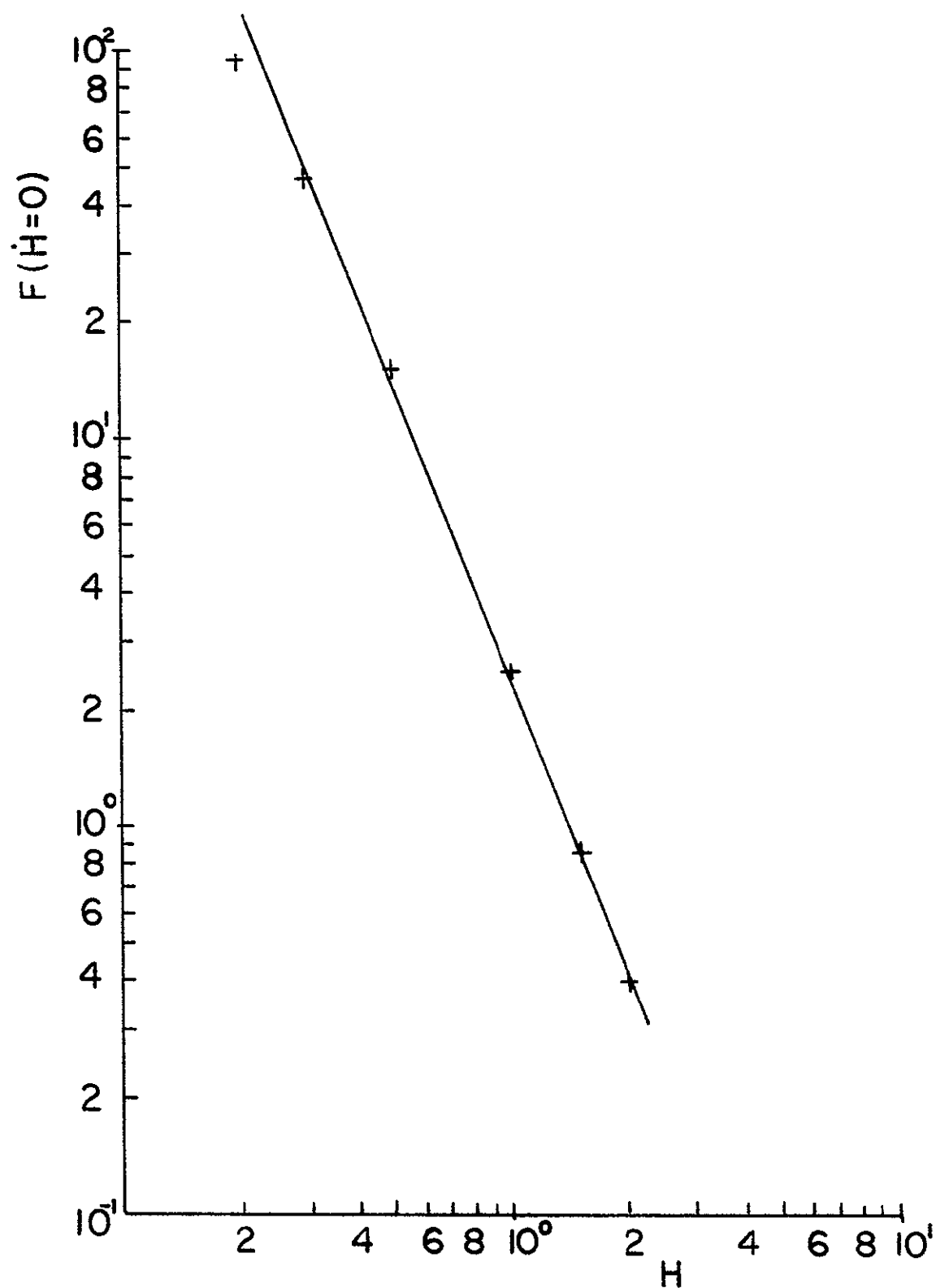


Fig.8 Variation of static, gas film force ($\dot{H}=0$) with the normalized film thickness

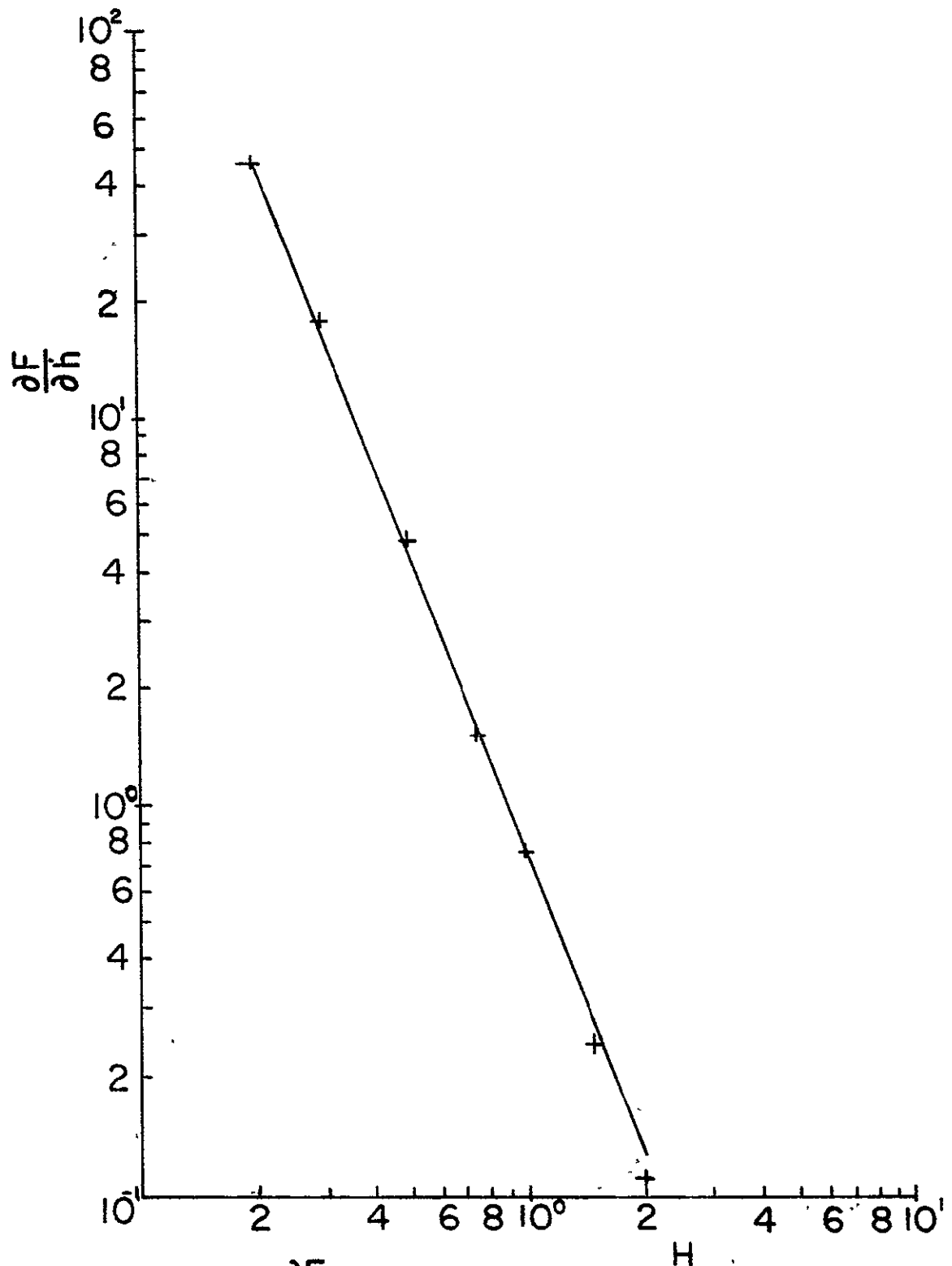


Fig.9 Variation $\frac{\partial F}{\partial h}$ with the normalized film thickness H

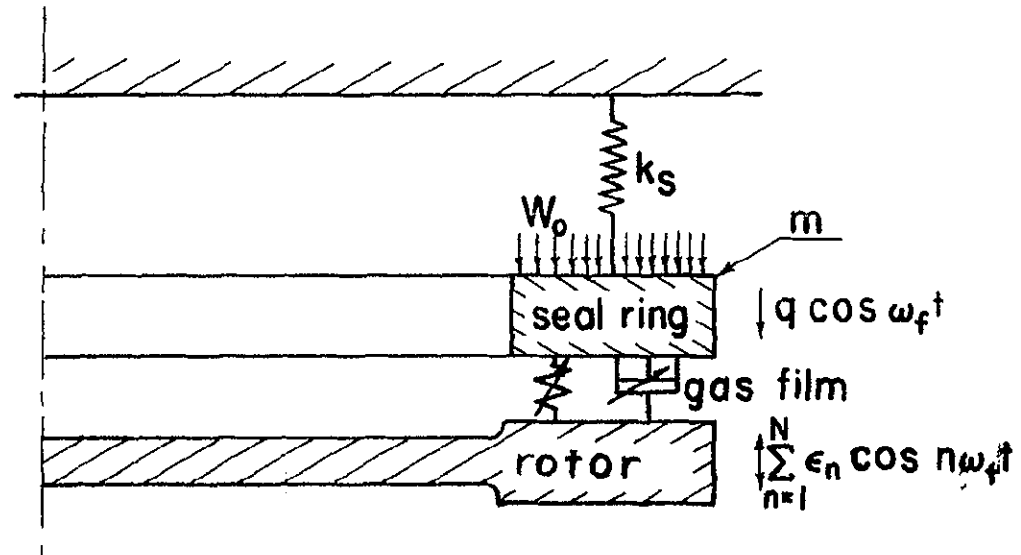


Fig.10 Simplified seal ring-rotor system

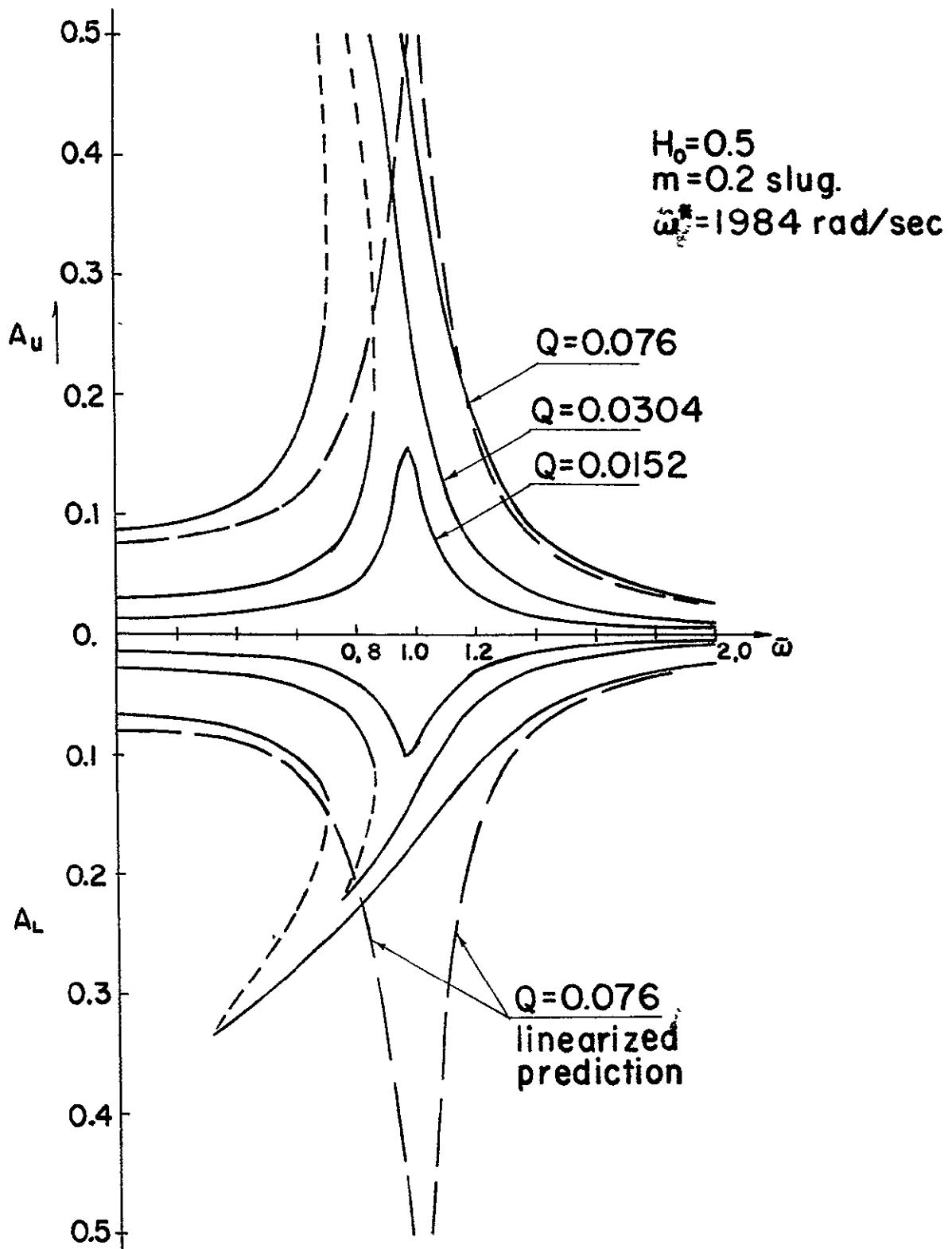


Fig.11 Nonlinear response for $H_0=0.5$, $m=0.2$ slug

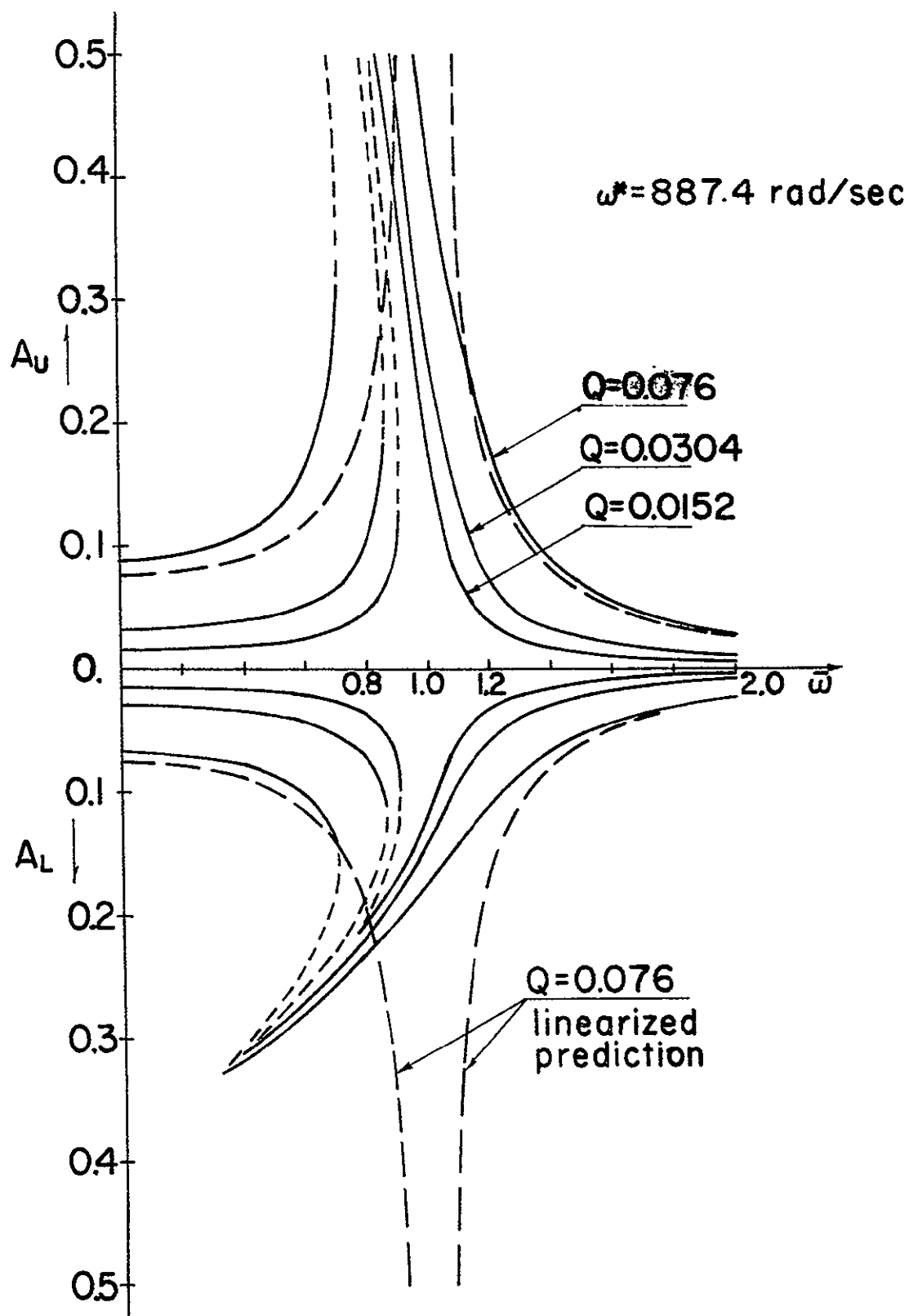


Fig.12 Nonlinear response for $H_0=0.5$, $m=1$ slug

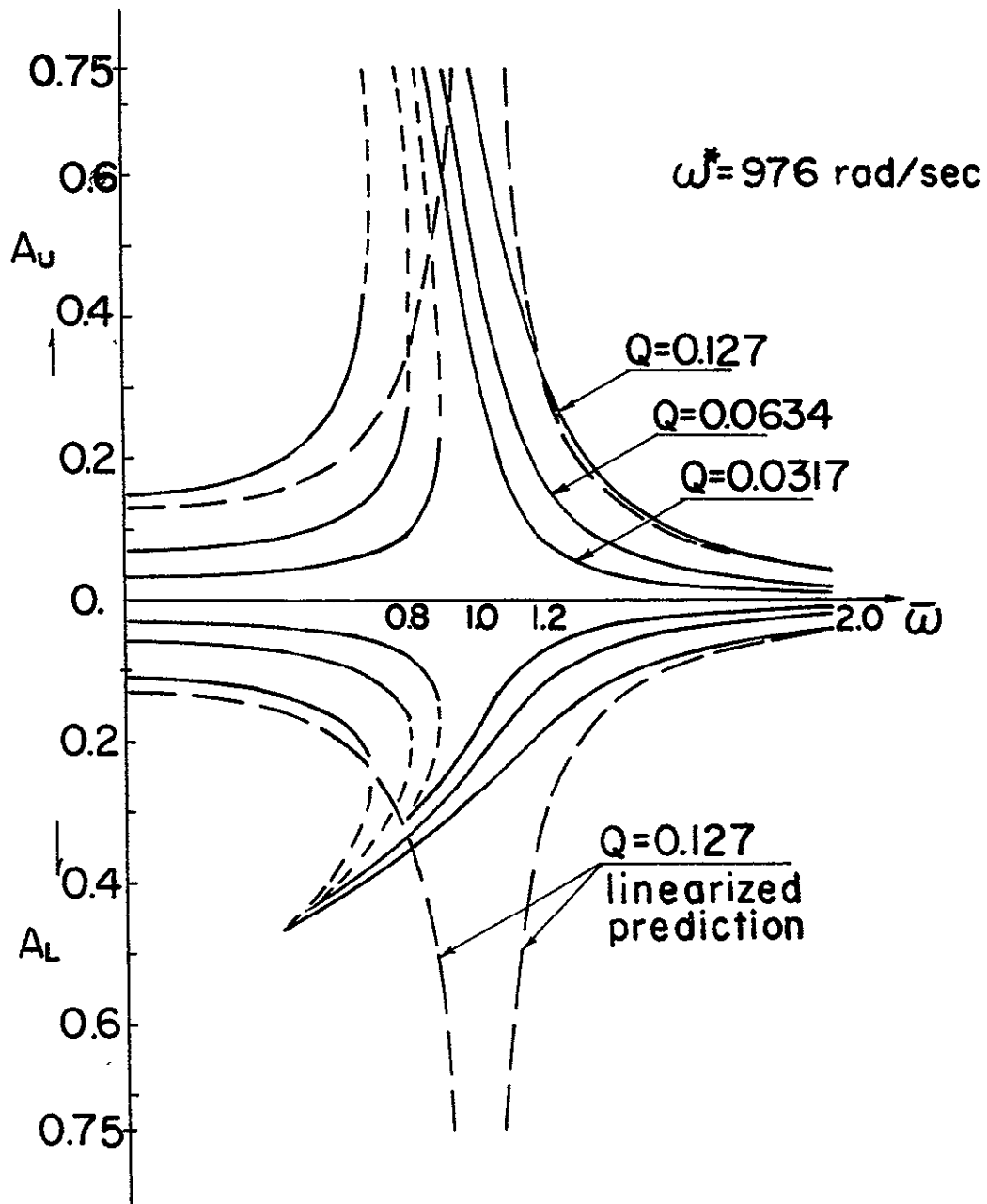


Fig.13 Nonlinear response for $H_b=0.75$, $m=0.2$ slug

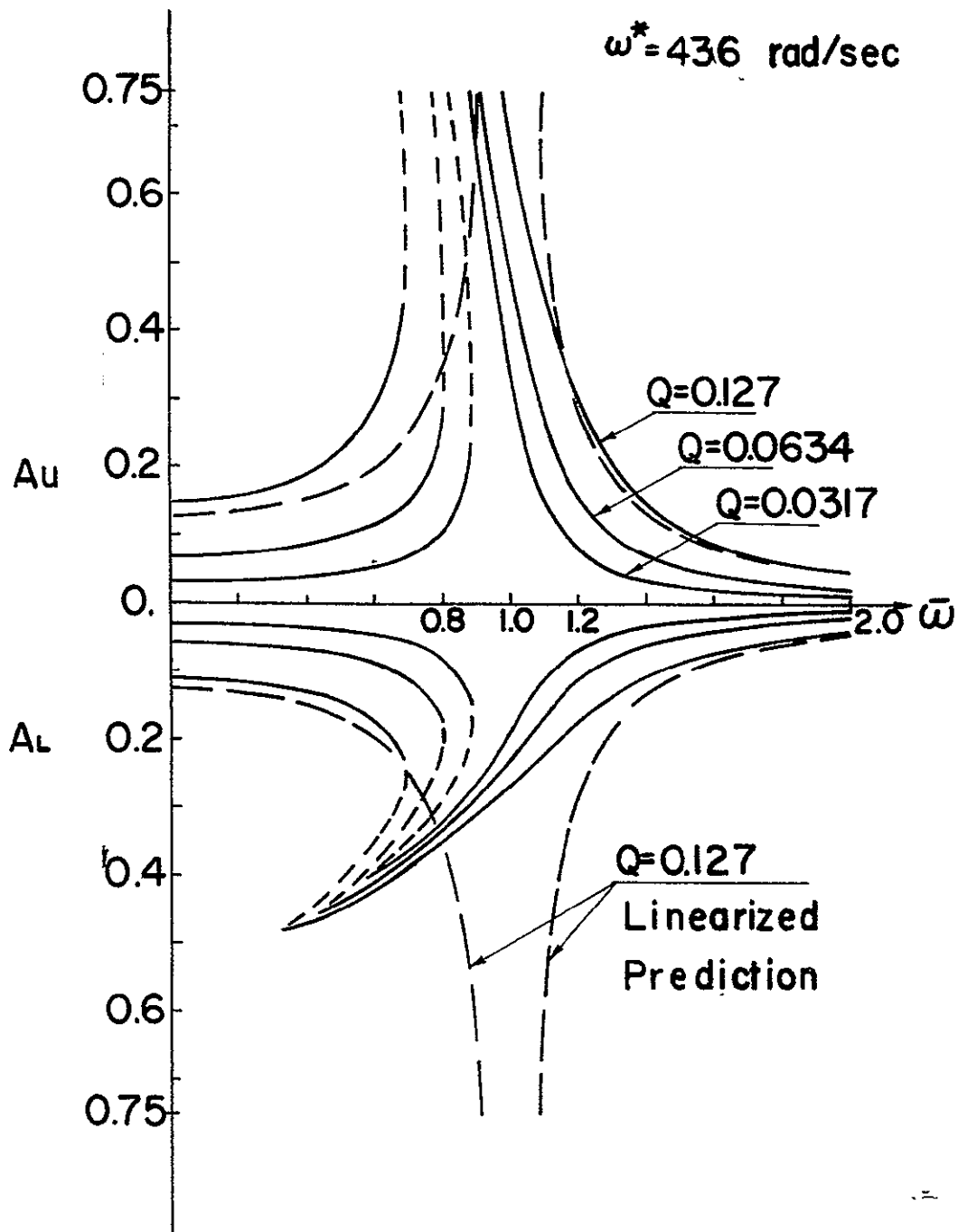


Fig.14 Nonlinear response for $H_0=0.75$, $m=1$ slug

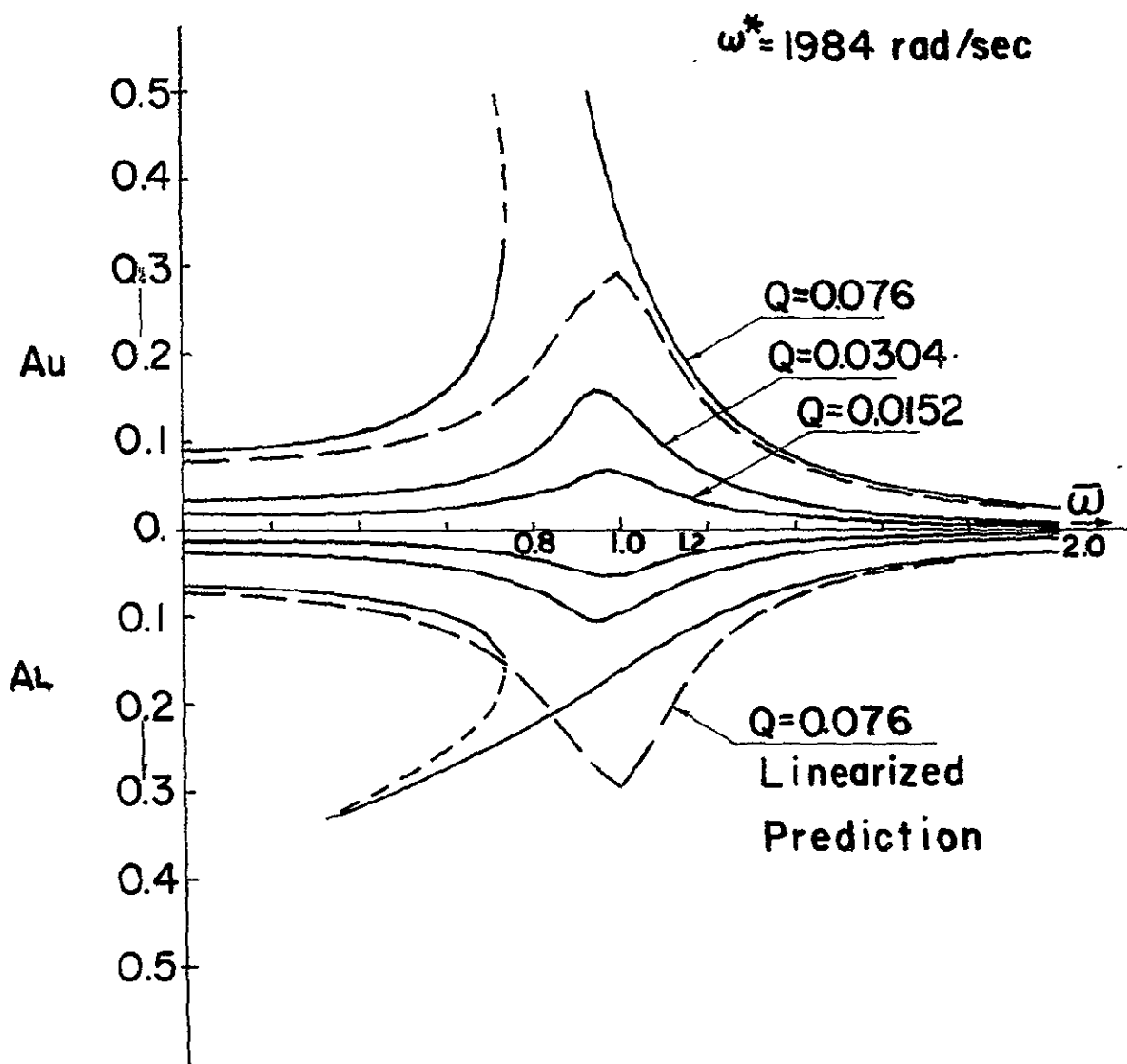


Fig.15 Nonlinear response for
 $H_0 = 0.5$, $m = 0.2$ slug, $C = 1.52$ lb_p/in/sec)

$\omega^* = 1984 \text{ rad/sec}$

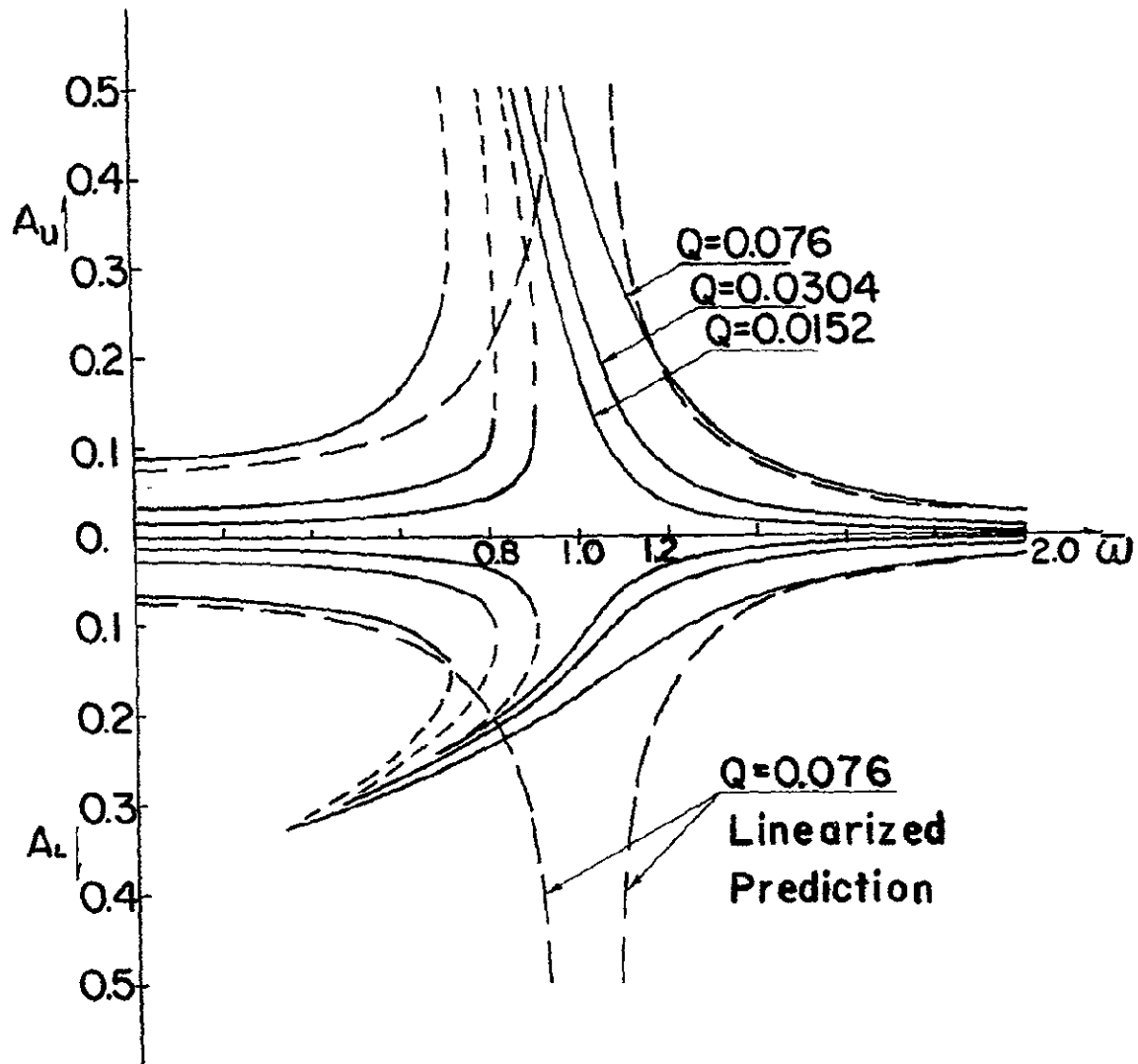


Fig. 16 Nonlinear response for $H_b=0.5$
 $m=0.25 \text{ slug } C_2=0.38 \text{ lb}_f/\text{ips}$

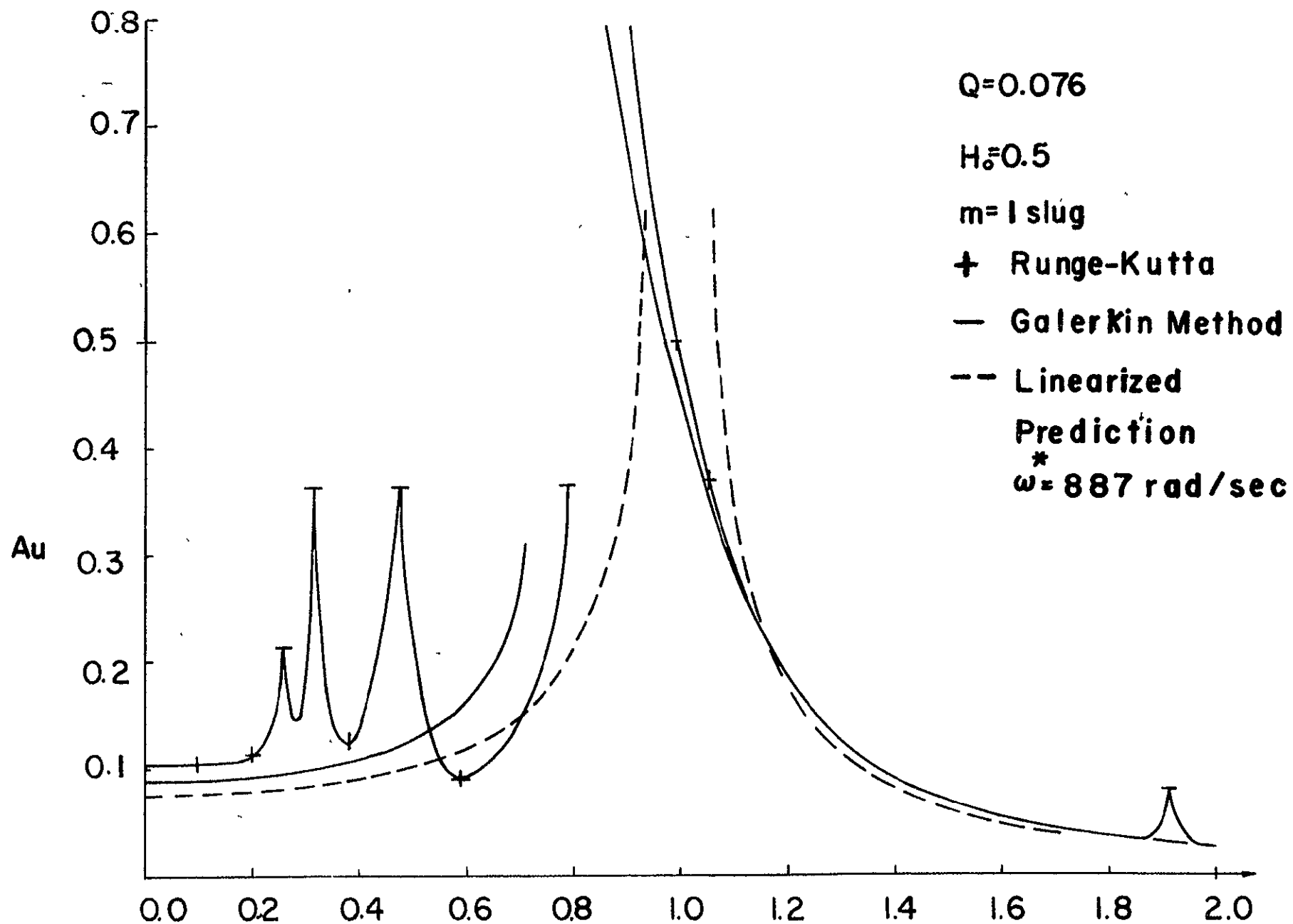


Fig.17 Comparison of the approximate and exact upward amplitudes of response

$Q=0.076$

$H_0=0.5$

$m=1 \text{ slug}$

+ Runge Kutta

— Galerkin Method

-- Linearized
Prediction

$=887 \text{ rad/sec}$

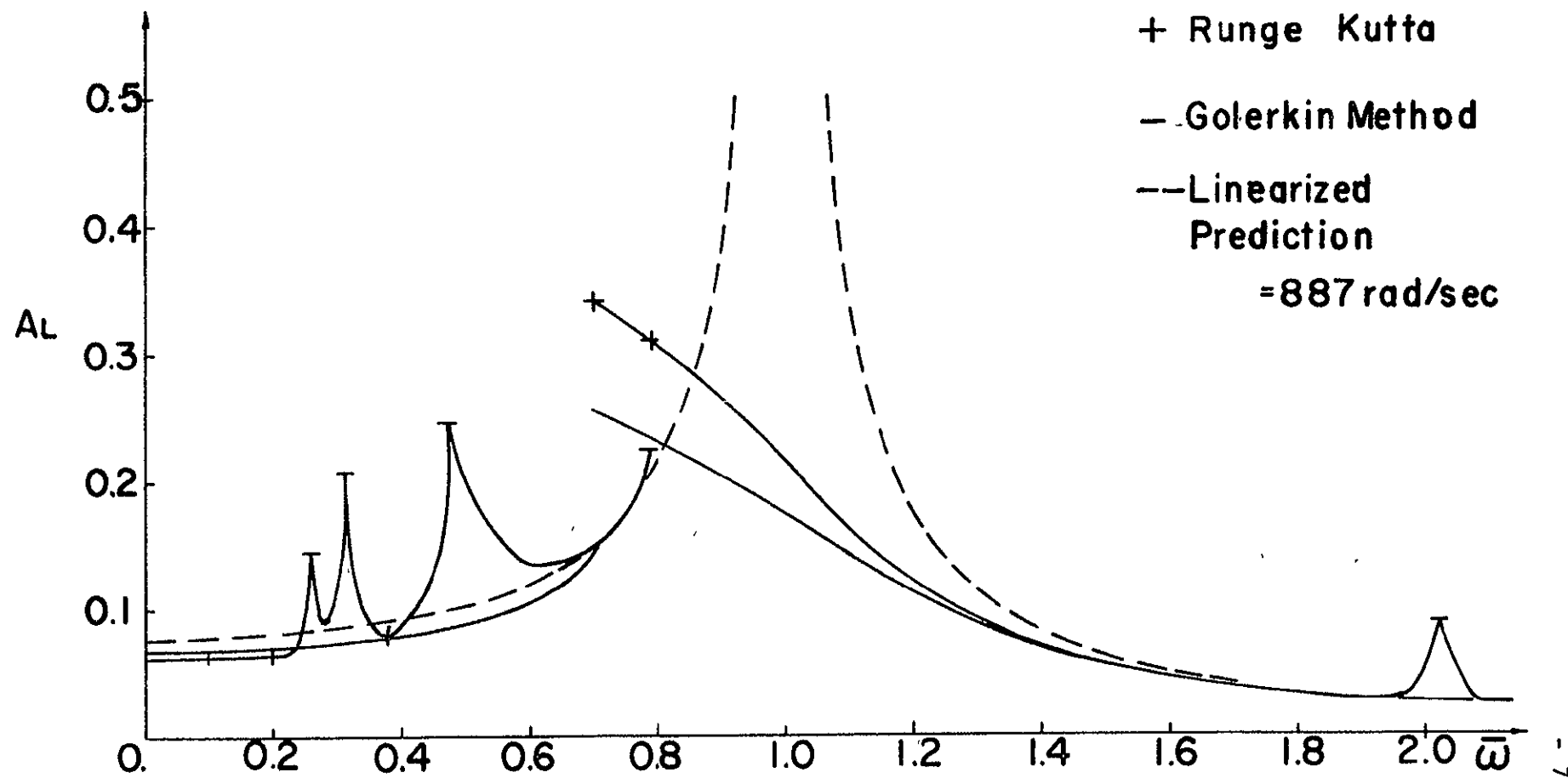


Fig.18 Comparison of the approximate and exact downward amplitude of response

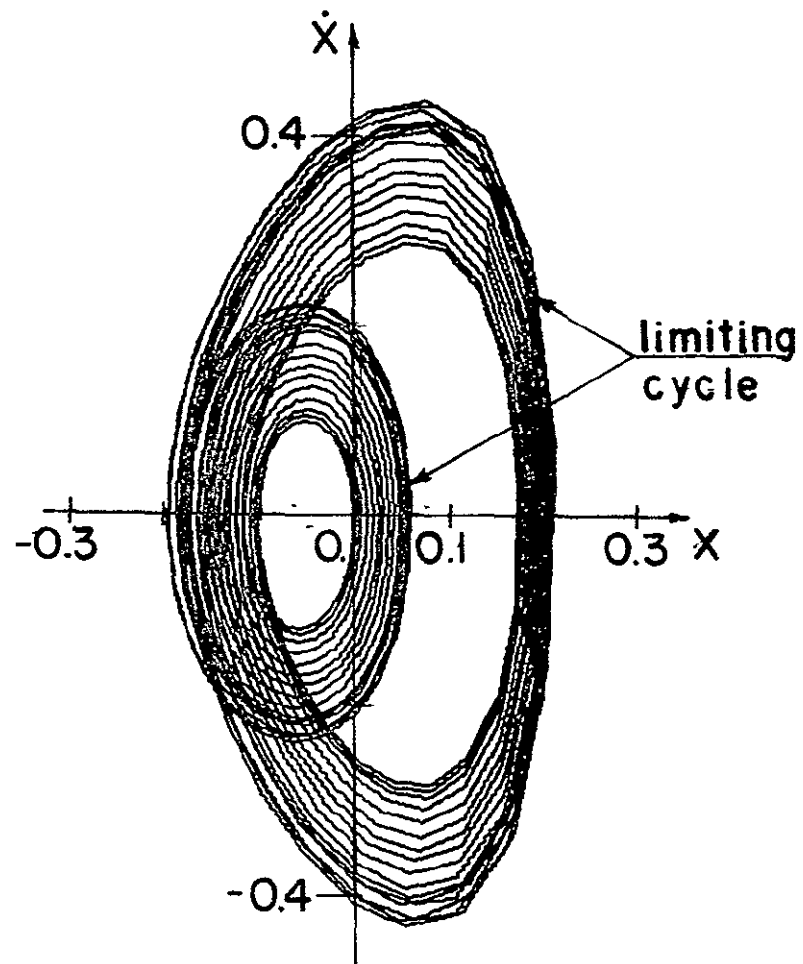


Fig.19 Phase plot with second harmonics
 $\bar{\omega}=0.507$

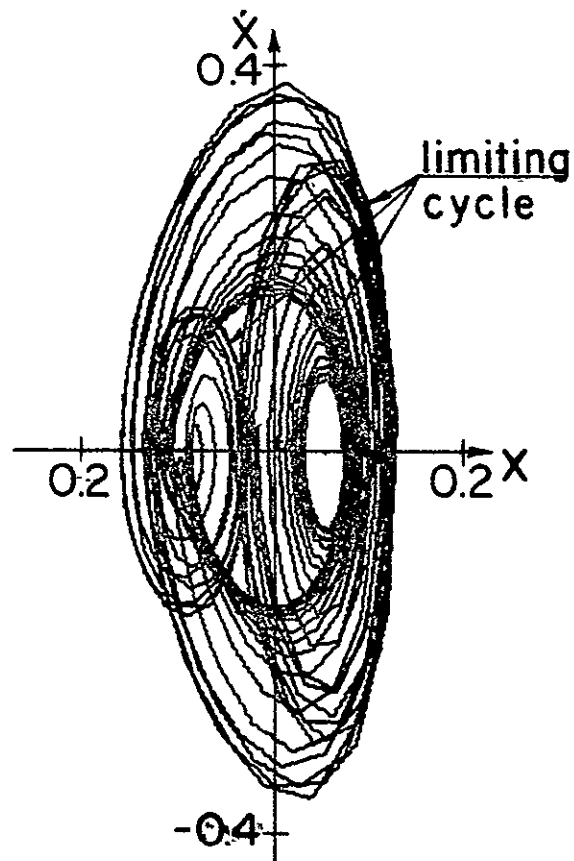


Fig.20 Phase plot with third harmonics
 $\bar{\omega}=0.338$

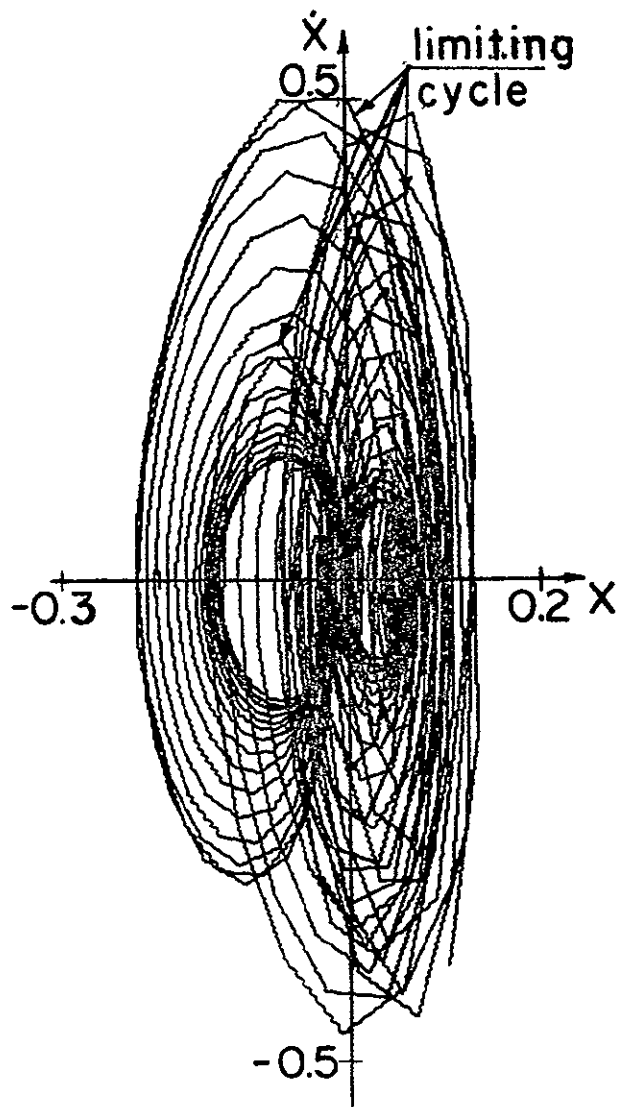


Fig.21 Phase plot with forth harmonics
 $\bar{\omega}=0.248$

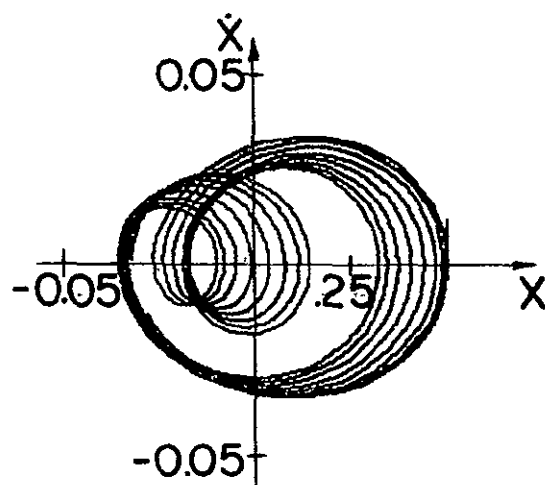


Fig.22 Phase plot with 2nd order
subharmonics
 $\bar{\omega} = 2.096$

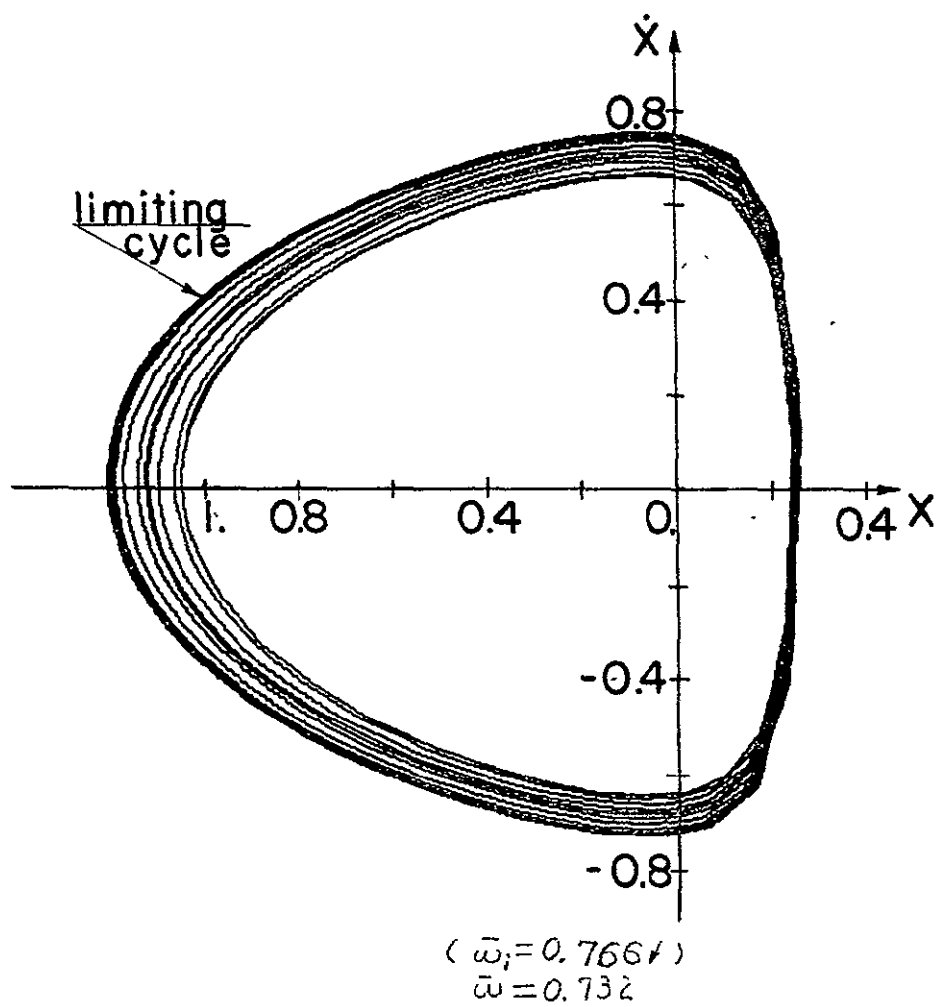


Fig.23 Phase plot with limiting cycle of large amplitude
 $\bar{\omega} = 0.732$

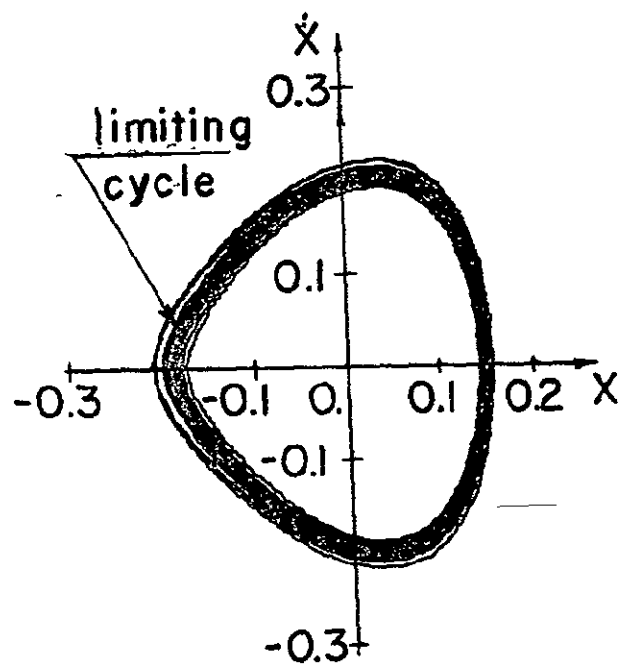


Fig.24 Phase plot with limiting cycle
of small amplitude
 $\bar{\omega}=0.745$

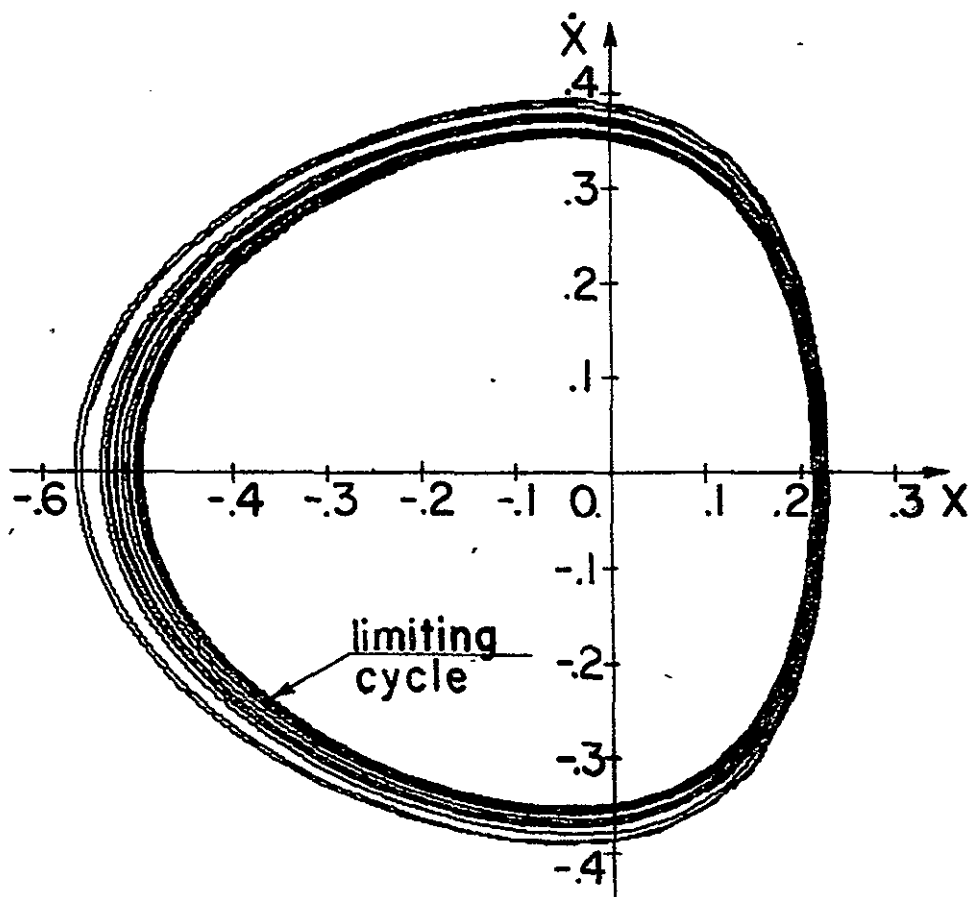


Fig.25 Phase plot at natural frequency
 $\bar{\omega}=1.0$

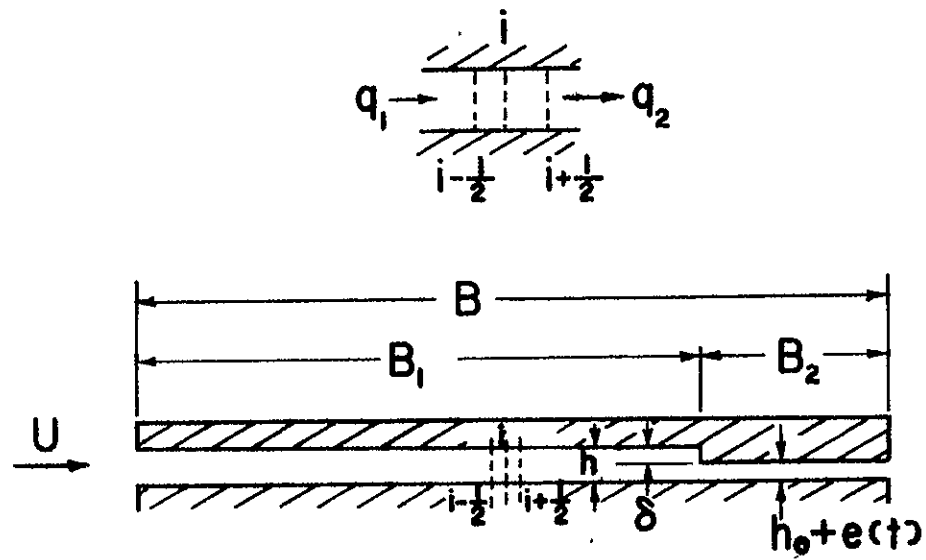


Fig.26 Flow balance and geometry of a infinitely wide Rayleigh step pad

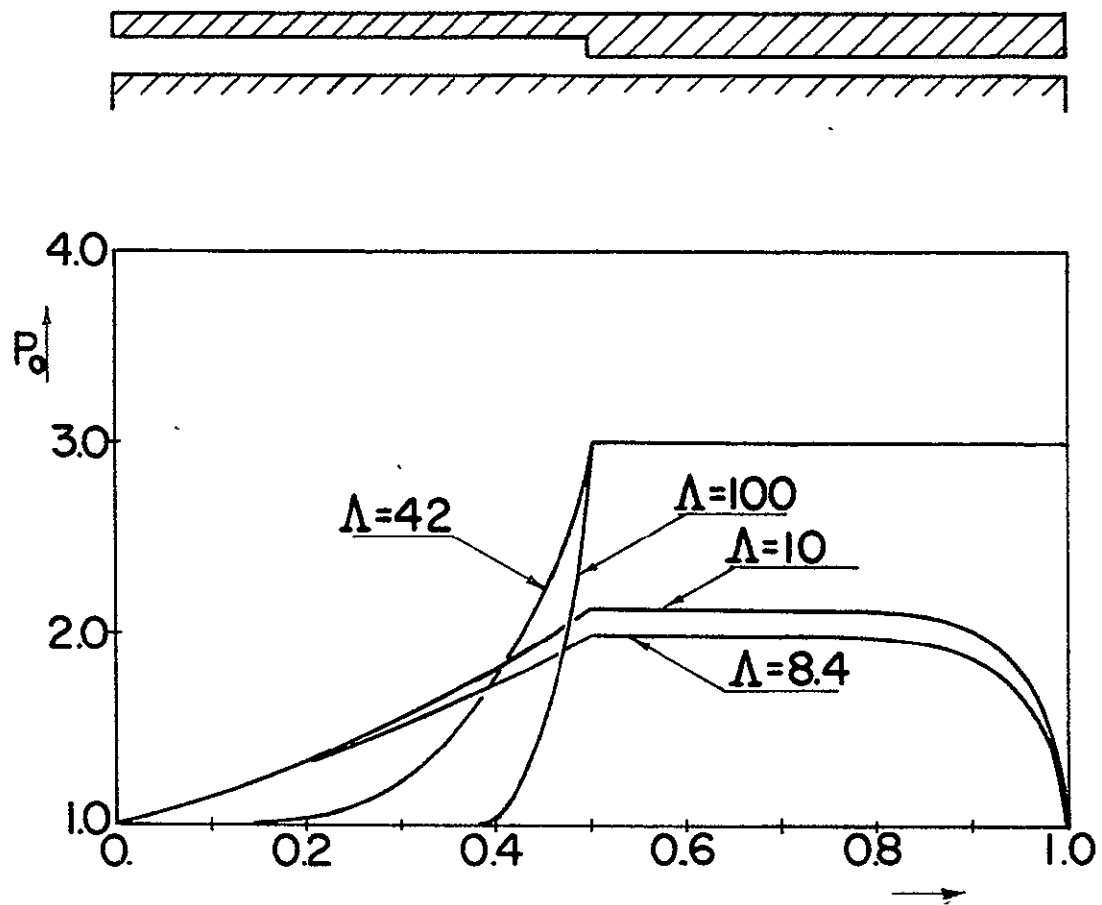


Fig.27 Pressure profile for $B_1/B=0.5$, $H_2=0.5$

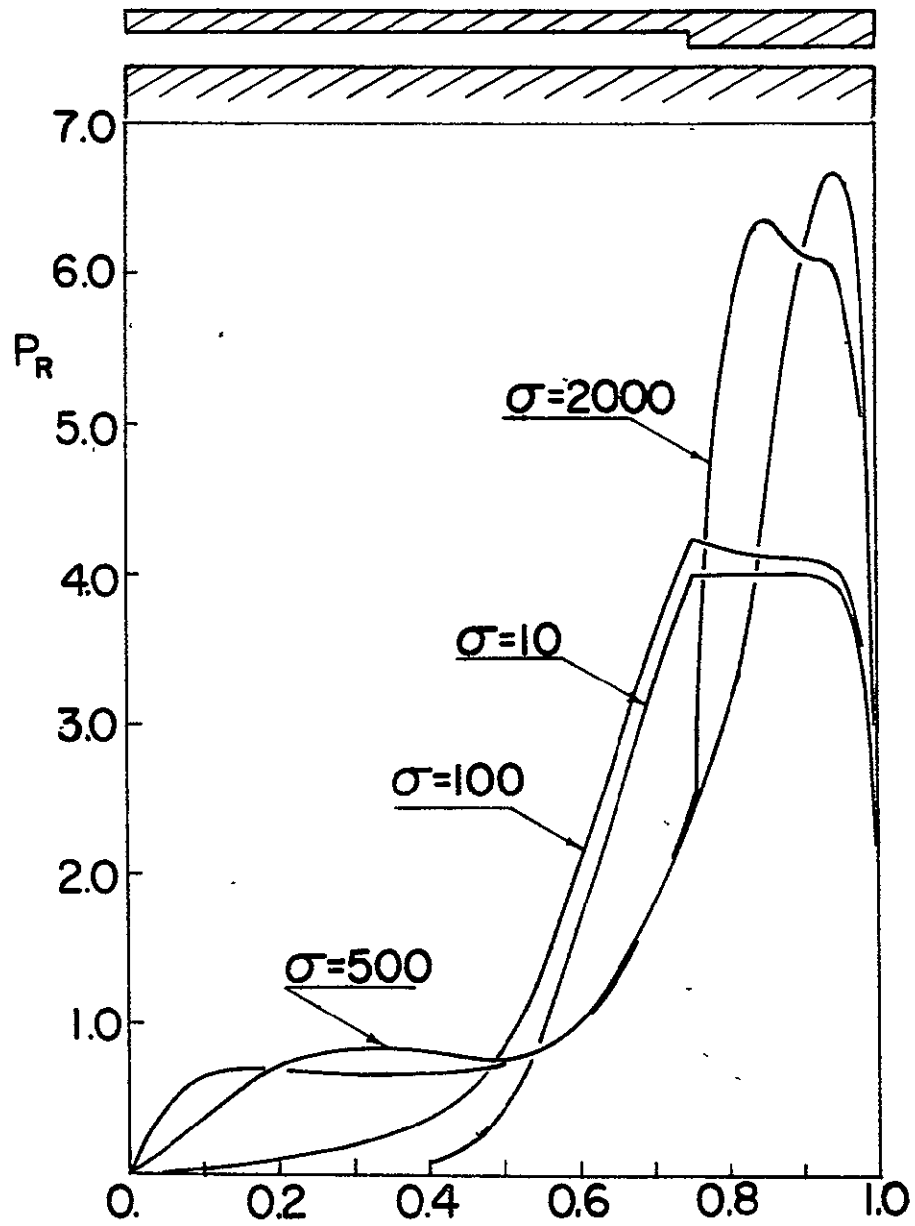


Fig.28 Real pressure profile for $\Lambda=42$, $H_2=0.5$,
 $B_1/B=0.75$

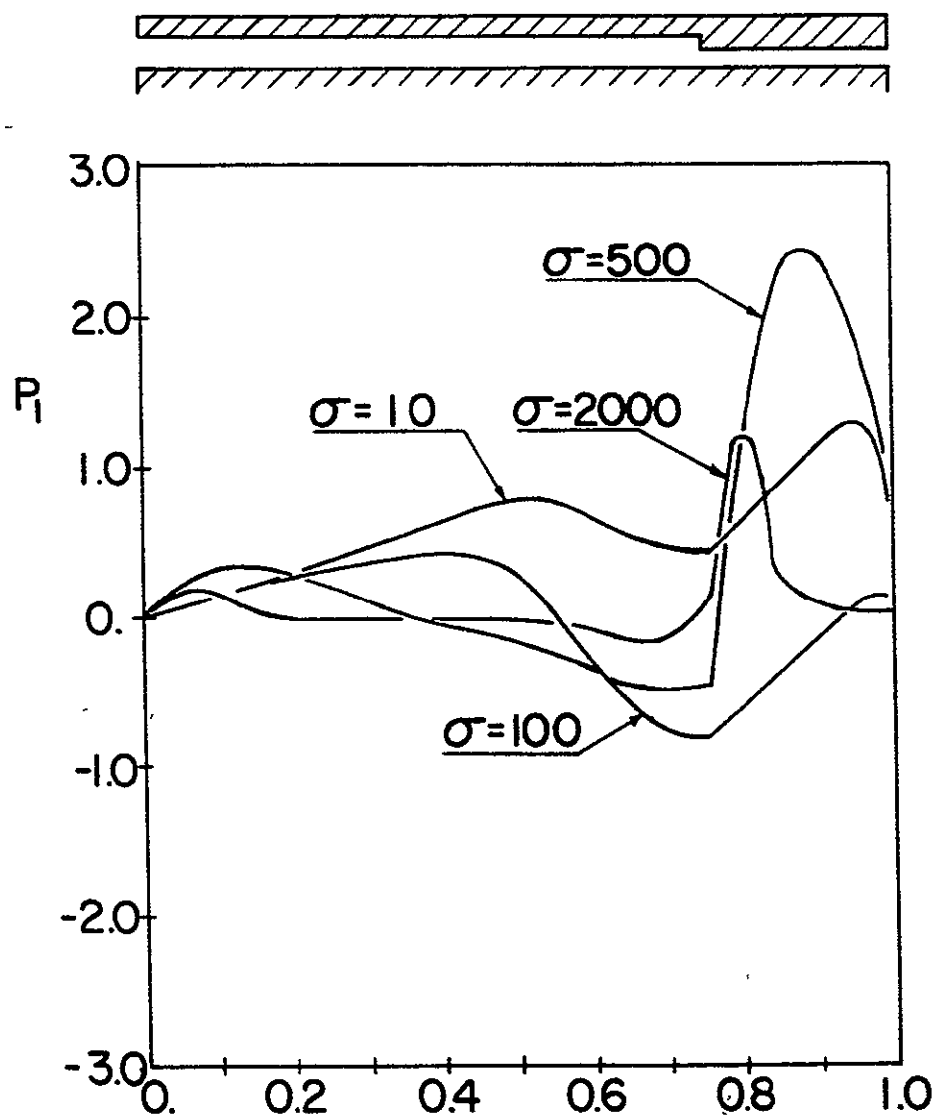


Fig.29 Imaginary pressure profile for $\Lambda=42$, $H=0.5$, $B_1/B=0.75$

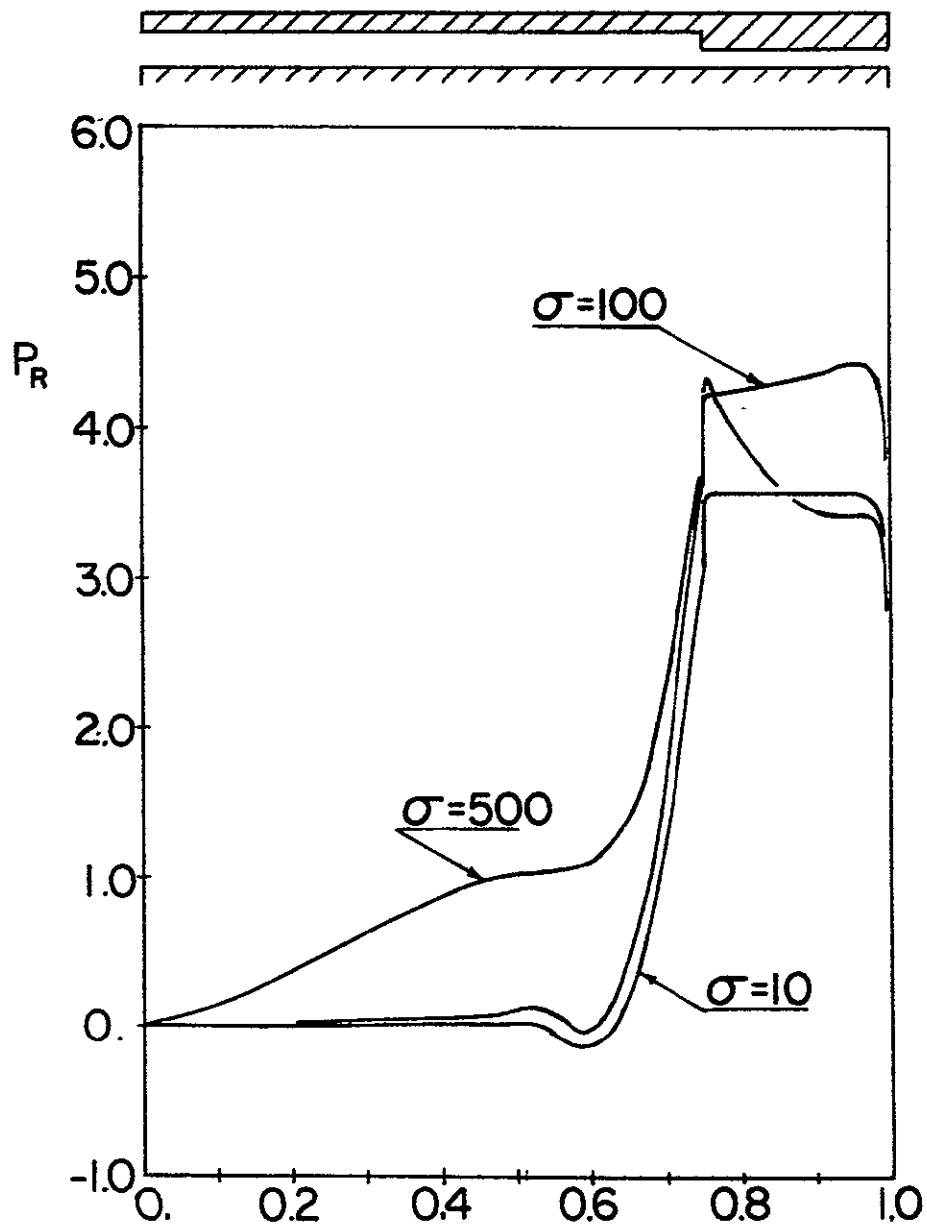


Fig.30 Real pressure profile for $\Lambda=100$, $H_2=0.5$, $B_1/B=0.75$

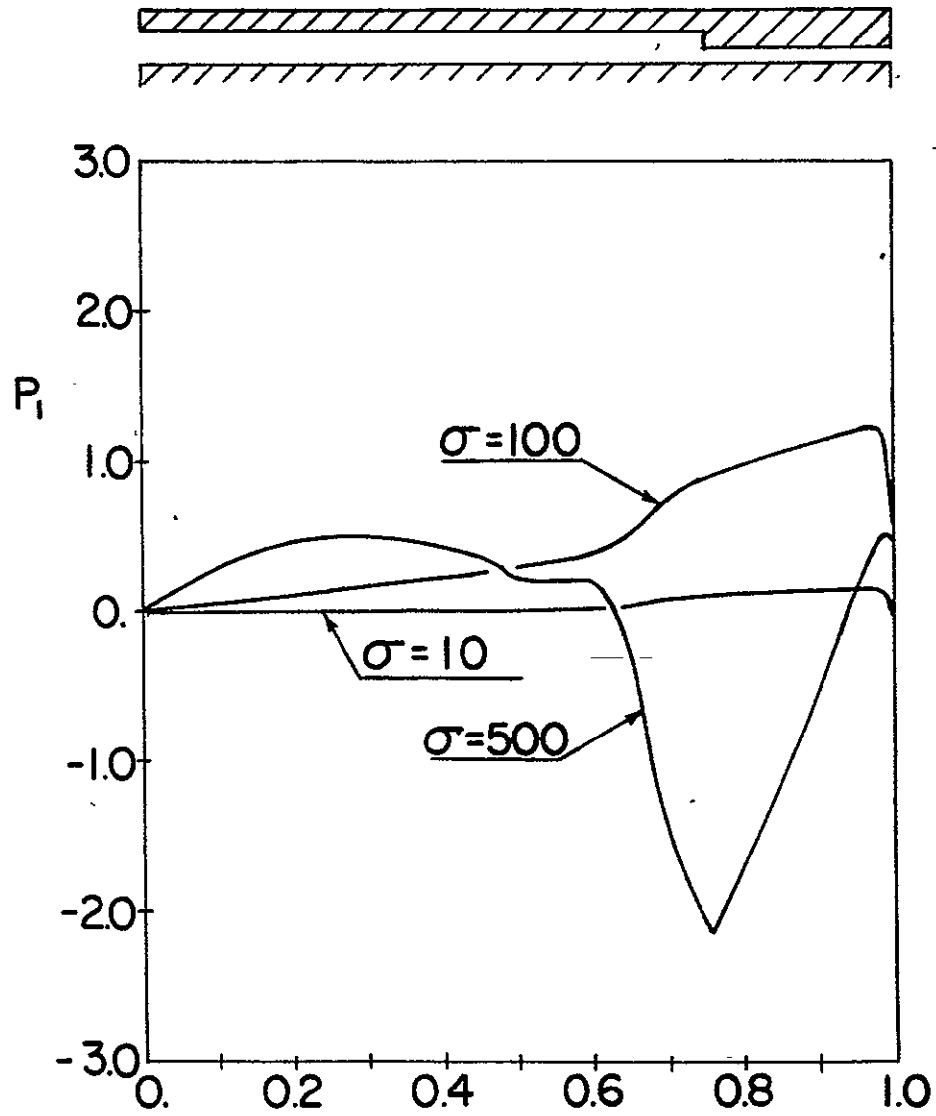


Fig.3I Imaginary pressure profile for $\Lambda=100$,
 $H_2=0.5$, $B_1/B=0.75$

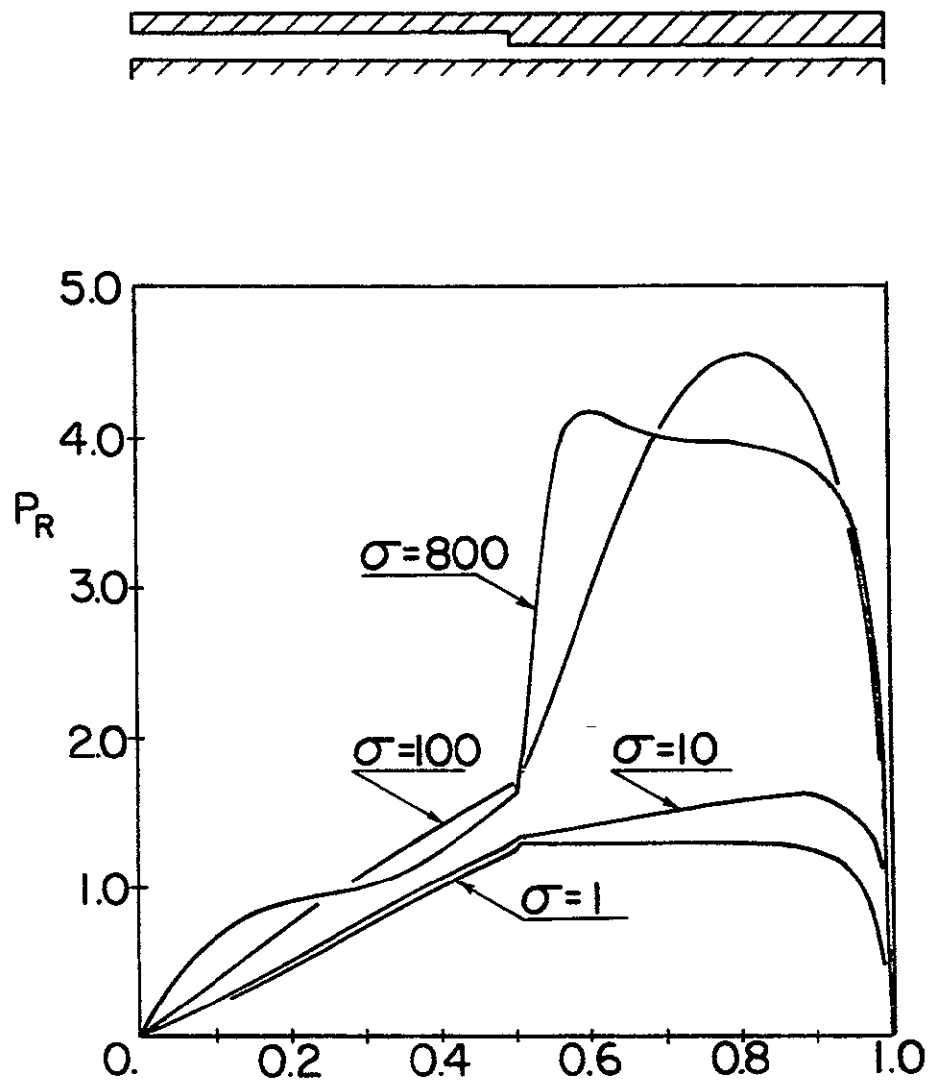


Fig.32 Real pressure profile for $\Lambda=8.4$, $H_2=0.5$, $B_1/B=0.5$.

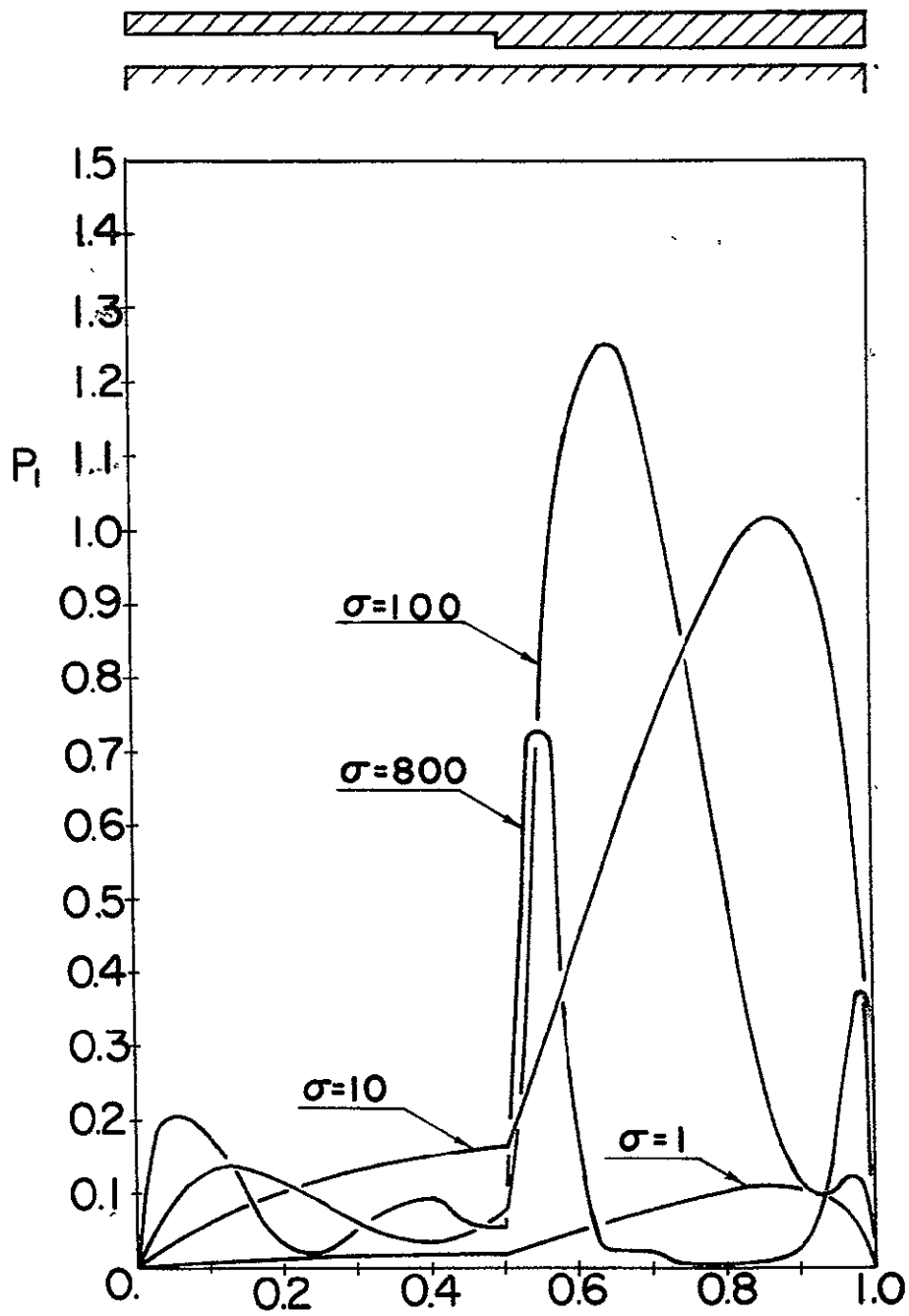


Fig.33 Imaginary pressure profile for $\Lambda=8.4$, $H_2=0.5$, $B_1/B=0.5$

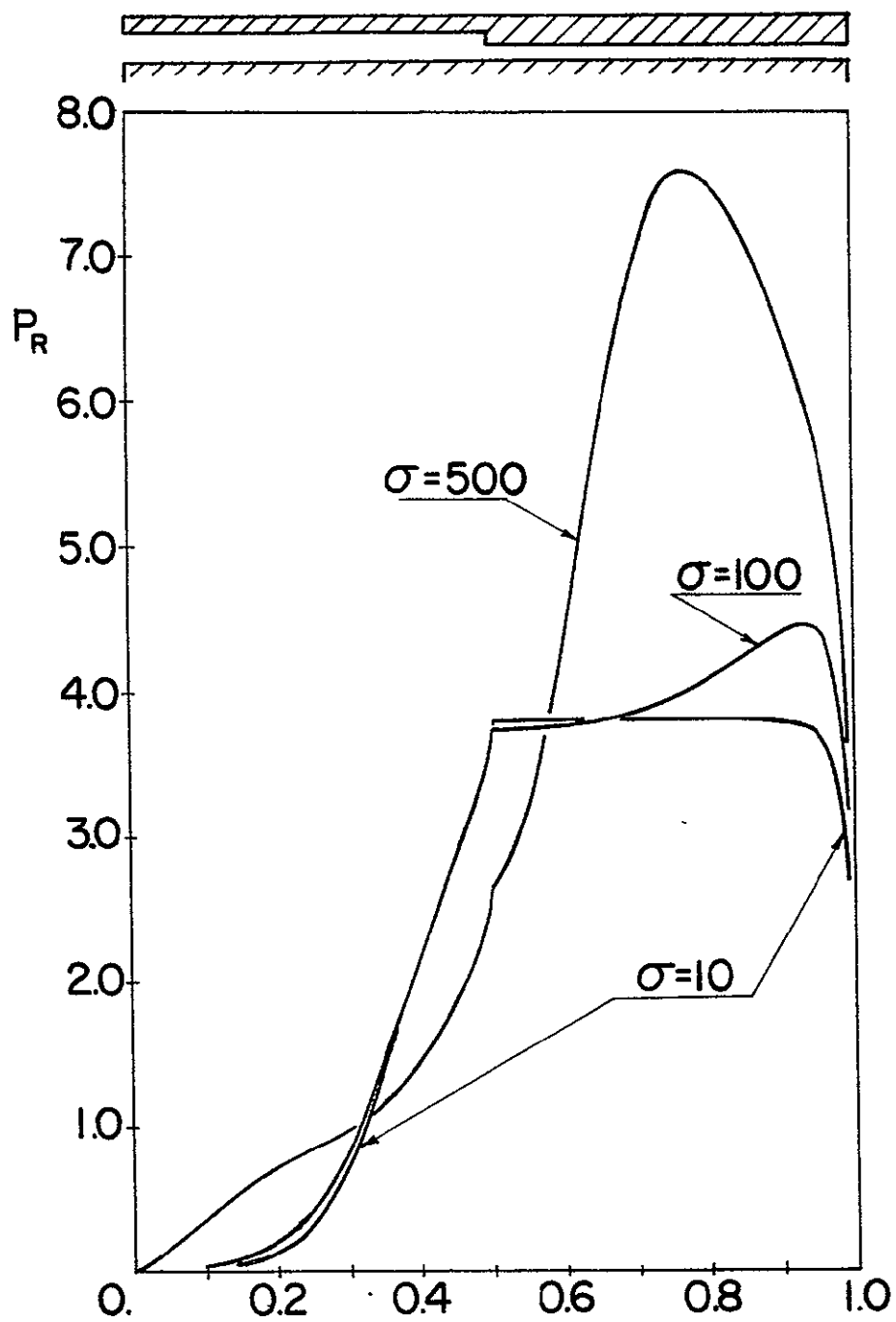


Fig.34 Real pressure profile for $\Lambda=42$, $H_2=0.5$, $B_1/B=0.5$

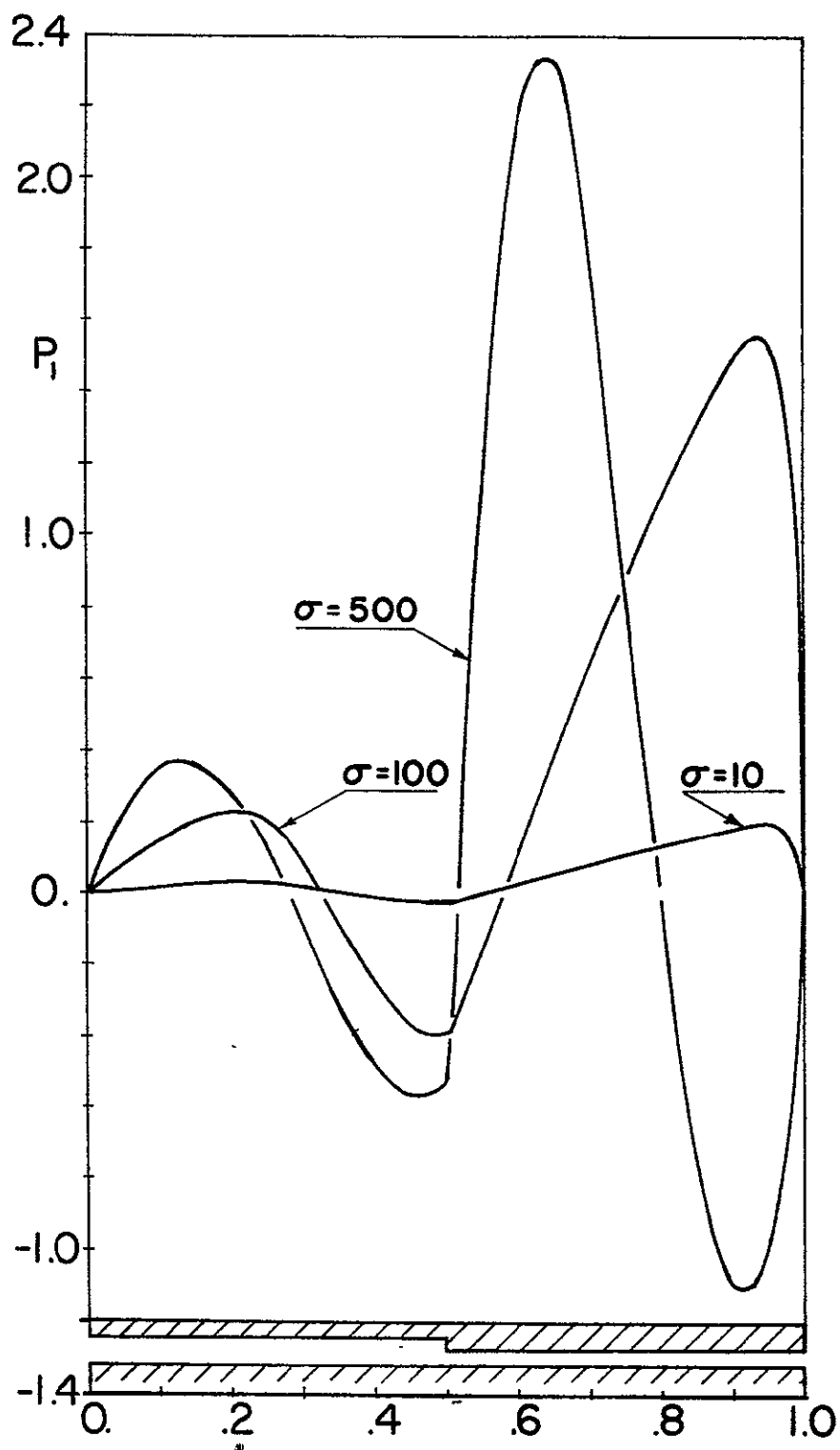


Fig.35 Imaginary pressure profile for $\Lambda=42$, $H_2=0.5$, $B_1/B=0.5$

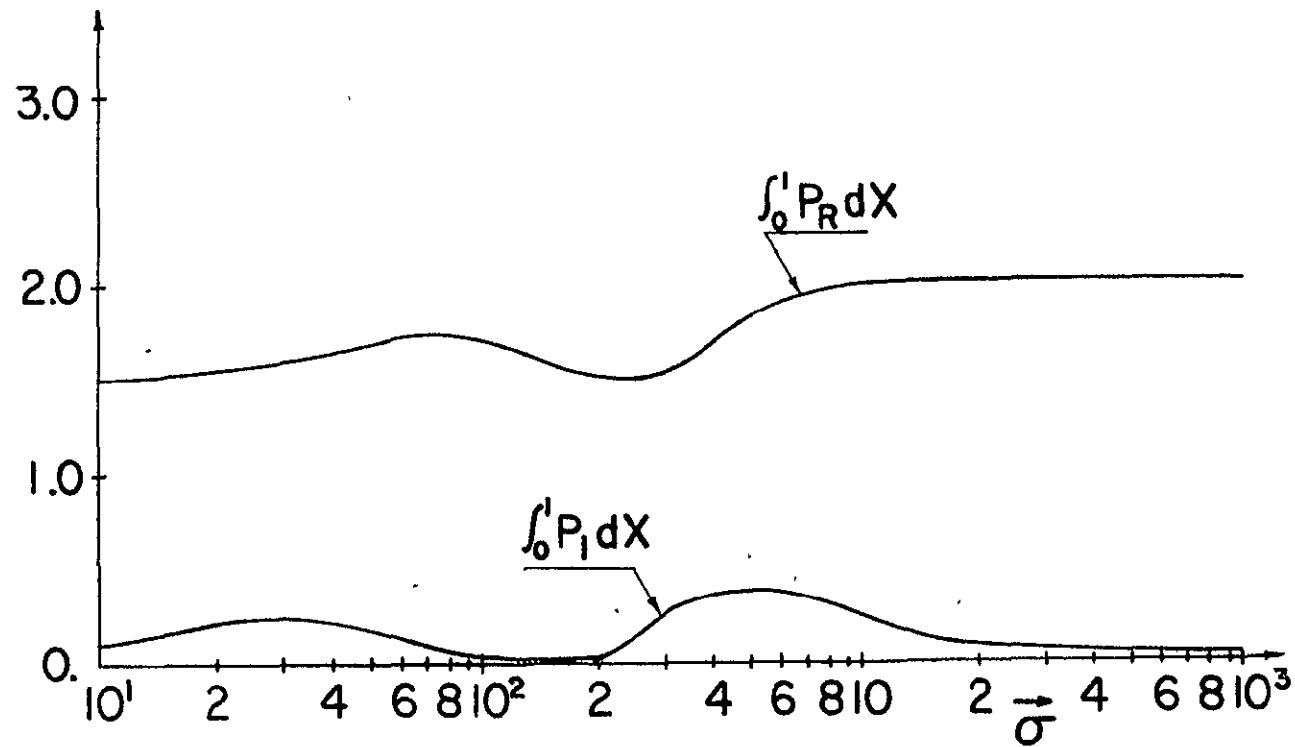


Fig.36 Variation of dynamic bearing forces with the excitation frequency, σ for $B_1/B=0.75$, $\Lambda=42$, $H_2=0.5$

```

PROGRAM RSEAL( INPUT,OUTPUT,TAPE5=INPUT,TAPE6=OUTPUT)
RAYTH
DIMENSION DR(17),DTH(33),HMINA(10),RPSA(10),PAA(10),VISA(10),TH(33
1),R(17),FRC(17),H(17,33),A1(17,33),A2(17,33),A3(17,33),A4(17,33),
2 A5(17,33),A6(17,33),A8(17,33),B(17),C(17),A(17,33),F(17),QSM(17,
317),E(17,17,33),G(17,33),DQ(17,33),P(17,33),Q(17,33),QQQ(33),
4 PP(17),HOUT(10),HDOT(10)
1 FORMAT(72H
1
2 FORMAT(16I5)
3 FORMAT(8F10.7)
+O-MAT (+5,5X,7E10.4/(8E10C4DD
5 FORMAT(6X,4HLAST,6X,4HNPAD,9X, 1HM, 9X, 1HN,8X, 2HIH,8X, 2HJH,7X
1 3HIHH,7X, 3HJHH, /)
6 FORMAT(8I10,/)
7 FORMAT(4X, 6HLKOUNT,5X 5HNDIAG,6X 4HIRRG, 6X,4HNPRES,/)
8 FORMAT(755H "OUTSIDE DIAMETER(INCHES)"
1,E12.5/)
9 FORMAT(55H "INSIDE DIAMETER(INCHES)"
1 E12.5/)
10 FORMAT(55H "THE ANGLE EXTENDING THE POCKET REGION(DEG.)"
1 E12.5/)
11 FORMAT(55H "THE ANGLE EXTENDING THE LAND REGION(DEG.)"
1 E12.5/)
12 FORMAT(55H "STEP DEPTH(INCHES)"
1 E12.5/)
13 FO=FORMAT(55H "OUTER WIDTH OF THE SHOUD(INCHES)"
+12+5/D
14 FORMAT(55H "INNER WIDTH OF THE SHOUD(INCHES)"
1 E12.5/)
15 FORMAT(55H "CONVERGENCE ERROR"
1 E12.5/)
16 FORMAT(54H "GRID SPACINGS IN THE RADIAL DIRECTION(INCHES)" /)
17 FORMAT(54H "GRID SPACINGS IN THE CIRCUMFERENTIAL DIRECTION(DEG)" /)
18 FORMAT(55H "MINIMUM FILM THICKNESS (INCHES)"
1 E12.5/)
19 FORMAT(55H "REVOLUTIONS PER SECOND"
1 E12.5/)
20 "O--ITTH", E12.5)
2
+2S -E0-S++
1 E12.5/)
22 FORMAT(55H "VISCOSITY(LB-SEC/+N$S2)"
1 E12.5/)
23 FORMAT(55H "LAMDA(6.*VIS$6.28$RPS$(RO/HMIN)**2/PA)"
1 E12.5/)
24 FORMAT(12H RB(I),TH(J) )
25 FO=FORMAT(25H "H, H-H, H-H, H-H, H-H, H-H"
2 -- 1TU15+ A1U+TJDTEIC D
27 FO=FORMAT(45H "F(5),BUFD,C(5DTA(5TI=1),A(1,1),AT(5,5+1)",10X,2HI=
1 ,I5,10X,2HJ=,I5)
28 FORMAT(25H "MATRIX IS SINGULAR AT J=13,16H,CASE ABANDONED./TH1)
29 FORMAT(29H "FINAL PRESSURE DISTRIBUTION. //)
30 FORMAT(77H "CASE CONVERGES TO F9.6,
1
14H AFTER 13,11H ITERATI

```

```

10NS)
31 FORMAT( / 10(1X,F11.7))
33 FORMAT('55H FILM THICKNESS AT O.D (INCHES) '
1 E12.5/)
34 FORMAT('755H TOTAL LOAD(LBS)'
1,E12.5/)
35 FORMAT('55H DIMENSIONLESS LOAD=LOAD/(AREA*PA) '
1 E12.5/)
36 FORMAT('55H HORSEPOWE= LOSS '
1 E12.5/,1H1)
37 FORMAT('55H STATIC SQUEEZE FILM VELO (IN/SEC) '
1 E12.5/)
38 FORMAT('15,5X,(8E10.4)')
3 +O-MATU55+ D+MENS+-NLESS STAT+C F+LM VELOC+TY W+TH HO=STEP DEPTH ,
1 E12.5/)
NR=5
NW=6
READ(NR,1)
90 READ(NR,2) LAST,NPAD,M,N,TH,JH,IHH,JHH,LKOUNT,NDTAG,IRRG,NPRE,NSYM
1,ND1
READ(NR,3) DO,DI,THG,THL,STEPD,WO,WI,ERROR
NN=N-1
MM=M-1
WRITE (NW,1)
IF (IRRG.NE.1) GO TO 91
READ(NR,3) (DR(I),I=1,MM)
READ(NR,3) (DTH(J),J=1,NN)
WRITE(NW,16)
WRITE(NW,20) (DR(I),I=1,MM)
WRITE(NW,17)
WRITE(NW,20) (DTH(J),J=1,NN)
TWD=(DO-DI)*0.5
IF (NSYM.EQ.1) TWD=TWD*0.5
TLG=THG+THL
DO 700 I=1,MM
700 DR(I)=DR(I)*TWD
DO 701 J=1,NN
701 DTH(J)=DTH(J)*TLG
GO TO 95
91 FMM=M-1
FNN=N-1
IHH1=IHH-1
AIHH1=IHH-IH
BIH1=M-IHH
IHI=IH-1
AIH1=IHI
IF (NSYM.EQ.1) GO TO 710
IF (IH .EQ. 1) GO TO 709
DO 92 I=1,IHI
92 DR(I)=WI/AIH1
709 DO 97 I=IH,IHH1
97 DR(I)=((DO-DI)*.5-WI-WO)/AIHH1
GO TO 720
710 FIHH1=IHH1

```

```

TEMP=(DO-DT)*0.25-WO/7FIHH1
DO 711 I=1,IHH1
711 DR(I)=TEMP
720 DO 98 I=IHH,MM
98 DR(I)=WO/BIH1
    JHH1=JHH-1
    AJHH1=JHH1
    BJH=N-JHH
    DO 93 J=1,JHH1
93 DTH(J)=THG/AJHH1
    DO 99 J=JHH,NN
99 DTH(J)=THL/BJH
95 CONTINUE
    READ (NR,4) NVISM,(VISA(I),I=1,NVISM),
    READ(NR,4)NRPSM,(RPSAT(I),I=1,NRPSM)
    READ(NR,4)NPAM,(PAA(I),I=1,NPAM)
    READ(NR,4)NHMM,(HMINAT(I),I=1,NHMM)
WRITE INPUT DATA
    READ (NR,3)      (HOUT(I),I=1,NHMM)
    READ (NR,4)      NHDTM,(HDOT(I),I=1,NHDTM)
    WRITE(NW,5)
    WRITE(NW,6)LAST,NPAD,M,N,IH,JH,IHH,JHH
    WRITE(NW,7)
    WRITE(NW,6)LKOUNT,NDIAG,IRRG,NPRE
    WRITE(NW,8)DO
    WRITE(NW,9)DI
    WRITE(NW,10)THG
    WRITE(NW,11)THL
    WRITE(NW,12)STEPD
    WRITE(NW,13)WO
    WRITE(NW,14)WI
    WRITE(NW,15)ERROR
    IF(NDIAG)731,731,730
730 WRITE(NW,16)
    WRITE(NW,20)(DR(I),I=1,MM)
    WRITE(NW,17)
    WRITE(NW,20)(DTH(J),J=1,NN)
731 CONTINUE
    DO 1000 NVIS=1,NVISM
    VIS=VISA(NVIS)
    DO 1000 NRPS=1,NRPSM
    RPS=RPSA(NRPS)
    DO 1000 NPA=1,NPAM
    PA=PAA(NPA)
    DO 96 I=1,M
    DO 96 J=1,N
96 Q(I,J)=1.
    DO 1000 N+DT31TN+DTM
    DO 1000 NHM=1,NHMM
    HMIN=HMINA(NHM)
    CONE=HOUT(NHM)/HMIN
    CONE1=CONE-1.
    WRITE (NW,33) HOUT(NHM)
    WRITE(NW,18)HMIN

```



```

WRITE(NW,19)RPS
WRITE(NW,21)PA
WRITE(NW,22)VIS
O=+TE UNOT3 D +DOTUN+DTD
PI=3.1416
RO=DO/2.0
RI=DI/2.
PLAM=6.*VIS*RPS*2.*PI*((RO/HMIN)**2.)/PA
CHDOT=HDOT(NHDT)/((2.*PI*RPS*HMIN)
CHDT=HDOT(NHDT)/((2.*PI*RPS*STEPD)
WRITE(NW,39) CHDT
STEP=STEPD/HMIN
WRITE(NW,23)PLAM
STEPH=STEP*0.5
CC=0.01745329
GENERATE COORDINATES
TH(1)=0.
NN=N-1
DO 100 J=1,NN
100 TH(J+1)=TH(J)+DTH(J)*CC
R(1)=DI/DO
MM=M-1
DO 105 I=1,MM
105 R(I+1)=R(I)+DR(I)/RO
DIDO=DI/DO
ODIDO=1.-DIDO
L6=1
K8=1
ADMY=1.
109 DO 107 J=1,N
107 H(L6,J)=ADMY
IF (K8.EQ.2) GO TO 108
L6=M
K8=2
ADMY=CONE
GO TO 109
108 DO 106 I=2,MM
RS9=R(I)
DO 106 J=1,N
106 H(I,J)=1.+CONE1*((RS9-DIDO)/ODIDO)**2
IF(NDIAG) I14,I14,I10
110 WRITE(NW,24)
WRITE(NW,20)(R(I),I=1,M)
WRITE(NW,20)(TH(J),J=1,M)
GENERATE A1(I,J) TO A6(I,J)
DO 112 I=1,M
112 WRITE (NW,20) (H(I,J),J=1,N)
114 DO 140 J=2,NN
DZ1=TH(J+1)-TH(J-1)
DZ2=2.*DZ1
DZ3=DZ2*(TH(J)-TH(J-1))
DZ3=1./DZ3
DZ4=1./(DZ2*(TH(J+1)-TH(J)))
DO 140 I=1,MM

```

```

HL=H(I,J-1)
HR=H(I,J+1)
HCH=(H(I,J-1)+H(I,J))*0.5
HRH=(H(I,J+1)+H(I,J))*0.5
HTH=(H(I+1,J)+H(I,J))*0.5
HTEMP=H(I-1,J)
IF(I.EQ.1)HTEMP=H(I,J)
HBH=(HTEMP +H(I,J))*0.5
+ F(J-JHH) 111,120,130
POINTS AT THE LEFT SIDE OF THE STEP
111 IF(I-IH) 130,115,116
POINTS ON THE BOTTOM EDGE
115 IF(NSYM.EQ.1) GO TO 116
735 HL=HL+STEP
HR=HR+STEP
HLH=HLH+STEP
HRH=HRH+STEP
IF(I.EQ.IH)HTH=HTH+STEP
IF(I.EQ.IHH)HBH=HBH+STEP
GO TO 130
116 IF(I-IHH) 117,735,130
POINTS IN THE POCKET
117 HL=HL+STEP
HR=HR+STEP
HCH=HCH+STEP
HRH=HRH+STEP
HTH=HTH+STEP
HBH=HBH+STEP
GO TO 130
120 IF(+-IH) 130,125,126
BOTTOM OR TOP CORNER
125 HL=HL+STEP
HLH=HCH+STEP
IF(I.EQ.IH) HTH=HTH+STEP
IF(I.EQ.IHH) HBH=HBH+STEP
GO TO 130
126 IF(I-IHH) 127,125,130
POINTS ALONG THE VERTICAL EDGE
127 HL=HL+STEP
HLH=HLH+STEP
HTH=HTH+STEP
HBH=HBH+STEP
GO TO 130
130 IF(NDIAG) 132,132,131
131 WRITE(NW,25)
WRITE(NW,20)HL,HR,HLH,HRH,HTH,HBH
GENERATE A1(I,J),ETC
132 RTEM=R(I-1)
DRT=DR(I-1)
IF(I.EQ.1)DRT=DR(I)
IF(I.EQ.1)RTEM=R(I)
TEMP1=PLAM*R(I)/DZ2
TEMP2= 1.0 / (4.0*(DR(I)+DRT) / RO)
A1(I,J)=TEMP1*HL

```

```

A2(I,J)=TEMP1*HR
A3(I,J)=DZ3*HLH**3/R(I)
A4(I,J)=DZ4*HRH**3/R(I)
A5(I,J)=TEMP2*HBH**3/(DRT /RO) *(R(I)+RTEM )
A6(I,J)=TEMP2*HMH**3/(DR(I)/RO) *(R(I)+R(I+1))
A8(I,J)=PLAM*R(I)*CHDOT
IF(NDIAG) 140,140,133
133 WRITE(NW,26)
WRITE(NW,20)A1(I,J),A2(I,J),A3(I,J),A4(I,J),A5(I,J),A6(I,J) ,
1 A8(I,J)
140 CONTINUE
KOUNT=1
141 DO 143 I=1,M
G(I,1)=0.
DO 142 K=1,M
142 E(I,K,1)=0.
143 CONTINUE
DO 370 J=1,N
DO 310 I=1,M
IF(J.EQ.1.OR. J.EQ.N) GO TO 210
IF( I .EQ. 1) GO TO 725
IF( I .EQ. M) GO TO 210
GO TO 726
725 IF(NSYM .NE.1) GO TO 210
726 SQP=SQRT(ABS(Q(I,J+1)))
SQM=SQRT(ABS(Q(I,J-1)))
SQQ=SQRT(ABS(Q(I,J)))
B(I)=A3(I,J)+A1(I,J)/(2.0*SQM)
C(I)=A4(I,J)-A2(I,J)/(2.0*SQP)
ASUM=A3(I,J)+A4(I,J)+A5(I,J)+A6(I,J)
F(I)=A3(I,J)*Q(I,J-1)+A1(I,J)*SQM
QTT=Q(I-1,J)
IF( I .EQ. 1 .AND. NSYM .EQ. 1) QTT=Q(I+1,J)
F(I)=F(I)+A5(I,J)*QTT -ASUM*Q(I,J)+A6(I,J)*Q(I+1,J)+A4(I,J)*Q
1(I,J+1)-A2(I,J)*SQP-A8(I,J)*SQQ
F(I)=-F(I)
DO 150 K=1,M
A(I,K)=0.0
IF(K.EQ.1) A(I,K)=-ASUM-A8*0.5/SQQ
A6TT=A6(I,J)
+F(I+ .EQ. 1 .AND. NSYM .EQ. 1) A6TT=A6(I,J)+A5(I,J)
+F(K.EQ.++1)A(I,K)=A6TT
IF(K.EQ.1)A(I,K)=A5(I,J)
150 CONTINUE
IF(J.NE.JHH) GO TO 305
IF(I.EQ.IH.OR.I.EQ.IHH) GO TO 151
IF(I.GT.IH.AND.I.LT.IHH) GO TO 152
GO TO 305
151 DMSP=STEP*0.5
GO TO 155
152 DMSP=STEP
155 SQQ=SQRT(ABS(Q(I,J)))
TEMP=AT(I,J)*DMSP/(H(I,J-1)+DMSP)
F(I)= F(I)-TEMP*SQQ

```

```

A(I,I)=A(I,I)+TEMP*0.575QQ
305 IF(NDIAG) 310,310,306
306 WRITE(NW,27)I,J
WRITE(NW,20)F(I),B(I),C(I),A(I,I-1),A(I,I),A(I,I+1)
GO TO 310
210 B(I)=0.
C(I)=0.
F(I)=0.
DO 211 K=1,M
A(I,K)=0.
IF(I.EQ.K)A(I,K)=1.
211 CONTINUE
GO TO 305
310 CONTINUE
DO 320 I=1,M
DO 320 K=1,M
320 QSMA(I,K)=A(I,K)+B(I)*E(I,K,J)
CALL MATINV(QSMA,M,BB,0,DET,ID)
GO TO (340,330),ID
340 DO 360 I=1,M
G(I,J+1)=0.
DO 360 K=1,M
G(I,J+1)=G(I,J+1)+QSMA(I,K)*(F(K)-B(K)*G(K,J))
E(I,K,J+1)=-QSMA(I,K)*C(K)
360 CONTINUE
370 CONTINUE
DMA=0.
DO 380 I=1,M
DMA=AMAX1(DMA,ABS(G(I,N+1)))
380 DQ(I,N)=G(I,N+1)
DO 400 JJ=2,N
J=N+2-JJ
DO 400 I=1,M
DUM=0.
DO 390 K=1,M
390 DUM=DUM+E(I,K,J)*DQ(K,J)
DUM=DUM+G(I,J)
DMA=AMAX1(DMA,ABS(DUM))
400 DQ(I,J+1)=DUM
DO 401 I=1,M
DO 401 J=I,N
401 Q(I,J)=Q(I,J)+DQ(I,J)
IF(NDIAG)405,405,402
402 DO 403 J=1,N
403 WRITE(NW,20)(DQ(I,J),I=1,M)
DO 404 J=1,N
404 WRITE(NW,20)(Q(I,J),I=1,M)
405 CONTINUE
GO TO 560
330 WRITE(NW,28)J
GO TO 1000
560 KOUNT=KOUNT+1
IF(KOUNT.GE.LKOUNT) GO TO 561
IF(DMA.GT.ERROR) GO TO 141

```

```

561 WRITE(NW,30)ERROR,KOUNT
IF(NPRE.EQ.1) WRITE(NW,29)
DO 576 J=1,N
DO 576 I=1,M
P(I,J)=SQRT(ABS(Q(I,J)))
576 CONTINUE
DO 585 I=1,M
IF(NPRE.EQ.1)WRITE(NW,31)(P(I,J),J=1,N)
DO 580 J=1,N
580 QQQ(J)=P(I,J)-1.
NN=N-1
PP(I)=0.
DO 581 J=1,NN
581 PP(I)=PP(I)+DTH(J)*(QQQ(J)+QQQ(J+1))*0.5
PP(I)=R(I)*CC*PP(I)
IF(ND1)585,585,800
800 WRITE(NW,31)PP(I)
585 CONTINUE
FPAD=NPAD
MM=M-1
WLOAD=0.
DO 589 I=1,MM
589 WLOAD=WLOAD+DR(I)*(PP(I)+PP(I+1))*0.5
WLOAD=WLOAD*RO*PA*FPAD
IF(NSYM.EQ.1)WLOAD=2.0*WLOAD
WBAR=WLOAD/(3.1416*(RO**2-RI**2)*PA)
IF(NSYM.EQ.1)WBAR=2.*WBAR
DO 600 I=1,M
IF(I.EQ.IH.OR.I.GT. IH) GO TO 593
591 FRC(I)=0.
NN=N-1
DO 592 J=1,NN
592 FRC(I)=FRC(I)+DTH(J)/H(I,J)
FRC(I)=FRC(I)*CC*R(I)**3
GO TO 600
593 IF (I.GT.IHH) GO TO 591
FRC(I)=0.
NN=N-1
DO 594 J=1,NN
IF(J.EQ.JHH.OR.J.GT.JHH) TEMP=1.0/H(I,J)
IF(J.LE.JHH)TEMP=1.0/(H(I,J)+STEP)
594 FRC(I)=FRC(I)+DTH(J)*TEMP
FRC(I)=FRC(I)*CC*R(I)**3
600 CONTINUE
MM=M-1
HPOW=0.
DO 605 I=1,MM
605 HPOW=HPOW+FRC(I)*DR(I)
HPOW=HPOW*VIS*6.2832*RPS*-O**3
HPOW=HPOW*FPAD*RPS*60./63000.0
HPOW=HPOW/HMIN
IF(NSYM.EQ.1) HPOW=2.0*HPOW
WRITE(NW,34)WLOAD
WRITE(NW,35)WBAR

```

```

WRITE (NW,36) HPOW
1000 CONTINUE
    IF (LAST) 90,90,1001
1001 STOP
    END

```

SUB-OUT+NE MATINVUATN1,BTM1,DETE- ,ID)
 MATRIX INVERSION WITH ACCOMPANYING SOLUTION OF LINEAR EQUATIONS
 NOVEMBER 1962 S GOOD DAVID TAYLOR MODEL BASIN AM MAT1

MAT10002
 MAT10003
 MAT10004

DIMENSION A(17,17),B(17,1),INDEX(17,3)

MAT10006
 MAT10007
 MAT10009

GENERAL FORM OF DIMENSION STATEMENT

EQUIVALENCE (IROW,JROW), (ICOLU ,JCOLU), (AMAX, T, SWAP)

MAT10012
 MAT10013
 MAT10014
 MAT10015
 MAT10016

INITIALIZATION

```

M=M1
N=N1
10 DETER =1.0
15 DO 20 J=1,N
20 INDEX(J,3) = 0
30 DO 550 I=1,N

```

MAT10018
 MAT10019
 MAT10020
 MAT10021
 MAT10022
 MAT10023
 MAT10024
 MAT10025
 MAT10026
 MAT10027
 MAT10028

SEARCH FOR PIVOT ELEMENT

```

40 AMAX=0.0
45 DO 105 J=1,N
    IF(INDEX(J,3)-1) 60, 105, 60
60 DO 100 K=1,N
    +F(INDEX(K,3)-1) 80, 100, 715
80 IF (      AMAX -ABS (A(J,K))) 85, 100, 100
    5 + -OW3J
    0 +COLU =K
    AMAX=ABS JA(J,K)
100 CONTINUE
105 CONTINUE
    INDEX(+COLU ,3) = INDEX(+COLU ,3) +1
260 INDEX(I,T)=IROW
270 INDEX(I,2)=ICOLU

```

MAT10030

 MAT10033
 MAT10034

 MAT10036

INTERCHANGE ROWS TO PUT PIVOT ELEMENT ON DIAGONAL

MAT10038
 MAT10039
 MAT10040

```

130 IF (IROW-ICOLU ) 140, 310, 140
140 DETER==DETER
150 DO 200 L=1,N
160 SWAP=ATIROW,L)
170 A(IROW,L)=A(ICOLU ,L)
200 A(ICOLU ,L)=SWAP
    +F(M) 310, 310, 210

```

MAT10043
 MAT10044

 MAT10047

210 DO 250 L=1,M	MAT10048
220 SWAP=B(+OW,L)	MAT10049
230 B(IROW,L)=B(ICOLU ,L)	
250 B(ICOLU ,L)=SWAP	
DIV+DE PIVOT ROW BY PIVOT ELEMENT	
310 PIVOT =A(ICOLU ,ICOLU)	MAT10052
DETER=DETER*PIVOT	MAT10000
330 A(+COLU ,+COLU)=1.0	MAT10053
340 DO 350 L=1,N	MAT10057
350 A(ICOLU ,L)=A(ICOLU ,L)/PIVOT	
355 +F(M) 380, 380, 360	MAT10059
360 DO 370 L=1,M	MAT10060
370 B(ICOLU ,L)=B(ICOLU ,L)/PIVOT	
-EDUCE NON-PIVOT -OWS	
380 DO 550 LI=1,N	MAT10062
390 IF(LI-ICOLU) 400, 550, 400	MAT10063
400 T=A(LI,ICOLU)	MAT10064
420 A(LI,ICOLU)=0.0	MAT10065
IF(T)430,550,430	
430 DO 450 L=1,N	MAT10069
450 A(LI,L)=A(LI,L)-A(ICOLU ,L)*T	
455 IF(M) 550, 550, 460	MAT10071
460 DO 500 L=1,M	MAT10072
500 B(LI,L)=B(LI,L)-B(ICOLU ,L)*T	
550 CONTINUE	MAT10074
INTERCHANGE COLUMNS	
600 DO 710 I=1,N	MAT10075
610 L=N+1-I	MAT10076
620 IF (INDEX(L,1)-INDEX(L,2)) 630, 710, 630	MAT10077
630 JROW=INDEX(L,1)	MAT10078
640 JCOLU=INDEX(L,2)	MAT10079
650 DO 705 K=1,N	MAT10080
660 SWAP=A(K,JROW)	MAT10081
670 A(K,JROW)=A(K,JCOLU)	
700 A(K,JCOLU)=SWAP	MAT10083
705 CONTINUE	MAT10084
710 CONTINUE	MAT10087
DO 730 K = 1,N	MAT10088
IF(INDEX(K,3)-I) 715,720,715	MAT10089
720 CONTINUE	MAT10090
730 CONTINUE	MAT10093
ID=1	MAT10094
740 =ETU=N	MAT10096
715 ID =2	MAT10091
GO TO 740	MAT10092
END	

Card 1 Format (72 H)

Identification Card

Card 2 Format (16I5)

Last - Integer to determine whether additional input data
are to be read

Last = 1 , no more input data

Last = 0 , more input data to be read from state-
ment 90.

NPAD - Number of pads (see Fig.A2)

M - Number of grids in the radial direction

N - Number of grids in the circumferential direction

IH - Grid number for the bottom edge of the step (see Fig. A2)
For NSYM=1, set IH-1

IHH - Grid number for the top edge of the step (see Fig. A2)

JH - Set JH=1

JHH - Grid number for the left edge of the step

LKOUNT - Maximum number of iterations allowed for the pressure
calculation (recommended value: 10-20)

NDIAG - Control for diagnostics

NDIAG = 1 , diagnostics print out

NDIAG = 0 , no diagnostics

IRRG - Control for irregular grids

IRRG = 1 , read in irregular grid spacings

IRRG = 0 , uniform grid spacing

NPRE - Control for printing out pressure profile

NPRE = 1 , print out pressure

NPRE = 0 , no pressure print out

NYSM - This integer is used to control whether pressure
calculation is made for a full pad or half a pad as
in the case where the pressure is symmetrical about

the center line (see Fig.A2).

NYSM = 0 , For calculation covering full pad

NYSM = 1 , For symmetrical pressure profiles where
where calculation is only made for half a pad.

ND1 - Set ND1 = 0 , for normal runs.

Card 3 Format (8F10.7)

DO - Outside diameter of thrust brg.,
 d_o in Fig.A1 (in.)

DI - d_i in Fig.A1 (in.)

THG - Angle extending the pocket region, θ_g in Fig.A2, (degrees)

THL - Angle extending the land region, θ_L in Fig.A2, (degrees)

STEPD - Depth of the step (in.)

WO - Outerwidth of the shroud, W_o in Fig.A2, (in.)

WI - Innerwidth of the shroud, W_i in Fig.A2 (in.)

ERROR - Convergence factor for pressure iteration.
(recommended value: .001 - .0002)

Card 4 Format (8F 10.7)

This card is required only when IRRG = 1

DR(I), I = 1, MM - Dimensionless irregular gird spacings in the radial
direction. (MM - M-1)

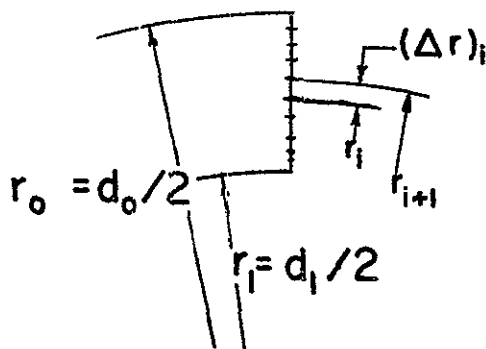


Fig.A1

$$DR(I) = \frac{(\Delta r)_i}{(r_o - r_i)}$$

$$= \frac{r_{i+1} - r_i}{r_o - r_i}$$

Card 5 Format (8F 10.7)

This card is required only when IRRG = 1

DTH(J), J = 1, NN - Dimensionless grid spacings in the circumferential direction. (NN = N-1)

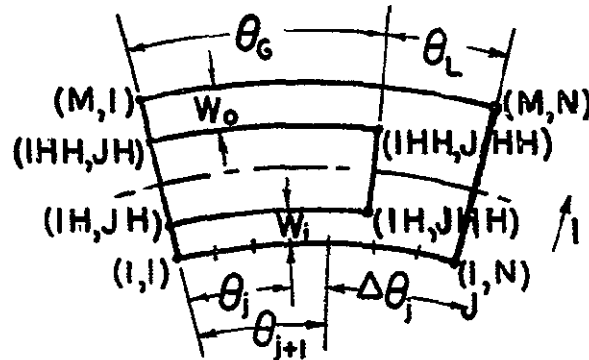


Fig. A-2

$$DTH(J) = \frac{(\Delta\theta)_j}{\theta_L + \theta_G} = \frac{\theta_{j+1} - \theta_j}{\theta_L + \theta_G}$$

Card 6 Format (I5, 5X, 7E 10.3)

NVISM - Total number of viscosities to be investigated in the production run.

VISA(I), I = 1, NVISM

The array of viscosities, (lb-sac/in²)

Card 7 Format (I5, 5X, 7E 10.3)

NRPSM - Total number of angular speeds to be investigated in the production run.

RPSA(I), I = 1, NRPSM

The array of angular speeds, (Rev. per sec.)

Card 8 Format (I5, 5X, 7E 10.3)

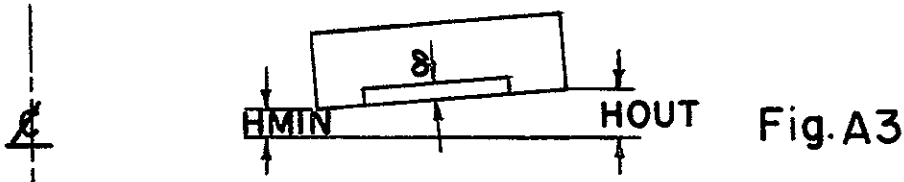
NPAM - Total number of ambient pressure to be investigated in the production run.

PAA(I), I = 1, NPAM

The array of ambient pressure, (PSI)

Card 9 Format (I5, 5X, 7E 10.3)

This card reads in the film thickness to be investigated in the production run. In the case of a parallel film, the film thickness in the land region will be read in the array designated as HMINA(I). In the case of non-parallel film with an axisymmetric coning of dishing, HMINA (I) represents the film thickness at the inside diameter in the land region. The film thickness at the outside diameter is HOUT(I) which read in Card 10.



The variables to be read in this card are:

NHMM - Total number of film thickness to be investigated in the production run.

HMINA(I), I = 1, NAMM

HMINA is the film thickness at the inside diameter in the land region (inch)

Card 10 Format (8F 10.7)

HOUT(I), I = 1, NHMM

- HOUT is the film thickness at the outside diameter in the land region. (inch)

Card 11 Format (I5, 5X, 7E 10.4/(8E10.4)

NHDTM - Total number of velocity or time variation of gas film thickness to be investigated in the production run.

HDOT(I) - Array of velocity or time variation of gas film thickness in in./sec.

```

PROGRAM RSGALN(INPUT,OUTPUT)
DIMENSION WN(30), QN(7), AG(9), AOG(9)
DIMENSION AHA(100), F1A(100), F2A(100), F3A(100), F4A(100), F1(9)
DIMENSION F5A(100), F6A(100), F7A(100), F8A(100), F9A(100)
THE TABLES ARE PREPARED IN THE FOLLOWING ORDER THAT (FJA(I), J=1,9)
= ( D1*I1, D2*I1A, D1*I4, D2*I4A, -D2*I1A0, -D2*I4A0, D2*I5/HO**2.5
, DI*I5A/HO**2.5, -D2*I5A0/HO**2.5 ).
DATA F1A(1)/0./, F2A(1)/7.854/, F3A(1)/3.1416/, F4A(1)/0./
DATA(F1A(I), I=2,60)/ 7.8555281E-02, 1.5720341E-01, 2.3603750E-01,
2 3.1515123E-01, 3.9463912E-01, 4.7459680E-01, 5.5512133E-01,
2 6.3631146E-01, 7.1826801E-01, 8.0109411E-01, 8.8489560E-01,
2 9.6978133E-01, 1.0558636E+00, 1.1432584E+00, 1.2320861E+00,
2 1.3224715E+00, 1.4145448E+00, 1.5084415E+00, 1.6043034E+00,
2 1.7022791E+00, 1.8025243E+00, 1.9052031E+00, 2.0104879E+00,
2 2.1185609E+00, 2.2296146E+00, 2.3438529E+00, 2.4614919E+00,
2 2.611E+00, 2.707 04 E+00, 2.8371835E+00, 2. 708745E+00,
2 3.10 2748E+00, 3.2527020E+00, 3.4014964E+00, 3.5560237E+00,
2 3.7166766E+00, 3.8387 1E+00, 4.0580843E+00, 4.23 7876E+00,
2 4.42 5206E+00, 4.6278602E+00, 4. 354321E+00, 5.0529163E+00,
2 5.2810529E+00, 5.5206483E+00, 5.7725837E+00, 6.0378224E+00,
2 6.3174205E+00, 6.6125372E+00, 6.9244476E+00, 7.2545570E+00,
2 7.6044175E+00, 7.9757465E+00, 8.3704491E+00, 8.7906429E+00,
2 9.2386874E+00, 9.7172183E+00, 1.0229187E+01, 1.0777908E+01/
DATAUF1AU+), I=61,100)/
2 1.1367114E+01, 1.2001018E+01, 1.2584396E+01, 1.3422673E+01,
2 1.4222038E+01, 1.5089573E+01, 1.6033412E+01, 1.7062939E+01,
2 1.8189023E+01, 1.942430 E+01, 2.0783580E+01, 2.2284206E+01,
2 2.3946707E+01, 2.5795465E+01, 2.7859629E+01, 3.0174285E+01,
2 3.2781965E+01, 3.5734627E+01, 3.9096287E+01, 4.2946530E+01,
2 4.7385298E+01, 5.2539475E+01, 5.8572095E+01, 6.5695462E+01,
2 7.4190157E+01, 8.4433212E+01, 9.6940826E+01, 1.1243492E+02,
2 1.31 5000E+02, 1.57010 5E+02, 1.8994101E+02, 2.3442157E+02,
2 2.9656997E+02, 3.871653 E+02, 5.2666744E+02, 7.5788976E+02,
2 1.1832960E+03, 2.1018302E+03, 4.7245976E+03, 1.8878381E+04/
DATA(F2A(I), I=2,60)/ 7.8586215E+00, 7.8725551E+00, 7.8958239E+00,
2 7.9284975E+00, 7.9706737E+00, 8.0224795E+00, 8.0840712E+00,
2 8.1556360E+00, 8.2373922E+00, 8.3295914E+00, 8.4325193E+00,
2 8.5464976E+00, 8.6718859E+00, 8.8090839E+00, 8.9585338E+00,
2 9.1207230E+00, 9.2961871E+00, 9.4855135E+00, 9.6893451E+00,
2 9.9083843E+00, 1.01433 8E+01, 1.0395223E+01, 1.0664772E+01,
2 1.0953037E+01, 1.1261104E+01, 1.1590152E+01, 1.1941467E+01,
2 1.2316453E+01, 1.2716640E+01, 1.3143699E+01, 1.3599453E+01,
2 1.4085 5E+01, 1.4605207E+01, 1.5159776E+01, 1.575221 E+01,
2 1.6385407E+01, 1.7062493E+01, 1.7786946E+01, 1.8562586E+01,
2 1.9393624E+01, 2.0284712E+01, 2.1240995E+01, 2.2268170E+01,
2 2.3372563E+01, 2.4561200E+01, 2.5841910E+01, 2.7223422E+01,
2 2.8715497E+01, 3.0329068E+01, 3.2076405E+01, 3.3971315E+01,
2 3.602 365E+01, 3.8268150E+01, 4.0707613E+01, 4.3370409E+01,
2 4.6282353E+01, 4.9472941E+01, 5.2975980E+01, 5.6830339E+01/
DATA(F2A(I), I=61,100)/
2 6.1080856E+01, 6.5779435E+01, 7.0986379E+01, 7.6772024E+01,
2 8.3218737E+01, 9.0423387E+01, .8500418E+01, 1.0758568E+02,
2 1.1784127E+02, 1.2946160E+02, 1.4268123E+02, 1.5778484E+02,

```

```

2 1.7512021E+02, 1.9511517E+02, 2.1829994E+02, 2.4533690E+02,
2 2.7706071E+02, 3.14532 6E+02, 3.5911751E+02, 4.1258599E+02,
2 4.7726736E+02, 5.5626382E+02, 6.5376773E+02, 7.7553624E+02,
2 9.2961755E+02, 1.12748 5E+03, 1.3858938E+03, 1.7298827E+03,
2 2.1980610E+03, 2.8519737E+03, 3.7937283E+03, 5.2009564E+03,
2 7C400 326E+03, 1C1041001E+04 1C7522447E+04, 3.0261024E+04,
2 5.9068684E+04, 1.3993135E+05, 4.7198425E+05, 3.7735728E+06/
++ OF A0++0+ 2060D/ 3.1419510E+00, 3.1429824E+00, 3.1447027E+00,
2 3.1471142E+00, 3.1502198E+00, 3.1540235E+00, 3.1585298E+00,
2 3.1637446E+00, 3.1696743E+00, 3.1763265E+00, 3.1837096E+00,
2 3.1918331E+00, 3.2007075E+00, 3.2103442E+00, 3.2207558E+00,
2 3.2319562E+00, 3.2439602E+00, 3.2567839E+00, 3.2704448E+00,
2 3.2849616E+00, 3.3003546E+00, 3.3166453E+00, 3.3338569E+00,
2 3.3520144E+00, 3.3711442E+00, 3.3912749E+00, 3.4124369E+00,
2 3.4346625E+00, 3.4579865E+00, 3.4824458E+00, 3.5080801E+00,
2 3.5349315E+00, 3.5630451E+00, 3.5924691E+00, 3.6232549E+00,
2 3.6554576E+00, 3.6891360E+00, 3.7243531E+00, 3.7611763E+00,
2 3.7996778E+00, 3.8399352E+00, 3.8820315E+00, 3.9260561E+00,
2 3.9721049E+00, 4.0202812E+00, 4.0706963E+00, 4.1234702E+00,
2 4.1787323E+00, 4.2366228E+00, 4.2972932E+00, 4.3609078E+00,
2 4.4276449E+00, 4.4976984E+00, 4.5712794E+00, 4.6486182E+00,
2 4.7299663E+00, 4.81559 1E+00, 4.9058188E+00, 5.0009572E+00/
DATA(F3A(I),I=61,100)/
2 5.1013801E+00, 5.2074911E+00, 5.3197370E+00, 5.4386134E+00,
2 5.5646716E+00, 5.6985265E+00, 5.8408664E+00, 5.9924634E+00,
2 6.1541 75E+00, 6.3270215E+00, 6.5120806E+00, 6.7106352E+00,
2 6.9241382E+00, 7.1542599E+00, 7.4029288E+00, 7.6723848E+00,
2 7.9652429E+00, 8.2845764E+00, 8.6340204E+00, 9.0179069E+00,
2 .44143 0E+00, .9109212E+00, 1.0434067E+01, 1.1020413E+01,
2 1.1681892E+01, 1.2433635E+01, 1.3295114E+01, 1.4291818E+01,
2 1.5457768E+01, 1.6839404E+01, 1.8501808E+01, 2.0539089E+01,
2 2.3092560E+01, 2.6384528E+01, 3.0785914E+01, 3.6965137E+01,
2 4.6260583E+01, 6.1798892E+01, 9.2971744E+01, 1.8680213E+02/
+AT1UF4AU+DT+32T60D/ 6. 736515E-02, 1.3755 14E-01, 2.0655024E-01,
2 2.7579871E-01, 3.4539021E-01, 4.1541249E-01, 4.8595458E-01,
2 5.5710716E-01, 6.2896280E-01, 7.0161625E-01, 7.7516481E-01,
2 8.4970863E-01, 9.2535102E-01, 1.0021989E+00, 1.0803631E+00,
2 1.1599589E+00, 1.2411062E+00, 1.3239304E+00, 1.4085626E+00,
2 1.4951401E+00, 1.5838073E+00, 1.6747161E+00, 1.7680265E+00,
2 1.8639077E+00, 1.9625385E+00, 2.0641085E+00, 2.1688189E+00,
2 2.2768835E+00, 2.3885300E+00, 2.5040014E+00, 2.6235570E+00,
2 2.7474742E+00, 2.8760502E+00, 3.0096038E+00, 3.1484776E+00,
2 3.2930400E+00, 3.4436882E+00, 3.6008507E+00, 3.7649907E+00,
2 3.9366095E+00, 4.1162504E+00, 4.3045037E+00, 4.5020110E+00,
2 4.7094711E+00, 4.9276467E+00, 5.1573713E+00, 5.3995573E+00,
2 5.6552054E+00, 5.9254154E+00, 6.2115978E+00, 6.5144879E+00,
2 6.8361620E+00, 7.1780548E+00, 7.5419812E+00, 7.9299605E+00,
2 8.3442447E+00, 8.7873513E+00, 9.2621024E+00, 9.7716694E+00/
DATA(F4A(I),I=61,100)/
2 1C031 627E+01, 1.0 10015E+01 1C1547415E+01, 1.2237038E+01,
2 1.2984832E+01, 1.3797611E+01, 1.4683210E+01, 1.5650673E+01,
2 1.6710487E+01, 1.7874863E+01, 1.9158091E+01, 2.0576979E+01,
2 2.2151398E+01, 2.3904986E+01, 2.5866029E+01, 2.8068606E+01,
2 3C0554070E+01, 3C3372 1E+01 3C6587731E+01, 4.0275 05E+01,

```

```
2 4.4535078E+01, 4.9489238E+01, 5.5297872E+01, 6.2168873E+01,
2 7.0377289E+01, 8.0293107E+01, 9.2423422E+01, 1.0747819E+02,
2 1.2647590E+02, 1.5091947E+02, 1.8310120E+02, 2.2665762E+02,
2 2.8763837E+02, 3.7671568E+02, 5.1416995E+02, 7.4249041E+02,
2 1.1634881E+03, 2.0745753E+03, 4.6822333E+03, 1.8789967E+04/
DATA(F5A(I),I=1,59)/ 0. , 2.7497442E-01,5.5045962E-01,
2 8.2696846E-01, 1.1050180E+00, 1.3851315E+00, 1.6678408E+00,
2 1.9536883E+00, 2.2432295E+00, 2.5370353E+00, 2.8356944E+00,
2 3.13 8161E+00, 3.4500330E+00, 3.7670041E+00, 4.0914178E+00,
2 4.4239953E+00, 4.7654945E+00, 5.1167138E+00, 5.4784962E+00,
2 5.8517341E+00, 6.2373745E+00, 6.6364245E+00, 7.0499568E+00,
2 7.4791171E+00, 7.9251312E+00, 8.3893125E+00, 8.8730716E+00,
2 9.3779257E+00, 9.9055097E+00, 1.0457588E+01, 1.1036068E+01,
2 1.1643017E+01, 1.2280673E+01, 1.2951473E+01, 1.3658065E+01,
2 1.4403336E+01, 1.5190438E+01, 1.6022818E+01, 1.6904250E+01,
2 1.7 38 77E+01, 1.831251E+01, 1.886382E+01, 2.1009798E+01,
2 2.2207604E+01, 2.3486560E+01, 2.4854161E+01, 2.6318738E+01,
2 2.7889564E+01, 2.9576990E+01, 3.1392586E+01, 3.3349322E+01,
2 3.5461763E+01, 3.7746313E+01, 4.0221486E+01, 4.2908234E+01,
2 4.5830332E+01, 4.9014836E+01, 5.2492622E+01, 5.6299036E+01/
DATA(F5A(I),I=60,100)/
2 6.0474671E+01, 6.5066298E+01, 7.0128000E+01, 7.5722544E+01,
2 8.1923058E+01, 8.8815087E+01, 9.6499133E+01, 1.0509380E+02,
2 1.1473976E+02, 1.2560462E+02, 1.3788928E+02, 1.5183581E+02,
2 1.6773775E+02, 1.8595332E+02, 2.0692274E+02, 2.3119103E+02,
2 2.5943838E+02, 2.9252105E+02, 3.3152694E+02, 3.7785238E+02,
2 4.3330926E+02, 5.0027714E+02, 5.8192238E+02, 6.8251978E+02,
2 8.0793374E+02, 9.6635414E+02, 1.1694491E+03, 1.4342207E+03,
2 1.7860852E+03, 2.2641687E+03, 2.9307839E+03, 3.8892080E+03,
2 5.3189242E+03, 7.5502829E+03, 1.1236044E+04, 1.7787769E+04,
2 3.0642697E+04, 5.9654177E+04, 1.4098798E+05, 4.7435606E+05,
2 3.7830331E+06/
DATA(F6A(I),I=1,59)/ 7.8540184E+00, 7.8555648E+00, 7.8602071E+00,
2 7.8679533E+00, 7.8788175E+00, 7.8928191E+00, 7.9099834E+00,
2 7.9303414E+00, 7.9539300E+00, 7.9807924E+00, 8.0109779E+00,
2 8.0445422E+00, 8.0815478E+00, 8.1220643E+00, 8.1661682E+00,
2 8.2139440E+00, 8.265483 E+00, 8.3208885E+00, 8.3802672E+00,
2 8.4437389E+00, 8.5114321E+00, 8.5834860E+00, 8.6600507E+00,
2 8.7412 3E+00, 8.8273737E+00, 8.9184 52E+00, 9.0148555E+00,
2 9.1166732E+00, 9.2241836E+00, 9.3376399E+00, 9.4573150E+00,
2 9.583502 E+00, 9.7165205E+00, 9.8567093E+00, 1.0004438E+01,
2 1.0160104E+01, 1.0324138E+01, 1.0497005E+01, 1.0679206E+01,
2 1.0871287E+01, 1.1073838E+01, 1.1287501E+01, 1.1512970E+01,
2 1.1751005E+01, 1.2002430E+01, 1.2268144E+01, 1.2549132E+01,
2 1.2 46467E+01, 1.29316132 E+01, 1.32495011E+01, 1.35848932E+01,
2 1.4224658E+01, 1.4623916E+01, 1.5048615E+01, 1.5500868E+01,
2 1.5983024E+01, 1.64976 3E+01, 1.7047788E+01, 1.7636566E+01/
DATA(F6A(I),I=60,100)/
2 1.8267678E+01, 1.8945226E+01, 1.9673837E+01, 2.0458740E+01,
2 2.1305867E+01, 2.221971E+01, 2.3214764E+01, 2.4293085E+01,
2 2.5467109E+01, 2.6748600E+01, 2.8151209E+01, 2.9690866E+01,
2 3.1386243E+01, 3.3259352E+01, 3.5336290E+01, 3.7648184E+01,
2 4.0232417E+01, 4.3134201E+01, 4.640 644E+01, 5.0123481E+01,
2 5.4362733E+01, 5.9231660E+01, 6.4863586E+01, 7.1429421E+01,
```

```

2 7.9151196E+01, 8.8321653E+01, 9.9333228E+01, 1.1272193E+02,
2 1.2 23557E+02, 1C4 4321E+02, 1C7641683E+02, 2.1104560E+02,
2 2.5760616E+02, 3.2235870E+02, 4.1630690E+02, 5.6028454E+02,
2 7.9777874E+02, 1.2326001E+03, 2.1668353E+03, 4.8210180E+03,
2 1. 06 072E+04/
DATAUF7AU+), +=1, 5 1/ 6C2 32000E+00, 6.2845747E+00, 6.2887012E+00,
2 6.2955873E+00, 6.3052457E+00, 6.3176945E+00, 6.3329570E+00,
2 6.3510618E+00, 6.3720431E+00, 6.3959406E+00, 6.4227999E+00,
2 6.4526727E+00, 6.4856166E+00, 6.5216958E+00, 6.5609815E+00,
2 6.6035514E+00, 6C64 4 11E+00, 6.6988937E+00, 6.7518606E+00,
2 6.8085018E+00, 6.8689366E+00, 6.9332940E+00, 7.0017134E+00,
2 7.0743452E+00, 7.1513519E+00, 7.2329084E+00, 7.3192034E+00,
2 7.4104401E+00, 7.5068376E+00, 7.6086319E+00, 7.7160774E+00,
2 7.8294482E+00, 7.9490401E+00, 8.0751721E+00, 8.2081888E+00,
2 8.3484623E+00, 8.4963949E+00, 8.6524219E+00, 8.8170147E+00,
2 8.9906842E+00, 9.1739847E+00, 9.3675184E+00, 9.5719399E+00,
2 9.7879622E+00, 1.0016362E+01, 1.0257989E+01, 1.0513769E+01,
2 1.0784718E+01, 1.1071 4 E+01, 1.1376685E+01, 1.1700271E+01,
2 1.2044190E+01, 1.2410079E+01, 1.2799751E+01, 1.3215214E+01,
2 1.3658700E+01, 1.4132695E+01, 1.4639974E+01, 1.5183642E+01/
DATA(F7A(I), I=60, 100)/
2 1.5767185E+01, 1.6394521E+01, 1.7070076E+01, 1.7798856E+01,
2 1.8586546E+01, 1.9439621E+01, 2.0365486E+01, 2.1372637E+01,
2 2.2470863E+01, 2.36714 1E+01, 2.4987684E+01, 2.6434811E+01,
2 2. 030 11E+01, 2. 7 726 E+01, 3C1759145E+01, 3.3946705E+01,
2 3.6396210E+01, 3.9151565E+01, 4.2266341E+01, 4.5806456E+01,
2 4C 53764E+01T 5C4510 25E+01, 5. 90 111E+01T 6.6212373E+01,
2 7.3640975E+01, 8.2480692E+01, 9.3116396E+01, 1.0607436E+02,
2 1.2208965E+02, 1.4221431E+02, 1.6799712E+02, 2.0179468E+02,
2 2.4733660E+02, 3.1081241E+02, 4.0311463E+02, 5.4489157E+02,
2 7C7 2 615E+02T 1C20 46 E+03, 2C1359358E+03T 4.7745321E+03,
2 1.8975671E+04/
DATA(F8A(I), I=1, 59)/ 0. , 2.7497442E-01, 5.5045962E-01,
2 8.26 6846E-01, 1.1050180E+00, 1.3851315E+00, 1.6678408E+00,
2 1.9536883E+00, 2.2432295E+00, 2.5370353E+00, 2.8356944E+00,
2 3.13 8161E+00, 3.4500330E+00, 3.7670041E+00, 4.0914178E+00,
2 4.4239953E+00, 4.7654945E+00, 5.1167138E+00, 5.4784962E+00,
2 5.8517341E+00, 6.2373745E+00, 6.6364245E+00, 7.0499568E+00,
2 7.4791171E+00, 7.9251312E+00, 8.3893125E+00, 8.8730716E+00,
2 9.3779257E+00, 9.9055097E+00, 1.0457588E+01, 1.1036068E+01,
2 1.1643017E+01, 1.2280673E+01, 1.2951473E+01, 1.3658065E+01,
2 1.4403336E+01, 1.5190438E+01, 1.6022818E+01, 1.6904250E+01,
2 1.7838877E+01, 1.8831251E+01, 1.9886382E+01, 2.1009798E+01,
2 2.2207604E+01, 2C3486560E+01, 2.4854161E+01, 2.6318738E+01,
2 2.7889564E+01, 2.9576990E+01, 3.1392586E+01, 3.3349322E+01,
2 3.5461763E+01, 3.7746313E+01, 4.0221486E+01, 4.2908234E+01,
2 4.5830332E+01, 4.9014836E+01, 5.2492622E+01, 5.6299036E+01/
DATA(F8A(+), I=60, 100)/
2 6.0474671E+01, 6.5066298E+01, 7.0128000E+01, 7.5722544E+01,
2 8.1923058E+01, 8.8815087E+01, 9.6499133E+01, 1.0509380E+02,
2 1.1473976E+02, 1.2560462E+02, 1.3788928E+02, 1.5183581E+02,
2 1.6773775E+02, 1.8595332E+02, 2.0692274E+02, 2.3119103E+02,
2 2.5943838E+02, 2.9252105E+02, 3.3152694E+02, 3.7785238E+02,
2 4.3330 26E+02, 5.0027714E+02, 5.8192238E+02, 6.8251978E+02,

```

```

2 8.07 3374E+02, 9.6635414E+02, 1.1694491E+03, 1.4342207E+03,
2 1.7860852E+03, 2.2641687E+03, 2.9307839E+03, 3.8892080E+03,
2 5.3189242E+03, 7.5502829E+03, 1.1236044E+04, 1.7787769E+04,
2 3.0642697E+04, 5.9664177E+04, 1.4098798E+05, 4.7435606E+05,
2 3.7830331E+06/
DATAUF AU+DT+31T 5 D/ 1C570 000E+01, 1.5714186E+01, 1.5732762E+01,
2 1.5763777E+01, 1.5807315E+01, 1.5863493E+01, 1.5932463E+01,
2 1.6014413E+01, 1.6109566E+01, 1.6218185E+01, 1.6340569E+01,
2 1.6477061E+01, 1.6628045E+01, 1.6793950E+01, 1.6975252E+01,
2 1.7172478E+01, 1.7386207E+01, 1.7617076E+01, 1.7865781E+01,
2 1.8133084E+01, 1.8419816E+01, 1.8726884E+01, 1.9055274E+01,
2 1.9406060E+01, 1.9780411E+01, 2.0179599E+01, 2.0605007E+01,
2 2.1058140E+01, 2.1540637E+01, 2.2054280E+01, 2.2601014E+01,
2 2.3182956E+01, 2.3802416E+01, 2.4461916E+01, 2.5164214E+01,
2 2.5912323E+01, 2.6709545E+01, 2.7559497E+01, 2.8466152E+01,
2 2.9433873E+01, 3.0467462E+01, 3.1572213E+01, 3.2753965E+01,
2 3.4019175E+01, 3.5374992E+01, 3.6829344E+01, 3.8391041E+01,
2 4.0069889E+01, 4.1876827E+01, 4.3824079E+01, 4.5925337E+01,
2 4.8195974E+01, 5.0653281E+01, 5.3316765E+01, 5.6208481E+01,
2 5.9353433E+01, 6.2780045E+01, 6.6520729E+01, 7.0612547E+01/
DATA(F9A(I),I=60,100)/
2 7.5098017E+01, 8.0026082E+01, 8.5453271E+01, 9.1445119E+01,
2 9.8077892E+01, 1.0544071E+02, 1.1363815E+02, 1.2279350E+02,
2 1.3305279E+02, 1.4458987E+02, 1.5761281E+02, 1.7237209E+02,
2 1C8 17108E+02T 2.0837956E+02, 2.3045146E+02, 2.5594812E+02,
2 2.8556931E+02, 3.2019491E+02, 3.6094160E+02, 4.0924100E+02,
2 4.66 4873E+02, 5.3649902E+02, 6.2112740E+02, 7.2519715E+02,
2 8.5468744E+02, 1.01793 2E+03, 1.2268227E+03, 1.4986157E+03,
2 1.8591183E+03, 2.3480042E+03, 3.0283905E+03, 4.0047739E+03,
2 5.4585626E+03, 7.7232913E+03, 1.1457308E+04, 1.8082732E+04,
2 3.1058803E+04, 6.0301284E+04, 1.4209818E+05, 4.7680527E+05,
2 3.7926419E+06/
10 FORMAT (9(E14.7),/)
11 FORMAT (4I5)
12 FORMAT (8F10.4)
13 FO=MAT (54H THE AMPLITUDE OF -ES-ONSE =
1 E14.7,/)
14 FORMAT (54H PHASE ANGLE DIFFERENCE (DEGREE) =
1 E14.7,/)
15 FORMAT (1H1)
16 FORMAT (54H THE GUESSED AMPLITUDE OF RESPONSE =
1 E14.7,/)
17 FORMAT (5(E14.7,6X),/)
18 FORMAT ( 5X6HQ(LB)=,17X3HHO=,12X8HM(SLUG)=,14X6HD(IN)=,8X12HW(RAD/
1 SEC)=)
19 FORMAT (F10.5,7(E14.7,1X),/)
20 FORMAT (2X3HHA=,5X,6HFI(1)=,9X,6HFI(3)=,9X3HFA=,12X,6HFI(7)=,9X,3H
1DA=,13X,4HDAO=,11X,2HF=)
21 FORMAT (54H THE CHARACTERISTIC FREQUENCY
1 E14.4,/)
22 FORMAT (54H THE NONDIMENSIONALIZED FREQUENCY
1 E14C4,/D
23 FO=MAT (+5,5X,(7F10.5))
24 FORMAT (54H THE ZERO-ORDER AMPLITUDE OF RESPONSE

```



```

1 E14.7,/)
25 FORMAT (54H THE NONDIMENSIONALIZED UPPER RESPONSE=
1 E14.7,/)
26 FORMAT (54H THE NONDIMENSIONALIZED LOWER RESPONSE=
1 E14.7,/)
BKS=C1, BCS=C2, AN1=N1=2.5, AN2=N2=2.5, TOL IS THE TOLERANCE OF
ERROR ALLOWED FOR THE SOLUTION, BMASST IS IN SEUG, AND DELTA IS
STEP IN INCHES.
AG(I), AND AOG(I) ARE I SERIES OF THE GUESSED VALUES OF AMPLITUDES,
A AND AO RESPECTIVELY. QN(I) THE GUESSED VALUES OF THE DYNAMIC
LOAD IN LBF. WN(I) ARE SERIES OF THE NONDIMENSIONALIZED FREQUENCY
TO BE USED IN THE CALCULATION.
-EAD 12, BKS, BCS, AN1, AN2
-EAD 12, HO, BMASST DELTAT TOL
READ 23, IG, (AG(I), I=1, IG)
-EAD 23, IG, (AOG(I), I=1, +G)
READ 23, LQ, (QN(I), I=1, LQ)
IA=0.
DO 110 IQ=1, LQ
-EAD 23, LW, (WN(I), I=1, LW)
PRINT 15
+AA=0C
QS=QN(IQ)
AMASS=BMASST/12.
AMDEL=DELTA*AMASS
HON1=HO**AN1
HON2=HO**AN2
HOPN1=HON1*HO
HOPN2=HON2*HO
WS2=BKS*AN1/AMDEL/HOPN1
WS=SQRT(WS2)
P=+NT 21, WS
DO 110 +W31, LW
+A=+Q-0.
WB=WN(IW)
W=WB*WS
PRINT 18
PRINT 17, QS, HO, BMASST, DELTA, W
PRINT 22, WB
WB2=WB*WB
WO=WS2*AMDEL
Q=QS/WO
HOMAX=HO*0.99
PI=3.1416
BK=BKS/WO
BC=BCS*WB/WS/AMASS
PHO1=PI*HON1
PHO2=PI*HON2
BI=BK/PHO1
B3=BC/PHO2
THE AMPLITUDE OF A FOR W=0., AO=0. IS ESTIMATED BY LINEAR INTERPOSITION.
IF (W.GT.0.) GO TO 50
IAA=1
AWO=Q*PI*HON1/BK

```

```

IF (AWO-F1A(50)) 41, 42, 43
42 A=0.5*HO
AO=0.
GO TO 50
41 I1=1
+2=50
GO TO 44
43 +1=50
I2=100
44 I3=(I1+I2)/2
ID=I2-I1+0.1
+F (+D-1D 45, 45, 46
46 IF (AWO-F1A(I3)) 47, 49, 48
47 I2=I3
GO TO 44
48 I1=I3
GO TO 44
45 AI=+1
A=(AI+(AWO-F1A(I1)))/(F1A(I2)-F1A(I1))/100.*HO
AO=0.
GO TO 50
4 A=+3/100.MHO
AO=0.
50 CONTINUE
GUESS THE VALUES OF A AND AO.
IF (IAA-1) 1,6,6
1 CONTINUE
+A=+A+1
IF (IA.GT.IG) GO TO 110
A=AG(IA)
AO=AOG(IA)
6 CONTINUE
--+NT 16T A
ITER=0.
103 CONTINUE
HA05=(1.+AO/HO)**2.5
+AO7=(1.+AO/HO)**3.5*HO
A+O3A/U+O+AOD
HA=AO*100.
HA=HA+1.
IHA=HA
+A+1
+1 0++AH+08A-+HA)*(F1A(IHA1)-F1A(IHA))
F+(2D3F2AU+HA)+(HA-+HA)*UF2AU++A1)-F2A(IHAD)
FI(3)=F3A(IHA)+(HA-IHA)*(F3A(IHA1)-F3A(IHA))
FI(4)=F4A(+HA)+U+A-IHA)*(F4A(IHA1)-F4A(IHA))
F+(5)3F5A(+HA)+(HA-+HA)*UF5A(IHA1D-F5A(IHAD)
FI(6)=F6A(IHA)+(HA-IHA)*(F6A(IHA1)-F6A(IHA))
FI(7)=F7A(IHA)+(HA-IHA)*(F7A(IHA1)-F7A(IHA))
FI(8)=F8A(IHA)+(HA-IHA)*(F8A(IHA1)-F8A(IHA))
FI(9)=F9A(IHA)+(HA-IHA)*(F9A(IHA1)-F9A(IHA))
FI(1)= FI(1)/HA05
FI(2)= FI(2)/HA07
FI(3)= FI(3)/HA05

```

```

FI(4)=FI(4)/HA07
FI(5)=-FI(5)/HA07
FI(6)=-FI(6)/HA07
FI(7)=FI(7)/HA05
FI(8)=FI(8)/HA07
FI(9)=-FI(9)/HA07
F=(FI(1)*B1-A*WB2)**2+(F+(3)*B3*A)**2-Q*Q
FA1=(FI(1)*B1-A*WB2)*(FI(2)*B1-WB2)*2.
FA2=(FI(3)*B3*A)*(FI(3)*B3+FI(4)*B3*A)*2.
FA=FA1+FA2
G=FI(7)-2.*PI
FAO=2.*(B1*FI(1)-A*WB2)*B1*FI(5)+(B3*A)**2*FI(3)*FI(6)*2.
DEL=FA*FI(9)-FAO*FI(8)
DA=(-F*F+( )+G*FAO)/DEL
DAO=(F*FI(8)-G*FA)/DEL
IF (ABS(DA).GT.0.5) GO TO 1
AO=AO+DAO
A=A+DA
P=+NT 20
PRINT 19,HA, FI(1), FI(3), FA, FI(7), DA, DAO, F
PRINT 10, FAO, DEL, G
ITER=ITER+1
IF (A.LE.0.) GO TO 1
AOB=ABS(AO)
AAO=ABS(A-AOB)
IF (AAO.GT.HOMAX) GO TO 1
IF (ITER.GT.15) GO TO 1
IF (ABS(DA).GT.TOL) GO TO 103
IF (ABS(DAO).GT.TOL) GO TO 103
R=FI(3)*BC*A/PHO2/(FI(1)*BK/PHO1-A*WB2)
ALPHA=ATAN(R)
ALPHA=ALPHA*180./3.1416
PRINT 24, AO
PRINT 13, A
AU=A+AO
ADOWN=A-AO
PRINT 25, AU
PRINT 26, ADOWN
PRINT 14, ALPHA
+AA=+AA+1
10 CONTINUE
END

```

Card 1 Format (8F10.5)

- BKS - Value of c_1 for the stiffness of the gas film force
 in lb_f .
- BCS - Value of c_2 for the damping of the gas film force in
 lb_f/ips .
- AN1 - Power n_1 for the stiffness force in terms of gas film
 thickness.
- AN2 - Power n_2 for the damping force in terms of gas film
 thickness.

Card 2 Format (8F10.5)

- HO - Normalized gas film thickness at equilibrium.
- BMASS .. Mass of the step ring in response in slug.
- DELTA .. Step depth of the pad in inches.
- TOL - Convergence factor for the amplitude iteration.

Card 3 Format (I5, 5X, (7F10.5))

- IG - Total number of the guessed amplitude A of the
 response.
- AG(I) - Array of the guessed amplitude A of the response.

Card 4 Format (I5, 5X, (7F10.5))

- IG - Total number of the guessed amplitude A_o of the response.
- ADG(I) - Array of the guessed amplitudes A_o of the response.

Card 5 Format (I5, 5X, (7F10.5))

- LQ - Total number of the force excitation to be investigated
 in the production run.
- QN(I) - Array of amplitude of force excitation in lb_f .

Card 6 Format (I5, 5X, (7F10.5))

- LW - Total number of the normalized forcing frequencies to
 be investigated.
- WN(I) - Array of normalized forcing frequencies.

If the sixth input statement is located within the doloop of
IQ = 1, LQ, LQ sets of card 6 are required.

```

PROGRAM RSRKIT(INPUT,OUTPUT,PUNCH,TAPE99)
COMMON Y, DY, ATABL, RTABL, IFVD, X, DX,W, BK, BC, Q, AMASS, DELTA
COMMON HO, TLAST, AY, FAC, WB2, HON1, HON2, HOPN1, HOPN2, AN1, AN2
COMMON XA, TA, XTA, IA, IA2, DXI, WLB, WB, SLOPE, TLW, WBO, XU
DIMENSION Y(2), DY(2), ATABL(2), -TABL(2), WO-K(18)
DIMENSION XA(1000), TA(1000), XTA(1000)
EXTERNAL DERIV, CNTRL, GRAPH
11 FORMAT (8F10.5)
12 FORMAT (54H MASS OF THE SEAL (SLUG) ,
1 E14.3,/)
13 FORMAT (54H DEPTH OF STEP DISCONTINUITY (IN) ,
1 E14.3,/)
14 FORMAT (54H NONDIMENSIONALIZED EQUILIBRIUM POSITION, HO ,
1 E14.3,/)
15 FORMAT (54H FREQUENCY OF PERIODIC FORCE, W (RAD/SEC) ,
1 E14.3,/)
16 FORMAT (54H AMPLITUDE OF THE PERIODIC FORCE APPLIED (LBS) ,
1 E14.3,/)
17 FORMAT (54H NONDIMENSIONALIZED DAMPING COEFFICIENT OF GAS FILM C ,
1 E14.3,/)
18 FORMAT (60H NONDIMENSIONALIZED MULTIPLE OF STIFFNESS S DISPLACEME
INT, K,E14.3,/)
19 FORMAT (54H NONDIMENSIONALIZED DISPLACEMENT ,
1 E14.3,/)
20 FORMAT (54H THE MULTIPLE OF TIME AND FREQUENCY (RAD) ,
1 E14.3,/)
21 FORMAT (3X7HDEGREE=,4X,11HPHASE(RAD)=,7X13HDISPLACEMENT=,11X9HVELO
ICITY=,/)
31 FORMAT (7X,23HDATA (XA(IA),IA=1, 70)/,2(E14.6,1H,))
32 FORMAT (5X,1H2,1X,4(E14.6,1H,))
33 FORMAT (7X,22HDATA (TA(IA),IA=1,94)/,4(F9.5,1H,))
34 FORMAT (5X,1H3,1X,6(F9.5,1H,))
35 FORMAT (7X,26HDATA (XTA(IAP),IAP=1,360)/,2(E14.6,1H,))
36 FORMAT (5X,1H2,1X,4(E14.6,1H,))
40 FORMAT (52H ERROR RETURN, DX=0 ,/)
41 FORMAT (52H NORMAL RETURN ,/)
42 FORMAT (52H ERROR RETURN, VARIABLE INTERVAL MODE ONLY ,/)
TLAST IS THE FINAL TIME OF THE INTERVAL IN INTEGRATION.
TLW IS THE FINAL TIME THAT THE SMOOTH VARIATION OF FREQUENCY ENDS.
WLB IS THE FINAL NONDIMENSIONALIZED FREQUENCY TO BE USED IN THE
TECHNIC OF SMOOTH VARYING FREQUENCY.
Y(1), Y(2), X ARE INITIAL CONDITIONS OF X, DX/DT, T RESPECTIVELY.
BKS=C1. BCS=C2. DELTA +S STEP IN INCHES. QS IS DYNAMIC LOAD IN
LB. AM IS MASS OF THE PAD IN SLUG. WB IS THE NONDIMENSIONALIZED
FREQUENCY. AN1=N1=2.5, AN2=N2=2.5 DXI IS THE TIME INCREMENT IN DEGREE.
READ 11, TLAST, TLW, WLB
READ 11, Y(1), Y(2), X
READ 11 , BKS, BCS, QS, AM, DELTA, HO, WB
0+
HON1=HO**AN1
HON2=HO**AN2
HOPN1=HON1*HO
HOPN2=HON2*HO

```

```

AMASS=AM/12.
AMDEL=AMASS*DELTA
WS2=BKS*AN1/AMDEL/HOPN1
WS=SQRT(WS2)
W=WB*WS
WB2=WB*WB
WL=WLB*WS
XO=X
SLOPE=(WLB-WB)/WB/(TLW-XO)
WBO3WB
WO=WS2*AMDEL
Q=QS/WO
BK=BKS/WO
BC=BCS/WS/AMASS
PRINT 12, AM
PRINT 13, DELTA
PRINT 14, HO
PRINT 15, W
PRINT 16, QS
PRINT 17, BC
PRINT 18, BK
DEFINE THE INITIAL VALUE OF Y(I)
XA(1)=Y(1)
TA(1)=X
XTA(1)=Y(2)
DEFINE X AS Y(1), AND DX/DT AS Y(2)
THE FOLLOWING IS PREPARED FOR RUNGE-KUTTA NUMERICAL INTEGRATION.
PI=3.1415926535
DX=DXI*PI/180.
FAC=10.**0.2
NTRY=1
N=2
IFVD=1
IBKP=1
ATABL(1)=0.001
ATABL(2)=0.001
RTABL(1)=0.001
RTABL(2)=0.001
IA2=1
IA=1
PRINT 21
CALL RKS3(DERIV,CNTRL,Y,DY,ATABL,RTABL,WORK,X,DX,N,IFVD,IBKP,NTRY,
1 IERR)
IF (IERR-0) 4, 5, 6
4 CONTINUE
PRINT 40
GO TO 3
5 CONTINUE
PRINT 41
GO TO 3
6 CONTINUE
PRINT 42
3 CONTINUE
THE FOLLOWING IS FOR THE PLOTS OF X AND DX/DT V.S. T.

```

```

CALL NAMPLT
CALL SCALE (XA,5.0,IA,1)
CALL SCALE (TA,40.0,IA,1)
CALL SCALE (XTA,5.0,IA,1)
CALL AXIS(0.0,0.0,7HT VALUE,7,40.0,0.0,TA(IA+1),TA(IA+2))
CALL AXIS (0.0,0.0,7HX VALUE,-7,8.,90.0,XA(IA+1),XA(IA+2))
CALL AXIS (1.0,0.0,8HXT VALUE,-8,8.0,90.0,XTA(IA+1),XTA(IA+2))
CALL LINE (TA,XA,IA,1,1,0)
CALL LINE (TA,XTA,IA,1,1,3)
CALL SYMBOL (3.0,9.0,0.20,16HPLOT OF X V.S. T,0.0,16)
CALL SYMBOL (4.0,10.0,0.20,20HPLOT OF DX/DT V.S. T,0.0,15)
CALL ENDPLT
THE FOLLOWING IS FOR THE PHASE PLOT OF X V.S. DX/DT.
RIA=IA
WIDTH=10.
WSPACE=10.
CALL SETUPC(0.,0.,0.,1.,-20.,2.,WIDTH,WSPACE)
CALL PARAM(GRAPH,1.,1.,RIA)
CALL ENDSURF
END

```

```

OB-OUTLINE DERIV
DIMENSION Y(2), DY(2), ATABL(2), -TABL(2), WORK(18)
DIMENSION XA(1000), TA(1000), XTA(1000)
COMMON Y, DY, ATABL, RTABL, IFVD, X, DX,W, BK, BC, Q, AMASS, DELTA
COMMON HO, TLAST, AY, FAC, WB2, HON1, HON2, HOPN1, HOPN2,AN1,AN2
COMMON XA, TA, XTA, IA, IA2, DX1, WLB, WB, SLOPE, TLW, WBO, XU
DY(1)=DY(1)/DT, DY(2)=DY(2)/DT.
DY(1)=Y(2)
DY(2)=(BK/HON1+Q*COS(X)-BK/(HO-Y(1))*AN1-BC*Y(2)*WB/(HO-Y(1))*AN
12)/WB2
RETURN
END

```

```

SUBROUTINE CNTRL(NTRY)
DIMENSION Y(2), DY(2), ATABL(2), RTABL(2)
DIMENSION XA(1000), TA(1000), XTA(1000)
COMMON Y, DY, ATABL, RTABL, IFVD, X, DX,W, BK, BC, Q, AMASS, DELTA
COMMON HO, TLAST, AY, FAC, WB2, HON1, HON2, HOPN1, HOPN2,AN1,AN2
COMMON XA, TA, XTA, IA, IA2, DX1, WLB, WB, SLOPE, TLW, WBO, XU
51 FORMAT (5X,I5.4(E14.6,6X))
54 FORMAT (54H THE DISPLACEMENT IS OUT OF RANGE )
IF Y(1) IS LESS THAN -4., OR Y(1) IS GREATER THAN HO, TERMINATE
THE NUMERICAL INTEGRATION.
AY=ABS(Y(1))
IF (AY.GT.4.0) GO TO 2
IF (Y(1)-HO) 1, 2, 2
2 CONTINUE

```



```

PRINT 54
NTRY=2
1 CONTINUE
IF (X-TLAST) 3, 3, 4
4 NTRY=2
3 CONTINUE
IA2=IA2+1
IADX=IA2*DXI
IA=IA2/4+0.0001
XTA(IA)=Y(2)
XA(IA)=Y(1)
TA(IA)=X
PRINT 51, IADX, X, Y(1), Y(2), WB
IF (WB-WLB) 11, 12, 12
11 WB=WBO*(1.+SLOPE*(X-XO))
GO TO 13
12 WB=WLB
13 CONTINUE
WB2=WB*WB
RETURN
END

```

```

SUBROUTINE GRAPH(T,XP,YP,ZP)
COMMON Y, DY, ATABL, RTABL, IFVD, X, DX, W, BK, BC, Q, AMASS, DELTA
COMMON HO, TLAST, AY, FAC, WB2, HON1, HON2, HOPN1, HOPN2, AN1, AN2
COMMON XA, TA, XTA, IA, IA2, DXI, WLB, WB, SLOPE, TLW, WBO, XU
DIMENSION Y(2), DY(2), ATABL(2), RTABL(2), WORK(18)
DIMENSION XA(1000), TA(1000), XTA(1000)
NP=T+.0001
XP=XA(NP)*5.
YP=0.0
ZP=XTA(NP)*5.
RETURN
END

```

Card 1 Format (8F10.5)

- TLAST - Final normalized time in radian for the integration.
- TLW - Final normalized time in radian for the changing of
 W during the integration.
- WLB - Final normalized forcing frequency.

Card 2 Format (8F10.5)

- Y(1) - The initial value of X.
- Y(2) - The initial value of \dot{X} , i.e. dX/dT .
- X - The initial time, T_i for the integration.

Card 3 Format (8F10.5)

- BKS - Value of c_1 in lb_f .
- BCS - Value of c_2 in lb_f/ips .
- QS - Value of q in lb_f .
- AM - Mass of the ring in response in slug.
- DELTA - Step depth, δ in inches.
- HO - Normalized equilibrium gas film thickness.
- WB - The initial normalized excitational frequency.

Card 4 Format (8F10.f)

- AN1 - Value of n_1 which is 2.5 in the case being investigated
 here.
- AN2 - Value of n_2 which is 2.5 in the case being investigated
 here.
- DXI - Time increments during the fixed interval of the numerical
 integration.

```

PROGRAM RSTAB(INPUT,OUTPUT)
DIMENSION SA(50), SB(50), SC(50), SD(50), SE(50), SF(50)
DIMENSION PO(50), PCR(50), PCI(50), DX(50), C(100), A(70,70)
DIMENSION CI(2,3,50), SUBV(50), VI(20)
DIMENSION XX(100), B(50,3), BH(50), AH(50), CH(50)
COMMON B1, ALAM, H1, TOL, NL, N2, B2, NL1, N21, NP, NP1, NL2, NL3
COMMON H2, H13, H23, HSUM
COMMON SA, SB, SC, SD, SE, SF
11 FORMAT (4F10.4,3I5)
12 FORMAT (8F10.5)
13 FORMAT (54H THE THRESHOLD FREQUENCY OF THE STEP SEAL
1 E14.4,/)
14 FORMAT (54H THE SQUEEZE FILM PARAMETER
1 E14.4,/)
15 FORMAT (54H THE BEARING NUMBER
1 E14.4,/)
16 FORMAT (54H MASS
1 E14.4,///)
17 FORMAT (54H RATIO OF MIN CLEARANCE HEIGHT TO DIFF. IN CLEARANCES
1 E14.4,/)
18 FORMAT (54H THE 1ST ORDER PRESSURISED LOAD
1 E14.4,/)
19 FORMAT ((8E14.4),/)
20 FORMAT (54H THE POINTS ARE TOO FEW
)
21 FORMAT (54H A AND/OR B IS OUT OF RANGE OF TABLE
)
22 FORMAT (54H THE GUESSED THRESHOLD FREQUENCY OF THE STEP SEAL
1 E14.4,/)
23 FORMAT (52H THE GRID DIFFERENCE
,/)
24 FORMAT (52H THE ZERO ORDER PRESSURE DISTRIBUTION
,/)
25 FORMAT (54H THE VALUE OF SMALLNESS
1 E14.4,/)
26 FORMAT (54H LOAD DUE TO THE IMAGINARY PART OF COMPLEX PRESSURE
1 E14.4,7)
27 FORMAT (5X,I5,(7F10.4))
29 FORMAT (7,(8E14.4,7))
30 FORMAT (52H THE IMAGINARY PART OF COMPLEX PRESSURE DISTRIBUTION,/)
31 FORMAT (52H THE REAL PART OF COMPLEX PRESSURE DISTRIBUTION
,/)
32 FORMAT (54H THE RATIO OF WIDTH OF STEP WITH HEIGHT H1
1 E14.4,/)
READ 11, B1, ALAM, H1, TOL, NL, N2, NV
READ 12, (VI(T),T=1,NV)
B2=1.-B1
NL1=NL-1
NL2=NL-2
NL3=NL-3
ND=NL2+NL2
N21=N2-1
NP=N2+1
NP1=NP+1
H12=H1**2
H13=H1**3
H2=H1+1.
H22=H2**2
H23=H2**3

```

```

READ 12, (DX(I),I=1,NL1)
READ 12, (PO(I),I=1,NL)
HSUM=H13+3.*H1*H2*(H1+H2)+H23
CALL NEWR(PO,DX)
CALL INTEG(0.,1.,DX,PO,NL,WLOAD,C1,FERR)
PRINT 32, B1
PRINT 15, ALAM
PRINT 17, H1
PRINT 14, SEG
PRINT 23
PRINT 19, (DX(I),I=1,NL1)
PRINT 24
PRINT 19, (PO(I),I=1,NL)
PRINT 25, TOL
A1=-ALAM*H1/2.
A2=-ALAM*(H1+H2)/4.
A3=-ALAM*H2/2.
THE COEFFICIENTS OF SMALL A, B, C, D, E, F AT EACH GRID POINT ARE
CALCULATED IN THE FOLLOWING AS SA, ... ETC.
DO 2 I=2,N21
SA(I)=H13/DX(I)
SC(I)=H13/DX(I-1)
SB(I)=-SA(I)-SC(I)
SD1=(PO(I+1)**2/DX(I)-PO(I)**2*(1./DX(I)+1./DX(I-1))+PO(I-1)**2
1 /DX(I-1))*3.*H12/4.
SD2=ALAM*(PO(I+1)-PO(I-1))/2.
SD(I)=SD1-SD2
SE(I)=H1*(DX(I)+DX(I-1))/2.
SF(I)=(DX(I)+DX(I-1))/2.
AH(I)=A1
CH(I)=-A1
BH(I)=0.
2 CONTINUE
SA(N2)=HSUM/8./DX(N2)
SC(N2)=H13/DX(N21)
SB(N2)=-SA(N2)-SC(N2)
SD1=((PO(NP)**2-PO(N2)**2)*(H12+H1*H2+H22)/DX(N2)+(PO(N21)**2-
1 PO(N2)**2)*3.*H12/DX(N21))/4.
SD2=ALAM*(PO(NP)-PO(N21))/2.
SD(N2)=SD1-SD2
SE(N2)=(H1+H2)*DX(N2)+2.*H1*DX(N21))/4.
SF(N2)=(DX(N2)+DX(N21))/2.
AH(N2)=A2
CH(N2)=-A1
BH(N2)=AH(N2)+CH(N2)
DO 3 I=NP1,NL1
SA(I)=H23/DX(I)
SC(I)=H23/DX(I-1)
SB(I)=-SA(I)-SC(I)
SD1=(PO(I+1)**2/DX(I)-PO(I)**2*(1./DX(I)+1./DX(I-1))+PO(I-1)**2
1 /DX(I-1))*3.*H22/4.
SD2=ALAM*(PO(I+1)-PO(I-1))/2.
SD(I)=SD1-SD2
SE(I)=H2*(DX(I)+DX(I-1))/2.

```

```

SF(I)=(DX(I)+DX(I-1))/2.
AH(I)=A3
CH(I)=-A3
BH(I)=0.
3 CONTINUE
SA(NP)=H23/DX(NP)
SC(NP)=HSUM78./DX(N2)
SB(NP)=-SA(NP)-SC(NP)
SD1=((PO(NP1)**2-PO(NP)**2)*3.*H22/DX(NP)+(PO(N2)**2-PO(NP)**2)*
1 (H12+H1*H2+H22)/DX(N2))/4.
SD2=ALAM*(PO(NP1)-PO(N2))/2.
SD(NP)=SD1-SD2
SE(NP)=(H1+H2)*DX(N2)+2.*H2*DX(NP))/4.
SF(NP)=(DX(NP)+DX(N2))/2.
AH(NP)=A3
CH(NP)=-A2
BH(NP)=AH(NP)+CH(NP)
CALCULATE ELEMENTS OF (A) AND (C) IN THE EQUATION AX=C.
B MATRIX IS USED TO SAVE A(I,J) WHICH ARE INDEPENDENT ON THE
DO 4 J=1,ND
DO 4 I=1,ND
A(I,J)=0.
4 CONTINUE
V=VI(1)
PRINT 22, V
AMASS=WLOAD/V**2
PRINT 16, AMASS
DO 5 J=2,NL3
I=J+1
JN=NL2+J
IN=JN+I
A(J,I)=SA(I)*PO(I+1)+AH(I)
A(JN,IN)=A(J,I)
A(J,J)=SB(I)*PO(I)+BH(I)
A(JN,JN)=A(J,J)
A(J,J-1)=SC(I)*PO(I-1)+CH(I)
A(JN,JN-1)=A(J,J-1)
A(J,JN)=SE(I)*V
A(JN,J)=A(J,JN)
C(J)=-SD(I)
C(JN)=SF(I)*PO(I)*V
B(J,3)=A(J,J+1)
B(J,2)=A(J,J)
B(J,1)=A(J,J-1)
5 CONTINUE
A(1,1)=SB(2)*PO(2)+BH(2)
A(NL1,NL1)=A(1,1)
A(1,2)=SA(2)*PO(3)+AH(2)
A(NL1,NL1)=A(1,2)
A(1,NL1)=SE(2)*V
A(NL1,1)=A(1,NL1)
C(1)=-SD(2)
C(NL1)=SF(2)*PO(2)*V
A(NL2,NL3)=SC(NL1)*PO(NL2)+CH(NL1)

```

```

A(ND,ND-1)=A(NL2,NL3)
A(NL2,NL2)=SB(NL1)*PO(NL1)+BH(NL1)
A(ND,ND)=A(NL2,NL2)
A(NL2,ND)=SE(NL1)*V
A(ND,NL2)=-A(NL2,ND)
C(NL2)=-SD(NL1)
C(ND)=SF(NL1)*PO(NL1)*V
B(1,1)=A(1,1)
B(1,2)=A(1,2)
B(NL2,1)=A(NL2,NL3)
B(NL2,2)=A(NL2,NL2)
DO 61 J=1,ND
XX(J)=C(J)
61 CONTINUE
CALL DETEQTA,XX,ND,DET)
IF (DET-0.) 108, 109, 108
109 STOP
108 CONTINUE
PCI(1)=0.
PCI(NL)=0.
PCR(1)=0.
PCR(NL)=0.
DO 7 J=NL1,ND
PCI(J-NL3)=XX(J)
7 CONTINUE
PRINT 30
PRINT 29, (PCI(I),I=1,NL)
CALL INTEG(0.,1.,DX,PCI,NL,PSM1,C1,IERR)
IF (IERR=1) 113, 114, 115
114 PRINT 20
STOP
115 PRINT 21
STOP
113 CONTINUE
PRINT 26, PSM1
DO 69 J=1, NL2
69 PCR(J+1)=XX(J)
PRINT 29, (PCR(I),I=1,NL)
PRINT 31
CALL INTEG(0.,1.,DX,PCR,NL,PRSM,C1,IERR)
PRINT 18, PRSM
AMASS=PRSM/V*#2
PRINT 16, AMASS
DO 121 IV=2,NV
V=VI(IV)
PRINT 22, V
DO 51 J=1,ND
DO 51 I=1,ND
A(I,J)=0.
51 CONTINUE
DO 52 J=2,NL3
I=J+1
JN=NL2+J
IN=JN+1

```

```

A(J,J-I)=B(J,1)
A(J,J)=B(J,2)
A(J,J+I)=B(J,3)
A(JN,IN)=A(J,I)
A(JN,JN)=A(J,J)
A(JN,JN-1)=A(J,J-1)
52 CONTINUE
A(1,1)=B(1,1)
A(1,2)=B(1,2)
A(NL2,NL3)=B(NL2,1)
A(NL2,NL2)=B(NL2,2)
A(NL1,NL1)=A(1,1)
A(NL1,NL)=A(1,2)
A(ND,ND-1)=A(NL2,NL3)
A(ND,ND)=A(NL2,NL2)
CALCULATE THE ELEMENTS OF A AND C WHICH VARY WITH RESPECT TO V.
DO 6 J=1,NL2
  I=J+1
  JN=J+NL2
  A(J,JN)=SE(I)*V
  A(JN,J)=A(J,JN)
  C(JN)=SF(I)*PO(I)*V
6 CONTINUE
DO 62 J=1,ND
  XX(J)=C(J)
62 CONTINUE
CALL DETEQ(A,XX,ND,DET)
IF (DET-0.) 111, 112, 111
112 STOP
111 CONTINUE
DO 8 J=NL1,ND
  PCI(J-NL3)=XX(J)
8 CONTINUE
PRINT 30
PRINT 29, (PCI(I),I=1,NL)
CALL INTEG(0.,1.,DX,PCI,NL,PSM2,CI,IERR)
IF (IERR-1) 116,117, 118
117 PRINT 20
STOP
118 PRINT 21
STOP
116 CONTINUE
PRINT 26, PSM2
DO 9 J=1, NL2
  PCR(J+1)=XX(J)
  PRINT 31
  PRINT 29, (PCR(I),I=1,NL)
  CALL INTEG(0.,1.,DX,PCR,NL,PRSM,CI,IERR)
  PRINT 18, PRSM
  AMASS=PRSM/V**2
  PRINT 16, AMASS
121 CONTINUE
END

```

```

SUBROUTINE INTEG(A,B,H,F,NP,VALUE,C,IERR)
* * * * *
SUBROUTINE INTEG
-----+-----
INTEGRATES THE NON EQUIDISTANTLY TABULATED FUNCTION F(X(I))
BETWEEN THE LIMITS A AND B.

A MODIFIED METHOD OF OVERLAPPING PARABOLAS IS EMPLOYED.

A SECOND ENTRY POINT 'INTEG2' IS PROVIDED FOR MORE THAN ONE
INTEGRATION ON THE SAME DIVISIONS OF X. THIS SAVES THE TIME
OF CALCULATING THE WEIGHTING FUNCTIONS.

ARGUMENTS -
A      LOWER LIMIT OF INTEGRATION.
B      UPPER LIMIT OF INTEGRATION.
X      ARRAY OF ARGUMENT VALUES. MUST BE MONOTONICALLY
      INCREASING AND MUST BE DIMENSIONED NP.
F      ARRAY OF FUNCTION VALUES. MUST BE DIMENSIONED NP.
NP     NUMBER OF POINTS. NP MUST BE GREATER THAN 3.
VALUE  RESULTANT VALUE OF THE INTEGRATION.
C      WEIGHTING FUNCTION PASSED TO THE MAIN PROGRAM
      FOR STORAGE.
IERR   RESULTANT ERROR PARAMETER.

REQUIRED SUBPROGRAMS - NONE

COMMON STORAGE -
THE WEIGHTING FUNCTION C IS STORED IN THE MAIN PROGRAM AND
REQUIRES THE FOLLOWING DIMENSION STATEMENT WHERE D.GE.NP.
      DIMENSION C(2,3,D)

ERROR INDICATIONS -
IERR = 0  INDICATES NO ERROR.
IERR = 1  INDICATES NP IS LESS THAN 4.
IERR = 2  INDICATES THE LIMITS OF INTEGRATION ARE OUT OF
      THE RANGE OF THE TABLE.

EDWARD G. TRACHMAN      8 JULY 1970  M.E. DEPT. 492-5640

* * * * *
DIMENSION X(50), F(50), C(2,3,50)
DIMENSION H(50), SUBV(50)

NP MUST BE GREATER THAN 3

IF (NP.LE.3) GO TO 96

CALCULATION OF INTERVALS OF X

NH=NP-1
X(1)=0.

```

INTEG002
 *INTEG003
 *INTEG004
 *INTEG005
 *INTEG006
 *INTEG007
 *INTEG008
 *INTEG009
 *INTEG010
 *INTEG011
 *INTEG012
 *INTEG013
 *INTEG014
 *INTEG015
 *INTEG016
 *INTEG017
 *INTEG018
 *INTEG019
 *INTEG020
 *INTEG021
 *INTEG022
 *INTEG023
 *INTEG024
 *INTEG025
 *INTEG026
 *INTEG027
 *INTEG028
 *INTEG029
 *INTEG030
 *INTEG031
 *INTEG032
 *INTEG033
 *INTEG034
 *INTEG035
 *INTEG036
 *INTEG037
 *INTEG038
 *INTEG039
 *INTEG040
 *INTEG041
 *INTEG042
 *INTEG043
 INTEG045
 INTEG046
 INTEG047
 INTEG048
 INTEG049
 INTEG050
 INTEG051
 INTEG052
 INTEG053

DO 10 I=1,NH	
10 X(I+1)=X(I)+H(I)	INTEG056
DO 20 I=1,NH	INTEG057
IF (I.EQ.1) GO TO 15	INTEG058
DEFINE COEFFICIENTS OF FIRST PARABOLA	INTEG059
C(1,1,I)=-(H(I))**3/(6.*H(I-1)*(H(I-1)+H(I)))	INTEG060
C(1,2,I)=H(I)*(3.*H(I-1)+H(I))/(6.*H(I-1))	INTEG061
C(1,3,I)=H(I)*(3.*H(I-1)+2.*H(I))/(6.*(H(I-1)+H(I)))	INTEG062
15 CONTINUE	INTEG063
IF (I.EQ.NH) GO TO 20	INTEG064
DEFINE COEFFICIENTS OF SECOND PARABOLA	INTEG065
C(2,1,I)=H(I)*(2.*H(I)+3.*H(I+1))/(6.*(H(I)+H(I+1)))	INTEG066
C(2,2,I)=H(I)*(H(I)+3.*H(I+1))/(6.*H(I+1))	INTEG067
C(2,3,I)=-(H(I))**3/(6.*H(I+1)*(H(I)+H(I+1)))	INTEG068
20 CONTINUE	INTEG069
ENTRY INTEG2	INTEG070
INITIALIZE SUMMATION VARIABLE	INTEG071
VALUE=0.0	INTEG072
IF (B=A) 40,92,30	INTEG073
B IS GREATER THAN A	INTEG074
30 ALIM = A	INTEG075
BLIM = B	INTEG076
SIGN = 1.0	INTEG077
GO TO 50	INTEG078
A IS GREATER THAN B	INTEG079
40 ALIM = B	INTEG080
BLIM = A	INTEG081
SIGN = -1.0	INTEG082
50 NH=NP-I	INTEG083
SETTING THE LOWER LIMIT OF INTEGRATION	INTEG084
DO 63 I=1,NH	INTEG085
PART A = 1.0	INTEG086
IF (ALIM-X(I)) 61,69,63	INTEG087
61 IF (I.EQ.1) GO TO 97	INTEG088
ALIM=X(I-1)	INTEG089
PART A=(X(I)-ALIM)/(X(I)-X(I-1))	INTEG090
GO TO 69	INTEG091
63 CONTINUE	INTEG092
69 CONTINUE	INTEG093
	INTEG094
	INTEG095
	INTEG096
	INTEG097
	INTEG098
	INTEG099
	INTEG100
	INTEG101
	INTEG102
	INTEG103
	INTEG104
	INTEG105
	INTEG106
	INTEG107

```

SETTING THE UPPER LIMIT OF INTEGRATION
DO 73 I=1,NH
PARTB = 1.0
IF (BLIM-X(I)) 71,79,73
71 IF (I.EQ.1) GO TO 97
BLIM = X(I)
PARTB=(BLIM-X(I-1))/(X(I)-X(I-1))
GO TO 79
73 IF (I.EQ.NP) GO TO 97
79 CONTINUE

CALCULATION OF INTEGRAL OVER SUBINTERVAL
DO 80 I=1,NH
SUBV(I) = 0.0
IF (X(I).EQ.ALIM) SUBV(I)=C(2,1,I)*F(I)+C(2,2,I)*F(I+1)+C(2,3,I)*
IF(I+2)
IF (I=NH) 102, 103, 103
103 CONTINUE
ADX=ABS(X(I+1)-BLIM)
IF (ADX.LT.1.E-5) SUBV(I)=C(1,1,I)*F(I-1)+C(1,2,I)*F(I)+C(1,3,I)*
1 F(I+1)
GO TO 101
102 CONTINUE
IF (X(I).GT.ALIM.AND.X(I+1).LT.BLIM) SUBV(I)=0.5*(C(1,1,I)*F(I-1)
I+(C(1,2,I)+C(2,1,I))*F(I)+(C(1,3,I)+C(2,2,I))*F(I+1)+C(2,3,I)*
2F(I+2))
101 CONTINUE
IF (PARTA.NE.1.OR.PARTB.NE.1) SUBV(I)=PARTA*PARTB*SUBV(I)

CALCULATE THE FINAL VALUE OF THE INTEGRAL
80 VALUE=VALUE+SUBV(I)
VALUE=SIGN*VALUE

SET ERROR PARAMETER FOR NORMAL RETURN
92 IERR = 0
RETURN

SET ERROR PARAMETER FOR TOO FEW POINTS
96 IERR = 1
RETURN

SET ERROR PARAMETER FOR A AND/OR B OUT OF RANGE OF TABLE
97 IERR = 2
RETURN
END

```

INTEG108
 INTEG109
 INTEG110
 INTEG111
 INTEG112
 INTEG113
 INTEG114
 INTEG115
 INTEG116
 INTEG117
 INTEG118
 INTEG119
 INTEG120
 INTEG121
 INTEG122
 INTEG123
 INTEG124
 INTEG125
 INTEG126
 INTEG127
 INTEG128
 INTEG129
 INTEG130
 INTEG131
 INTEG132
 INTEG133
 INTEG134
 INTEG135
 INTEG136
 INTEG137
 INTEG138
 INTEG139
 INTEG140
 INTEG141
 INTEG142
 INTEG143
 INTEG144
 INTEG145
 INTEG146
 INTEG147
 INTEG148
 INTEG149
 INTEG150
 INTEG151
 INTEG152

```

SUBROUTINE DETEQ(A,B,N,DET)
DIMENSION A(70,70),B(70),IPVOT(70)
DET=1.0
DO 11 J=1,N
11 IPVOT(J)=0.0
DO 121 I=1,N
T=0.0
DO 51 J=1,N
IF (IPVOT(J)-1) 21,51,21
21 DO 50 K=1,N
IF (IPVOT(K)-1) 31,50,50
31 IF (ABS(T)-ABS(A(J,K))) 41,50,50
41 IROW=J
ICOL=K
T=A(J,K)
50 CONTINUE
51 CONTINUE
IF (ABS(T)-1.E-8) 131,131,55
55 IPVOT(ICOL)=I
IF (IROW-ICOL) 61,81,61
61 DET=-DET
DO 71 L=1,N
T=A(IROW,L)
A(IROW,L)=A(ICOL,L)
71 A(ICOL,L)=T
T=B(IROW)
B(IROW)=B(ICOL)
B(ICOL)=T
81 TEMP=A(ICOL,ICOL)
DET=DET*TEMP
A(ICOL,ICOL)=1.
DO 91 L=1,N
91 A(ICOL,L)=A(ICOL,L)/TEMP
B(ICOL)=B(ICOL)/TEMP
DO 121 L1=1,N
IF (L1-ICOL) 101,121,101
101 T=A(L1,ICOL)
A(L1,ICOL)=0.
DO 111 L=1,N
111 A(L1,L)=A(L1,L)-A(ICOL,L)*T
B(L1)=B(L1)-B(ICOL)*T
121 CONTINUE
RETURN
131 DET=0.0
RETURN
END

```

```

SUBROUTINE NEWRT(PO,DX)

```

```

DIMENSION AA(50), BB(50), CC(50), DD(50), EE(50), FF(50), DX(50)
DIMENSION AT(50), BT(50), CT(50), PO(50), DP(50), FI(50), FIDP(50,3)
COMMON B1, ALAM, H1, TOL, NL, N2, B2, NL1, N21, NP, NP1, NL2, NL3

```

```

COMMON H2, H13, H23, HSUM
COMMON AA, BB, CC, DD, EE, FF
11 FORMAT (4F10.4,2I5)
12 FORMAT (8F10.5)
13 FORMAT (6XE14.4,3(6X,E14.4),/)
14 FORMAT (17X3HFI=,3X17HDFI/DP(J),J=1,2,3,/)
15 FORMAT (3X2HT=,22X3HDX=,17X3HPO=,/)
16 FORMAT (5X15,2(6XE14.4),/)
17 FORMAT (54H 'PRESSURE IS SMALLER THAN THE AMBIENT PRESSURE' )
18 FORMAT (5X15,3(6XE14.4),/)
19 FORMAT (1H1)
DO 2 I=2, N21
  AA(I)=H23/2./DX(I)
  CC(I)=H23/2./DX(I-1)
  BB(I)=-AA(I)-CC(I)
  FF(I)=ALAM*H2/2.
  DD(I)=-FF(I)
  EE(I)=0.
2 CONTINUE
  AA(N2)=HSUM/DX(N2)/16.
  CC(N2)=H23/2./DX(N21)
  BB(N2)=-AA(N2)-CC(N2)
  FF(N2)=FF(N21)
  DD(N2)=-ALAM*(H2+H1)/4.
  EE(N2)=DD(N2)+FF(N2)
DO 3 I=NP1, NL1
  AA(I)=H13/2./DX(I)
  CC(I)=H13/2./DX(I-1)
  BB(I)=-AA(I)-CC(I)
  FF(I)=ALAM*H1/2.
  DD(I)=-FF(I)
  EE(I)=0.
3 CONTINUE
  AA(NP)=H13/2./DX(NP)
  CC(NP)=HSUM/DX(N2)/16.
  BB(NP)=-AA(NP)-CC(NP)
  DD(NP)=DD(NP1)
  FF(NP)=ALAM*(H1+H2)/4.
  EE(NP)=DD(NP)+FF(NP)
104 CONTINUE
DO 5 I=2, NL1
  J=I-1
  A(J)=AA(I)*PO(I+1)+DD(I)
  B(J)=BB(I)*PO(I)+EE(I)
  C(J)=CC(I)*PO(I-1)+FF(I)
  FI(J)=A(J)*PO(I+1)+B(J)*PO(I)+C(J)*PO(I-1)
  FI(J)=-FI(J)
5 CONTINUE
DO 6 I=3, NL2
  J=I-1
  FIDP(J,1)=CC(I)*2.*PO(I-1)+FF(I)
  FIDP(J,2)=BB(I)*2.*PO(I)+EE(I)
  FIDP(J,3)=AA(I)*2.*PO(I+1)+DD(I)
6 CONTINUE

```

```

FIDP(1,2)=BB(2)*2.*PO(2)+EE(2)
FIDP(1,3)=AA(2)*2.*PO(3)+DD(2)
FIDP(NL2,1) = CC(NL1)*2.*PO(NL2)+FF(NL1)
FIDP(NL2,2) = BB(NL1)*2.*PO(NL1)+EE(NL1)
CALL TDLEQ (FIDP,FI,DP,NL2)
DO 7 I=2, NL1
PO(I)=PO(I)+DP(I-1)
IF (PO(I)-0.) 101, 101, 7
101 PRINT 17
DO 23 IP=1, NL1
PRINT 18, IP, DX(IP), PO(IP), DP(IP-1)
23 CONTINUE
STOP
7 CONTINUE
RMAX=TOL/2.
DO 8 K=1, NL2
R=DP(K)
IF (R-RMAX) 8, 8, 102
102 RMAX=R
8 CONTINUE
IF (RMAX-TOL) 103, 103, 104
103 CONTINUE
PRINT 15
DO 9 IP=1,NL1
PRINT 16, IP, DX(IP), PO(IP)
9 CONTINUE
PRINT 19
RETURN
END

```

```

SUBROUTINE TDLEQ (A,C,X,N)
SUBROUTINE SOLVES A TRIDIAGONAL SYSTEM OF LINEAR EQUATIONS
DIMENSION A(50,3), C(50), X(50), B(50,2), D(50)
START
J=N
B(1,1)=A(1,2)
B(1,2)=A(1,3)
D(1)=C(1)
JJ=J-1
DO 5 K=2,JJ
IF (ABS(B(K-1,1))-ABS(B(K-1,2)))3, 4, 4
3 B(K,1)=A(K,2)*B(K-1,1)/B(K-1,2)-A(K,1)
B(K,2)=A(K,3)+B(K-1,1)/B(K-1,2)
D(K)=(C(K)*B(K-1,1)-A(K,1)*D(K-1))/B(K-1,2)
GO TO 5
4 B(K,1)=A(K,2)-A(K,1)*B(K-1,2)/B(K-1,1)
B(K,2)=A(K,3)
D(K)=C(K)-A(K,1)*D(K-1)/B(K-1,1)
5 CONTINUE
7 X(J)=(C(J)*B(J-1,1)-A(J,1)*D(J-1))/(A(J,2)*B(J-1,1)-A(J,1)*B(J-1,2
1))

```

```
      K=J-1
15  X(K)=(D(K)-B(K,2)*X(K+1))/B(K,1)
      IF (K-1) 100, 100, 10
10  K=K-1
      GO TO 15
100 RETURN
      END
```

Card 1 Format (5F10.4, 3I5)

- B1 - Ratio of B_1/B .
- ALAM - Bearing number, Λ .
- H1 - Normalized gas film thickness, H_2 .
- Tol - Smallness for convergence.
- NL - Total grid number for the step pad including two
 end points.
- N2 - Total grid number for the left edge of the step pad
 with $H = H_2$.

Card 2 Format (8F10.5)

- VI(I) · Array of the squeeze numbers to be solved.

Card 3 Format (8F10.5)

- DX(I) - Array of increments of X defined as $\Delta X_i = X_{i+1} - X_i$
 such that $\sum_{i=1}^N DX(I) = 1$.

Card 4 Format (8F10.5)

- PO(I) - Array of the guessed zero order pressure profile Po , i
 on the pad with $Po, 1 = Po, n = 1$.